

1 **CCSP Synthesis and Assessment Product 1.2**
2 **Past Climate Variability and Change in the Arctic and at High**
3 **Latitudes**

4
5 **Chapter 7 Past Extent and Status of the Greenland Ice Sheet**

6
7 **Chapter Lead Author:** Richard B. Alley, The Pennsylvania State
8 University

9 **Contributing Authors:**

- 10 John T. Andrews, University of Colorado, Boulder
11 Garry K.C. Clarke, University of British Columbia, Vancouver, CA
12 Kurt M. Cuffey, University of California, Berkeley
13 Svend Funder, University of Copenhagen, DK
14 Shawn J. Marshall, University of Calgary, Alberta, CA
15 Jerry X. Mitrovica, University of Toronto, Ontario, CA
16 Daniel R. Muhs, US Geological Survey, Denver, CO
17 Bette Otto-Bliesner, National Center for Atmospheric Research, Boulder,
18 CO

19
20

20 **ABSTRACT**

21 The Greenland Ice Sheet is expected to shrink or disappear with warming, based on a
22 survey of paleoclimatic and related information. Recent observations show that the
23 Greenland Ice Sheet has melted more in years with warmer summers. Mass loss by
24 melting is therefore expected to increase with warming. But whether the ice sheet
25 shrinks or grows, and at what pace, depend also on changes in snowfall and iceberg
26 production. This is a complicated system, and reconstructions of past climate and ice
27 sheet configuration (the “paleo record”) are a valuable source of information, providing
28 an essential complement to process-based models. The paleo record shows that the
29 Greenland Ice Sheet has consistently lost mass when the climate warmed and grown
30 when the climate cooled. Such changes have occurred even at times of slow or zero sea-
31 level change, so changing sea level cannot be the cause of at least some of the ice sheet
32 changes. In contrast, there are no documented ice sheet changes that occurred
33 independent of temperature changes. Moreover, snowfall has increased when the climate
34 warmed, but the ice sheet lost mass nonetheless; increased accumulation in the ice sheet
35 center has not been sufficient to counteract increased melt and flow near the edges. Most
36 of the documented changes (of both ice sheet and forcings) spanned multi-millennial
37 periods, but limited data show that rapid response to rapid forcings has occurred. In
38 particular, regions near the ice margin have been observed to respond on a decadal
39 timescale. However, major changes of central regions of the ice sheet are thought to take
40 centuries to millennia, and this is supported by the limited paleo data. The paleo record
41 does not yet give any strong constraints on how rapidly a major shrinkage or nearly
42 complete loss of the ice sheet could occur. The available evidence suggests near-total

43 loss has occurred for warming of more than a few degrees above mean 20th century
44 values, but this threshold is poorly defined (perhaps as little as 2°C or more than 7°C).
45 The paleo archives are sufficiently sketchy that temporary ice-sheet growth in response to
46 warming, or ice-sheet changes induced by factors other than temperature, may have
47 occurred in the past without being recorded.

48

49 **7.1 The Greenland Ice Sheet**

50

51 **7.1.1. Overview**

52

53 The Greenland Ice Sheet (**Figure 7.1**) contains by far the largest volume of ice of any
54 present-day northern-hemisphere mass. The **ice sheet** is approximately 1.7 million
55 square kilometers (km²) in area, extending as much as 2200 km north-to-south. The
56 maximum ice thickness is 3367 m, with an average thickness of 1600 m (Thomas et al.,
57 2001), and a volume of 2.9 million km³ (Bamber et al., 2001). Some of the bedrock
58 beneath this ice has been depressed below sea level by the weight of the ice, and a little
59 of this bedrock would remain below sea level following removal of the ice and rebound
60 of the bedrock (Bamber et al., 2001). However, most of the ice that rests on bedrock is
61 above sea level and so would contribute to sea-level rise if melted, with an estimated sea-
62 level rise from total ice-sheet loss of about 7.3 m (Lemke et al., 2007).

63

64

65 The ice sheet consists primarily of old snow that has been squeezed to ice under the
66 weight of new snow that accumulates every year. Snow accumulation on the upper
67 surface tends to increase ice-sheet size. Ice sheets lose mass primarily by the runoff of
68 meltwater from low-elevation regions and by the formation of icebergs that break off the
69 ice margins and drift away to melt elsewhere (**calving**). **Sublimation**, snowdrift (Box et
70 al., 2006), and melting or freezing at the **bed** beneath the ice are minor terms in the
71 budget, although melting beneath floating extensions called **ice shelves** before icebergs
72 break off may be important (see 7.1.2, below).

73

74 Estimates of net snow accumulation on the Greenland Ice Sheet have been presented
75 by Hanna et al. (2005) and Box et al. (2006), among others. Hanna et al. (2005) found
76 for 1961-1990 (an interval of moderately stable conditions before more-recent warming)
77 that surface snow accumulation (precipitation minus evaporation) was about 573 Gt/yr
78 (**Gigatons** per year), with 280 Gt/yr of meltwater runoff leaving the ice sheet; the
79 difference of 293 Gt/yr is similar to the estimated iceberg **calving flux** within the broad
80 uncertainties (Reeh, 1985; Bigg, 1999; Reeh et al., 1999). (For reference, return of 360
81 Gt of ice to the ocean would raise global sea level by 1 mm; Lemke et al., 2007.) More
82 recently, trends have been observed toward warming, increasing snowfall, and more
83 rapidly increasing meltwater runoff (Hanna et al., 2005; Box et al., 2006). Large
84 interannual variability causes the statistical significance of many of these trends to be
85 relatively low, but the independent trends exhibit internal consistency (e.g., warming is
86 expected to increase both melting and snowfall based on modeling experiments and

87 simple physical arguments, and both trends are observed in independent studies; Hanna et
88 al., 2005; Box et al., 2006).

89

90 Increased iceberg calving has also been observed in response to faster flow of many
91 outlet glaciers and shrinkage or loss of ice shelves (see 7.1.2, below, for discussion of the
92 parts of an ice sheet) (e.g., Rignot and Kanagaratnam, 2006; Alley et al. 2005). The
93 Intergovernmental Panel on Climate Change (IPCC; Lemke et al., 2007) found that
94 “Assessment of the data and techniques suggests a mass balance of the Greenland Ice
95 Sheet of between +25 and -60 Gt (-0.07 to 0.17 mm) **SLE [sea level equivalent]** per year
96 from 1961-2003 and -50 to -100 Gt (0.14 to 0.28 mm SLE) per year from 1993-2003,
97 with even larger losses in 2005”. Updates are provided by Alley et al. (2007) (**Figure**
98 **7.2**) and by Cazenave (2006). Rapid changes have been occurring in the ice sheet, and in
99 the ability to observe the ice sheet, so additional updates are virtually certain to be
100 produced.

101

102 The long-term importance of these observed trends is considerably uncertain—short-
103 lived oscillation, or harbinger of further shrinkage? This uncertainty motivates some of
104 the interest in the history of the ice sheet.

105

106

107 **7.1.2 Ice-sheet behavior**

108

109 Where delivery of snow or ice (typically as snowfall) exceeds removal (typically by
110 meltwater runoff), a pile of ice develops. Such a pile that is observed to notably deform
111 and flow is called a **glacier, ice cap** or **ice sheet**. (For a more comprehensive overview,
112 see Paterson, 1994; Hughes, 1998; Van der Veen, 1999; or Hooke, 2005, among well-
113 known texts.) Use of these terms is often ambiguous. “**Glacier**” most typically refers to
114 a relatively small mass in which flow is directed down one side of a mountain, whereas
115 “**ice cap**” refers to a small mass with flow diverging from a central dome or ridge, and
116 “**ice sheet**” to a very large ice cap of continental or subcontinental scale. A faster-
117 moving “jet” of ice flanked by slower-flowing parts of an ice sheet or ice cap may be
118 referred to as an **ice stream**, but also as an **outlet glacier** or simply **glacier** (especially if
119 the configuration of the underlying bedrock is important in delineating the faster-moving
120 parts), complicating terminology. Thus, the prominent Jakobshavn Glacier (Jakobshavn
121 Isbrae, or Jakobshavn ice stream) is part of the ice sheet on Greenland, flowing in a deep
122 bedrock trough but with slower-moving ice flanking the faster-moving ice near the
123 surface.

124

125 A glacier or ice sheet spreads under its own weight, deforming internally. The
126 deformation rate increases with the cube of the **driving stress**, which is proportional to
127 the ice thickness and to the surface slope of the ice. Motion also may occur through
128 sliding over the interface between the bottom of the ice and what lies beneath it, i.e. its
129 substrate. Ice motion is typically slow or zero where the ice is frozen to the substrate, but
130 is faster where the ice-substrate interface is close to the melting point. Ice motion can also
131 take place through the deformation of subglacial sediments. This mechanism is

132 important only where subglacial sediments are present and thawed. The contribution of
133 these basal processes ranges from essentially zero to almost all of the total ice motion.
134 Except for floating ice shelves (see below in this section), Greenland's ice generally does
135 not exhibit the gross dominance by basal processes seen in some West Antarctic ice
136 streams.

137

138 Most glaciers and ice sheets tend toward a steady configuration. Snow accumulation
139 in higher, colder regions supplies mass, which flows to lower, warmer regions where
140 mass is lost by melting and runoff or by iceberg **calving**, with the bergs drifting away to
141 melt elsewhere.

142

143 Some ice masses tend to an oscillating condition, marked by ice buildup during a
144 period of slow flow, and then a short-lived surge of rapid ice flow; however, under steady
145 climatic conditions, these oscillations repeat with some regularity and without huge
146 changes in the average size across cycles. Accelerations in ice flow, whether as part of a
147 surging cycle, or in response to long-term ice-sheet evolution or climatically forced
148 change, may occur through several mechanisms. These mechanisms include thawing of a
149 formerly frozen bed, increase in meltwater reaching the bed causing increased lubrication
150 (Zwally et al., 2002; Joughin et al., 1996; Parizek and Alley, 2004), and changes in
151 meltwater drainage causing retention of water at the base of the glacier, which increases
152 lubrication (Kamb et al., 1985). Ice-flow slowdown can similarly be induced by
153 reversing these causes.

154

155 Recently, attention has been focused on changes in ice shelves. Where ice flows into
156 an ice-marginal water body, iceberg calving may occur from **grounded** (non-floating)
157 **ice**. However, the flowing ice instead may remain attached to the glacier or ice sheet as it
158 flows into the ice-marginal body of water. The attached ice floats on the water and
159 calves from the end of the floating extension, which is called an **ice shelf**. Ice shelves
160 frequently run aground on local high spots in the bed of the water body on which they
161 float. Ice shelves that occupy embayments or fjords experience friction from the rocky or
162 icy sides that restrains ice flow. Loss of friction from these restraints then allows faster
163 flow of the ice feeding the ice shelf (Payne et al., 2004; Dupont and Alley, 2005; 2006).

164
165 Although numerous scientific papers have dealt with the possibilities of changing
166 lubrication or loss of ice-shelf buttressing affecting ice flow, comprehensive ice-flow
167 models generally have not incorporated these processes. These comprehensive models
168 also did not accurately project the ice-flow accelerations observed recently in Greenland
169 and in some parts of the Antarctic ice sheet (Alley et al., 2005; Lemke et al., 2007;
170 Bamber et al., 2007). This issue is cited by IPCC (2007), which provided sea-level
171 projections “excluding future rapid dynamical changes in ice flow” (Table SPM3, WG1)
172 and noted that this prevented “a best estimate or an upper bound for sea level rise” (p.
173 SPM 15). A paleoclimatic perspective can help inform consideration of these issues.

174
175 As noted above in this section, when subjected to a step forcing (e.g., a rapid climatic
176 warming from one sustained level to another), an ice sheet typically responds by evolving
177 to a new steady state in response (Paterson, 1994). For example, an increase in

178 accumulation rate causes thickening of the ice sheet. The thicker ice sheet discharges
179 mass faster and, if the ice margin does not move as the ice sheet thickens, it becomes on
180 average steeper, which also speeds ice discharge. These changes eventually cause the ice
181 sheet to approach a new configuration that is in balance with the new forcing (a new
182 steady state). For central regions of cold ice sheets, the time required to complete most of
183 the response to a step accumulation-rate change (i.e., the response time) scales with the
184 thickness divided by the accumulation rate. These characteristic times are a few
185 thousands of years (millennia) for the modern Greenland Ice Sheet and a few times
186 longer for the ice-age ice sheet (e.g., Alley and Whillans, 1984; Cuffey and Clow, 1997).
187

188 A change in ice-margin position will steepen or flatten the mean slope of the ice sheet,
189 speeding or slowing flow, with the first influence felt near the ice-sheet edge. This, in
190 turn, causes a “wave” of adjustment that propagates toward the ice-sheet center. Fast-
191 flowing marginal regions can be affected within years, whereas the full response of the
192 slow-flowing central regions to a step-change at the coast requires a few millennia.

193
194 Warmer ice deforms more rapidly than colder ice. In inland regions, ice sheet
195 response to temperature change is somewhat similar to response to accumulation-rate
196 change with cooling causing slower deformation, which favors thickening hence higher
197 ice flux through the increased thickness (and perhaps with increasing surface slope also
198 speeding flow), re-establishing equilibrium. However, because most of the deformation
199 occurs in deep ice, and a surface-temperature change requires many millennia to
200 penetrate to that deep ice to affect deformation, most of the response is delayed for a few

201 millennia or longer while the temperature change penetrates to the deep layers, and then
202 the response requires a few more millennia. The calculation is not simple, because the
203 motion of the ice carries its temperature along with it. If melting of the upper surface of
204 an ice sheet develops over a region in which the bottom of the ice is frozen to the
205 substrate, thawing of that basal interface may be caused by penetration of surface
206 meltwater to the bed if water-filled crevasses develop at the surface. The actual
207 penetration of the water-filled crevasse is likely to occur in much less than a single year,
208 perhaps in only a few minutes, rather than over centuries to millennia (Alley et al., 2005).
209

210 Numerous ice-sheet models (e.g., Huybrechts, 2002) demonstrate the relative
211 insensitivity of the inland thickness to these environmental parameters. This insensitivity
212 has allowed reasonably accurate ice-sheet reconstructions using computational models
213 that assume **perfectly plastic ice behavior** and a fixed **yield strength** (Reeh 1984; the
214 only piece of information needed in these reconstructions of inland-ice configuration is
215 the footprint of the ice sheet, with no specification of accumulation rate hence mass flux,
216 for example). This insensitivity can be understood from very simple physics.

217

218 As noted above in this section, the driving stress for ice deformation increases linearly
219 with ice thickness and with the surface slope, and the ice-deformation rate increases with
220 the cube of this driving stress. Velocity from deformation is obtained by integrating the
221 deformation rate through thickness, and ice flux is the depth-averaged velocity multiplied
222 by thickness, so the ice flux increases with the cube of the surface slope and the fifth
223 power of the thickness for ice frozen to the bed. (Allowing a thawed bed retains strong

224 dependence on surface slope and thickness, but with different numerical values.) If the
225 ice-marginal position is fixed (say, because the ice has advanced to the continental-shelf
226 edge and cannot advance farther across the very deep water), then the typical surface
227 slope of the ice sheet is also proportional to the ice thickness (divided by the fixed half-
228 width), giving an eighth-power dependence of ice flux on inland thickness. Although an
229 eighth-power dependence is not truly perfectly plastic, it does serve to greatly limit
230 inland-thickness changes—doubling the inland thickness would increase ice flux 256-
231 fold. Because of this insensitivity of the inland thickness to many controlling parameters,
232 changes in ice-sheet volume are controlled more by changes in the areal extent of the ice
233 sheet than by changes in the thickness in central regions.

234

235 Such simple mechanistic scalings of ice sheet behaviors can be useful heuristically,
236 and often have been used to interpret ice-sheet behavior in the past. However, in modern
237 usage, our physical understanding of ice sheet behaviors is implemented in fully coupled
238 three-dimensional (or reduced-dimensional) **ice-dynamical models** (e.g., Huybrechts,
239 2002; Parizek and Alley, 2004; Clarke et al., 2005), which are used to assimilate and
240 understand the relevant data.

241

242

243 **7.2 Paleoclimatic Indicators Bearing on Ice-Sheet History**

244

245 The basis for paleoclimatic reconstruction is discussed in Cronin (1999) or Bradley
246 (1999), among other sources. Here, additional attention is focused on those indicators

247 that help in reconstruction of the history of the ice sheet. Marine indicators are discussed
248 first, followed by terrestrial archives.

249

250

251 **7.2.1 Marine Indicators**

252

253 As discussed in section 7.3 below, the Greenland Ice Sheet has often been more
254 extensive than it is now, and much of that extension occurred into regions now below sea
255 level. Furthermore, iceberg-rafted debris and meltwater from the ice sheet can leave
256 records in marine settings related to the extent and flux of ice-sheet ice. Marine
257 sediments also preserve important indicators of temperature and of other conditions that
258 may have affected the ice sheet.

259

260 Research cruises to the marine shelf and slope margins of west and east Greenland
261 dedicated to understanding changes over the times most relevant to its history have been
262 undertaken only in the last ten to twenty years. Initially, attention was focused along the
263 east Greenland shelf (Marienfeld, 1992b; Mienert et al., 1992; Dowdeswell et al., 1994a),
264 but in the last few years several cruises have extended to the west Greenland margin as
265 well (Lloyd, 2006; Moros et al., 2006). Research on adjacent deep-sea basins, such as
266 Baffin Bay or Fram Basin off North Greenland, is more complicated because the late
267 Quaternary (<450 ka) sediments record inputs from several adjacent ice sheets (Dyke et
268 al., 2002; Aksu, 1985; Andrews et al., 1998a; Hiscott et al., 1989). Regardless, it must be
269 emphasized that the existing geographic coverage of research on the Greenland shelf is

270 limited. Temporally, the majority of marine cores from the Greenland shelf contain
271 records that span the retreat from the last ice age (<15 ka—we use calendar years rather
272 than radiocarbon years unless indicated; conversions include those of Stuiver et al., 1998
273 and Fairbanks et al., 2005; all ages specified by “ka” or “Ma” are in years before present,
274 where “present” is conventionally taken as the year 1950). The use of datable volcanic
275 ashes (**tephras**—a recognizable tephra/ash layer from a single eruption is often found
276 across broad regions and has the same age in all cores) from Icelandic sources offers the
277 possibility of linking records from around Greenland from the time of the layer known as
278 Ash Zone II (~54 ka) to the present (with appropriate cautions; Jennings et al., 2002a).

279

280 The sea-floor around Greenland is relatively shallow in places, above “**sills**” formed
281 during the **rifting** that opened the modern oceans. Such sills connect Greenland to
282 Iceland via the Denmark Strait, and Greenland to Baffin Island via Davis Strait. These
283 500-600 m deep sills separate archives of ice sheet histories into “northern” and
284 “southern” components. Even farther north, sediments shed from north Greenland are
285 especially transported into the Fram Basin of the Arctic Ocean (Darby et al., 2002).

286

287 Ocean surface circulation around Greenland today, which transports debris-bearing
288 icebergs from the ice sheet, is largely controlled by a clockwise pattern with cold, fresh
289 waters exiting the Arctic Ocean via Fram Strait and flowing southward along the east
290 Greenland margin as the East Greenland Current (Hopkins, 1991). These waters turn
291 north after rounding the southern tip of Greenland. In the vicinity of Denmark Strait,
292 warmer water from the Atlantic (modified Atlantic Water from the Irminger Current)

293 turns and flows parallel to the East Greenland Current. This surface current is called the
294 West Greenland Current once it has rounded the southern tip of Greenland. On the east
295 Greenland shelf, this modified Atlantic Water becomes an “intermediate-depth” water
296 mass (reaching to the deeper parts of the continental shelf, but not to the depths of the
297 ocean beyond the continental shelf), which moves along the deeper topographic troughs
298 on the continental shelf and penetrates into the margins of the calving Kangerdlugssuaq
299 ice stream (Jennings and Weiner, 1994; Syvitski et al., 1996). In Baffin Bay, three water
300 masses have been identified. Arctic Water occurs in the upper 100-300 m in all areas,
301 and this water mass is underlain by West Greenland Intermediate Water (modified
302 Atlantic Water) between 300-800 m. Deep Baffin Bay Water occurs throughout the Bay
303 at depths >1200 m (Tang et al., 2004).

304

305 Some of the interest in the Greenland Ice Sheet is linked to the possibility that
306 meltwater could greatly affect the formation of deep waters in the North Atlantic.
307 Furthermore, changes in deep-water formation in the past are linked to climate changes
308 that affected the ice sheet (e.g., Alley, 2007). The major deep-water flow is directed
309 southward through and south of Denmark Strait (McCave and Tucholke, 1986). The
310 sediment deposit known as the Erik Drift off southwest Greenland is a product of this
311 flow (Stoner et al., 1995). Convection in the Labrador Sea results in the formation of an
312 upper component of this North Atlantic Deep Water.

313

314 Based on marine cores and seismic data, reconstructions of the variations in the
315 Greenland Ice Sheet over the last glacial cycle (and, occasionally, into older times) have

316 been based on (see subsections of 7.2.1, below, for explanations): a) the presence of ice-
317 rafted debris and indications of changes in sediment sources; b) evidence for glacial
318 deposition onto **trough-mouth fans**; c) stable-isotope and biotic data that indicate times
319 of meltwater release from the ice sheet; and, d) geophysical data pertaining to seafloor
320 erosion and deposition. Each is discussed briefly in the next subsections.

321

322

323 **7.2.1a Ice-rafted debris (IRD) and provenance**

324

325 Coarse-grained rock material (such as sand and pebbles) cannot be carried far from a
326 continent by wind or current, so the presence of such materials in marine cores is of great
327 interest. Small amounts might be delivered in tree roots or attached to uprooted kelp
328 holdfasts (Gilbert, 1990; Smith and Bayliss-Smith, 1998), and rarely a meteorite might be
329 encountered, but large quantities of coarse rock material found far from land indicate
330 transport in ice, and so this material is called ice-rafted debris, or IRD. Both sea ice and
331 icebergs can carry coarse material, complicating interpretations. However, iceberg IRD
332 usually includes some number of grains larger than 2 mm in size and consistent with the
333 grain-size distributions of glacially transported materials, whereas the sediment entrained
334 in sea ice is typically finer grained (Lisitzin, 2002). In order to evaluate the links
335 between the Greenland Ice Sheet and ice-rafted debris events in marine cores, it is also
336 necessary to be able to link that debris to specific geographic/bedrock areas of the
337 Greenland Ice Sheet or adjacent ice sheets (i.e. identify its provenance or site of origin).
338 However, such studies are only in their infancy. Proxies for sediment source include

339 **radiogenic isotopes** (such as ϵNd ; Grousset et al., 2001; Farmer et al., 2003),
340 **biomarkers** that can be linked to different outcrops of dolomite (Parnell et al., 2007),
341 sediment magnetic properties (Stoner et al., 1995), or quantitative mineralogical
342 assessment of sediment composition (Andrews, 2008).

343

344

345 **7.2.1b Trough mouth fans**

346

347 Sediment is often transferred across the continental shelf along large troughs, forming
348 major depositional features called trough-mouth fans (TMF) where the troughs widen and
349 flatten at the continental rise (Vorren and Laberg, 1997; O'Cofaigh et al., 2003). These
350 features are important archives for understanding history of the sediment sources,
351 including ice sheets. Along the east Greenland margin, trough-mouth fans exist off
352 Scoresby Sund (Dowdeswell et al., 1997), the Kangerdlugssuaq Trough (Stein, 1996),
353 and the Angamassalik Trough (St. John and Krissek, 2002). Along the west Greenland
354 margin, the most conspicuous such fan is the massive body off Disko Bay associated with
355 erosion by Jakobshavn Glacier and other outlet glaciers in that region. During periods
356 when the ice sheet reaches the shelf break, glacial sediments are shed downslope as
357 debris flows (i.e. coarse diamictons), whereas periods when the ice sheet is well-back
358 from the shelf break are marked by sediments containing materials from the open-marine
359 environment (including shells of foraminifera) and land-derived materials (including ice-
360 rafted debris).

361

362

363 **7.2.1c Foraminifera, including stable-isotopic ratios of shells**

364

365 Foraminifera – mostly marine, single-celled planktonic animals with chalky shells –
366 are widely distributed, and shells of surface-dwelling (planktic) and bottom-dwelling
367 (benthic) species are commonly found in many sediments. The species present provide
368 information on environmental conditions, and chemical and isotopic characteristics of the
369 shells provide additional information. Variations in the ratios of the stable isotopes of
370 oxygen, ^{18}O to ^{16}O ($\delta^{18}\text{O}$) are especially widely used. These ratios respond to changes in
371 the global ice volume. Water containing the lighter isotope (^{16}O) evaporates from the
372 ocean more readily, and ice sheets are ultimately composed of that evaporated water, so
373 during times when the ice sheets are larger, the ocean is isotopically heavier. This effect
374 is rather well-known, and can be corrected for with considerable confidence if the age of
375 a sample is known. Temperature also affects $\delta^{18}\text{O}$, with warmer temperatures favoring
376 incorporation of the lighter isotope into the shell. Near ice sheets, abrupt changes to light
377 values are most commonly associated with meltwater events delivering isotopically light
378 and fresh water (Jones and Keigwin, 1988; Andrews et al., 1994). Around the Greenland
379 Ice Sheet, most such records are from near-surface planktic foraminifera of the species *N.*
380 *pachyderma* sinistral (Fillon and Duplessy, 1980; van Kreveld et al., 2000; Hagen and
381 Hald, 2002), although there are some data from benthic foraminifera (Andrews et al.,
382 1998a; Jennings et al., 2006).

383

384

385 **7.2.1d Seismic and geophysical data**

386

387 Detailed seismic investigations have been conducted along some of the major shelf
388 troughs and on the trough-mouth fans. Emphasis has been placed on high-resolution
389 studies of the sediments nearest the sea floor (seismostratigraphy; O'Cofaigh et al., 2003),
390 although some deeper-looking data are available (airgun profiles; Stein, 1996; Wilken
391 and Mienert, 2006). Sonar reveals the shape of the upper surface of the sediment,
392 showing features such as the tracks left by drifting icebergs contacting and plowing
393 through the sediment (Dowdeswell et al., 1994b; Dowdeswell et al., 1996; Syvitski et al.,
394 2001), and the streamlining of the sediment surface caused by glaciation.

395

396

397 **7.2.2 Terrestrial Indicators**

398

399 Land-based records, like their marine equivalents, can reveal the history of ice-extent
400 changes, as well as the climatic conditions that existed around the ice sheet at various
401 times. Terrestrial records are often more discontinuous in space and time than are marine
402 records, because net erosion (which removes the sediments containing climatic records)
403 is dominant on land whereas net deposition occurs in most marine settings. Nonetheless,
404 usefully complete records of many time intervals have been assembled from terrestrial
405 indicators. Here, a range of indicators is summarized briefly. This treatment is
406 representative rather than comprehensive. Furthermore, the great wealth of indicators,
407 and the interwoven nature of their interpretation, preclude any simple subdivision.

408

409

410 *7.2.2a Geomorphic indicators*

411

412 The land surface itself records the action of ice, and thus provides information on ice-
413 sheet history. Glacial deposits known as **moraines** are especially instructive, but others
414 are also important.

415

416 Moraines are sediment deposited around glaciers from material carried on, in, or under
417 the moving ice (e.g., Sugden and John, 1976). A preserved moraine may mark the
418 maximum extent reached by ice during some advance, or a still-stand during retreat.
419 Normally, older moraines are destroyed by ice readvance, although remnants of moraines
420 overrun by a subsequent advance are occasionally preserved and identifiable, especially if
421 the readvance was made by ice frozen to its bed and so nearly or completely stationary
422 where the ice met the moraine. Because most older moraines are reworked by
423 subsequent advances, moraines are primarily restricted to recording the timing of the
424 most recent glacial maximum, and pauses or subsidiary readvances during retreat.

425

426 Limiting ages of moraines can be estimated from radiocarbon (carbon-14) dating of
427 carbon-bearing materials incorporated in a moraine (the moraine must be younger than
428 those materials) or deposited in lakes that formed on or behind moraines following ice
429 retreat (the moraine must be older than those materials). Increasingly, moraines are dated
430 by measurement of beryllium-10 or other isotopes produced in boulders by cosmic rays

431 (e.g., Gosse and Phillips, 2001). Because cosmic rays penetrate only about 1 m in rock,
432 boulders that are quarried from beneath the ice following erosion of ~1 m or more of
433 overlying material, or large boulders that fall on the ice and are rolled over during
434 transport, typically start with no cosmogenic nuclides in their upper surfaces, and
435 accumulate those nuclides proportional to exposure time. Corrections for loss of nuclides
436 by boulder erosion, for inheritance of nuclides from before deposition, and other factors
437 may be nontrivial but potentially reveal further information. Additional techniques of
438 dating can sometimes be used, including historical records and the increase over time in
439 lichen-colony size (e.g., Locke et al., 1979; Geirsdottir et al., 2000), soil development,
440 and breakdown of rocks (clast weathering).

441

442 Related information on glacial behavior and ages is also available from the land
443 surface. For ages of events, a boulder need not be in a moraine to be dated using
444 cosmogenic isotopes, and surfaces **striated** and polished by glacial action can be dated
445 similarly. Glacial retreat often reveals wood or other organic material that died when
446 overrun during an advance, and that can also be dated using radiocarbon techniques.

447

448 With small glaciers, the highest elevation to which a moraine extends is often close to
449 the equilibrium-line altitude at the time when the moraine formed (that is, the altitude
450 above which net snow accumulation occurred, and below which mass loss occurred—
451 mass moves into the glacier above that elevation and out below that elevation, controlling
452 the deposition of rock material). Glaciation produces identifiable landforms, especially if
453 the ice is thawed at the base and thus sliding freely over its substrate, so contrasts in

454 landform appearance can be used to map limits of glaciation, or of wet-based glaciation,
455 where moraines are not available.

456

457 Glaciers respond to many environmental factors, but for most glaciers the balance
458 between snow accumulation and melting is the major control on glacier extent.
459 Furthermore, with notable exceptions, melting is usually affected more by climate change
460 than is accumulation. The equilibrium vapor pressure (“the ability of warmer air to hold
461 more moisture”) increases roughly 7% per °C; across a range of glaciers that balance
462 snow accumulation by melting, the increase in melting is approximately 35%(±10%) per
463 °C (e.g., Oerlemans, 1994; 2001; Denton et al., 2005). Thus, glacier extent can often be
464 used as a proxy for melt-season duration and temperature, primarily summertime
465 temperature.

466

467

468 *7.2.2b Biological indicators and related features*

469

470 Living things are sensitive to climate. The species found in a tropical rain forest are
471 obviously quite different from those found on the **tundra**. By comparing modern species
472 from different places with different climates, or by looking at changes in species at one
473 place over the short instrumental record, the relationship to climate can be estimated.
474 Assuming that this relationship has not changed over time, longer records of climate then
475 can be estimated from older occurrences of different species (e.g., Schofield et al., 2007),
476 providing information on the climatic forcing affecting the ice sheet.

477

478 Lake sediments are especially valuable as sources of biotic indicators, because of the
479 continuous sedimentation process (which yields a continuous record) and the rich
480 ecosystems in and around lakes (e.g., Bjorck et al., 2002; Ljung and Bjorck, 2004;
481 Andresen et al., 2004). Pollen (e.g., Ljung and Bjorck, 2004; Schofield et al., 2007),
482 microfossils, and macrofossils (including chironomids, or midge flies; Brodersen and
483 Bennike, 2003) are all used to great advantage in reconstructing past climates. The
484 isotopic composition of shells or of inorganic precipitates in lakes records some
485 combination of water-isotopic composition and temperature. Physical aspects of lake
486 sediments, including those linked to biological processes (e.g., loss on ignition, which
487 primarily measures the relative abundance of organic matter in the sediment) are also
488 related to climate. In places where the weight of the ice previously depressed the land
489 below sea level and subsequent rebound raised the land back above sea level and formed
490 lakes (see 7.2.2c, below), the timing of the onset of lacustrine conditions, and the modern
491 height of the lake, together provide key information on the ice-sheet history (e.g.,
492 Bennike et al., 2002).

493

494 Raised marine deposits in Greenland and surroundings provide an additional and
495 important source of biological indicators of climate change. The interplay of changing
496 sea level, geological processes of uplift and subsidence, and isostatic response (ice-sheet
497 growth depressing the land and subsequent shrinkage allowing rebound, with a lagged
498 response; again, see 7.2.2c, below), cause many marine deposits to now reside above sea
499 level. Biological materials within those deposits, and especially shells, allow radiocarbon

500 or uranium-thorium dating (see 7.2.2d, below), providing a history of relative sea level
501 that can be used to infer ice-sheet loading histories, and allow climatic reconstruction
502 based on the species present (e.g., Dyke et al., 1996).

503

504

505 ***7.2.2c Glacial isostatic adjustment (GIA) and near-field relative sea-level indicators***

506

507 Within the geological literature, sea level is generally defined as the distance between
508 the sea surface and sea bottom. (This convention contrasts with the concept of absolute
509 sea level, where the position of the sea surface is measured relative to some absolute
510 datum, such as the center of the Earth.) This definition of sea level is consistent with
511 geological markers of past sea-level change (e.g., ancient shorelines, shells, driftwood,
512 etc.), which reflect changes in the height of either of the two bounding surfaces (i.e., an
513 ancient shoreline can be exposed because the surface of the ocean dropped, or land
514 uplifted, or a net combination of land and ocean height changes). Over the time periods
515 considered in this report, the dominant process responsible for such changes, at least on a
516 global scale, is the mass transfer between ice reservoirs and oceans associated with the
517 ice-age cycles, and the deformational response of the Earth to this transfer of mass. This
518 deformational response is formally termed **glacial isostatic adjustment (GIA)**.

519

520 The growth and shrinkage of ice have generally been sufficiently slow that glacial
521 isostatic adjustment of the solid Earth is characterized by both immediate **elastic** and
522 slow **viscous** (i.e., flow) effects. As an example, if a large ice sheet were to form

523 instantly and then persist for more than a few thousand years, the land would experience
524 near-instantaneous elastic sinking, followed by slow subsidence toward isostatic
525 equilibrium in response to movement of deep, hot rock outward from beneath the ice
526 sheet. Roughly speaking, the final depression will be about 30% of the thickness of the
527 ice; thus, the ancient Laurentide ice sheet that covered most of Canada and the
528 northeastern U.S, and reached a peak thickness of 3-4 km, produced a crustal depression
529 of approximately 1 km. (For comparison, the ice sheet contained enough water to make a
530 layer ~70 m thick across the world oceans, much less than the local deformation beneath
531 the ice.) Outside the depressed region covered by an ice load, the land is gradually
532 pushed upward to form a so-called **peripheral bulge**. As the ice subsequently melts, the
533 central region of depression rebounds, and sites within this area are subject to a sea-level
534 fall that will continue for thousands of years beyond the end of the melting phase. For
535 example, sites in Hudson Bay are presently experiencing a sea-level fall of order 1 cm/yr
536 despite the disappearance of most of the Laurentide ice sheet by 8 ka. Moreover, the
537 reduction of ice cover causes the peripheral bulge to subside, leading to a sea-level rise in
538 such areas (e.g., along the U.S. east coast) that also continues to the present. As one
539 considers sites farther away from the high-latitude ice cover, in the so-called far field, the
540 sea-level change is dominated during deglaciation by the addition of meltwater into the
541 global oceans. However, in periods of stable ice cover, for example during the present
542 interglacial, changes in sea-level continue to occur as a consequence of the ongoing
543 gravitational and deformational effects of glacial isostatic adjustment. As an example,
544 glacial isostatic adjustment is responsible for a fall in sea level of ~3 m over the last
545 5,000 years in parts of the equatorial Pacific, with the associated exposure of corals and

546 ancient shoreline features of this age (Mitrovica and Peltier, 1991; Mitrovica and Milne,
547 2002; Dickinson, 2001). We return to this point in section 7.2.2d, below.

548

549 Near-field relative sea-level changes, where the term “relative” denotes the height of
550 an ancient marker relative to the present-day level of the sea, have commonly been used
551 to constrain models of the geometry of ice complexes, particularly since the Last Glacial
552 Maximum [~24 ka] (e.g., Lambeck et al., 1998; Peltier, 2004). Fleming and Lambeck
553 (2004) compared a set of ~600 relative sea-level data points, from sites collected in
554 Greenland from all but the southeast coast and the west coast near Melville Bugt, with
555 numerical models of the glacial isostatic adjustment process to constrain the post-Last
556 Glacial Maximum history of the Greenland Ice Sheet. The Fleming and Lambeck (2004)
557 data set comprised primarily fossil mollusk shells that lived at or below the sea surface
558 but that now are exposed above sea level; because of the unknown depth at which the
559 mollusks lived, they provide a limiting value on sea level. However, Fleming and
560 Lambeck (2004) also included observations on the transition of modern lakes from
561 formerly marine conditions, and constraints associated with the present (sub-sea) location
562 of initially terrestrial archaeological sites (see also Weidick, 1996; Kuijpers et al., 1999).
563 Tarasov and Peltier (2002, 2003) analyzed their own compilation of local sea-level
564 records by coupling glacial isostatic adjustment and climatological models, inferring ice
565 history extending to the last interglacial.

566

567 Like all glacial isostatic adjustment models, these studies are hampered by
568 uncertainties in the **viscoelastic structure** of the Earth (Mitrovica, 1996), which is

569 generally prescribed by the thickness of the elastic plate and the radial profile of viscosity
570 within the underlying mantle, and this uncertainty has implications for the robustness of
571 the inferred ice history. In addition, the analysis of sea-level records in Greenland is
572 complicated by signals from at least two other non-local sources: (1) the adjustment of
573 the peripheral bulge associated with the (de)glaciation of the larger North American
574 Laurentide ice sheet, since this bulge extends over Greenland (e.g., Fleming and
575 Lambeck, 2004); and (2) the net addition of meltwater from contemporaneous melting
576 (or, in times of glaciation, growth) of all other global ice reservoirs. Therefore, some
577 constraints on the volume and extent of the Laurentide ice sheet, and the volume of more
578 distant ice sheets and glaciers, are required for the analysis of sea-level data from
579 Greenland.

580

581

582 *7.2.2d Far-field indicators of relative sea-level high-stands*

583

584 Past changes in Greenland Ice Sheet volume are recorded in far-field sea level. All
585 other sources of sea-level change, as well as that due to the glacial isostatic adjustment
586 process, are also recorded in far-field sea-level records, so a single history of sea level
587 provides information related to ice-volume change (and to other factors such as thermal
588 expansion/contraction of ocean water), but no information on the relative contribution of
589 individual sources.

590

591 The record of past sea level can be reconstructed in many ways. An especially
592 powerful method of reconstruction utilizes the record of marine deposits or emergent
593 coral reefs that are now found above sea level on geologically relatively stable coasts and
594 islands (that is, in regions not being affected rapidly by processes linked to plate
595 tectonics.). Such records are literally “high-water marks,” or “bathtub rings” of past high
596 sea levels. Coastal landforms and deposits provide powerful and independent records of
597 sea-level history compared to the often-cited deep-sea oxygen-isotope record of glacial
598 and interglacial periods. Coastal landforms have two advantages over the deep-sea
599 oxygen-isotope record for sea-level history: (1) if corals are present, they can be dated
600 directly; and (2) depending on the geological setting, estimates of paleo-sea level can be
601 made.

602

603 Coastal landforms record high stands of the sea when coral-reef growth can “keep up”
604 with the rising sea level (upper panel in **Figure 7.3**) or when marine terraces can be
605 eroded into bedrock during a stable sea-level high stand (lower panel in **Figure 7.3**).
606 Thus, emergent marine deposits, either reefs or terraces, on a geologically active, rising
607 coastline record interglacial periods (**Figure 7.4**). On a geologically stable or slowly
608 sinking coast, reefs will be emergent only from sea-level stands that were higher than
609 present (**Figure 7.4**). Past sea levels can thus be determined from stable coastlines or
610 even rising coastlines, if reasoned models of uplift rates can be made. Emphasis is
611 especially placed on geologic records of high sea-level stands that are found on
612 geologically relatively stable coasts. Although valuable geologic records occur on rising
613 coasts, estimates of past sea level derived from such coasts are always dependent on

614 assumptions about the rate of **tectonic** uplift, and therefore will carry with them more
615 uncertainty.

616

617 The direct dating of emergent marine deposits is possible because uranium (U) is
618 dissolved in ocean water but thorium (Th) and protactinium (Pa) are not. Certain marine
619 organisms, particularly corals, co-precipitate U directly from seawater during growth.
620 All three of the naturally occurring isotopes of U, ^{238}U and ^{235}U (both primordial parents)
621 and ^{234}U (a decay product of ^{238}U), are therefore incorporated into living corals. ^{238}U
622 decays to ^{234}U , which in turn decays to ^{230}Th . The parent isotope ^{235}U decays to ^{231}Pa .
623 Thus, activity ratios of $^{230}\text{Th}/^{234}\text{U}$, $^{238}\text{U}/^{234}\text{U}$, and $^{231}\text{Pa}/^{235}\text{U}$ can provide three
624 independent clocks for dating the same fossil coral (e.g., Edwards et al., 1997). Since the
625 1980s, most workers have employed thermal ionization mass spectrometry (TIMS) to
626 measure U-series nuclides, which has increased precision, requires much smaller
627 samples, and can extend the useful time period for dating back to at least ~500,000 yr.

628

629 The coastlines where the most reliable records of past high sea levels can be found are
630 in the tropics and subtropics, where ocean temperatures are warm enough that coral-reef
631 growth is possible. Within this broad equatorial region, the ideal coastlines for studies of
632 past high sea levels are those that are distant from boundaries of tectonic plates, and thus
633 occur near geologically relatively quiescent continental margins or as islands well within
634 the interiors of large tectonic plates. Even in such locations, however, there can be
635 important uncertainty in interpreting past sea levels. We highlight two major reasons for
636 this uncertainty.

637

638 First, many islands well within the crustal tectonic plate covering the Pacific Ocean,
639 for example, are part of hot spot volcanic chains. (A major source of internal heat, called
640 a hot spot, leads to a volcano on the overriding tectonic plate; as the plate drifts laterally,
641 the slower-moving hot spot becomes positioned below a different part of the plate, and a
642 new volcano is formed as the previously active volcano becomes extinct. Eventually, a
643 chain of volcanoes is produced, such as the Hawaiian-Emperor seamount chain). The
644 weight of a growing volcano depresses the land isostatically in the same way that the
645 weight of an ice sheet does, and the cold upper elastic layer of the Earth flexes to form a
646 topographic high around the low caused by the volcano. Oahu, in the Hawaiian Island
647 chain, is a good example of an island that is apparently experiencing slow uplift, and an
648 associated local sea-level fall, due to volcanic loading on the “Big Island” of Hawaii
649 (Muhs and Szabo, 1994).

650

651 Second, the existence of a sea-level highstand of a given age in a stable geologic
652 setting does not necessarily imply that ice volumes were lower at that time relative to the
653 present day, even if the highstand is dated to a previous interglacial. As discussed above,
654 glacial isostatic adjustment, since it involves slow viscous flow of rock, produces global-
655 scale changes in sea-level even during periods when ice volumes are stable. As an
656 example, over the last 5,000 years, motion of ocean water away from the equatorial
657 regions toward the ancient ice complexes in order to fill the void left by the subsidence of
658 the peripheral bulge regions associated with the ice sheets has led to an ongoing sea-level
659 fall of order approximately 0.5 mm/yr in those far-field equatorial regions (Mitrovica and

660 Peltier, 1991; Mitrovica and Milne, 2002). This process, known as equatorial ocean
661 syphoning, is responsible for the development of so-called 3-meter beaches and exposed
662 coral reefs that have been dated to the end of the last deglaciation and that are endemic to
663 the equatorial Pacific (e.g., Dickinson, 2001). Thus, the interpretation of such apparent
664 highstands requires correction for glacial isostatic adjustments such that the residual
665 record reflects true changes in ice volume.

666

667

668 *7.2.2e Geodetic indicators*

669

670 Geodetic data are yielding both “local” and “non-local” constraints on recent ice-sheet
671 mass changes. As an example, land-based measurements of changes in gravity and
672 crustal motions estimated using the Global Positioning System (GPS) are being used to
673 monitor deformation associated with ongoing and recent changes in the mass distribution
674 of the periphery of the Greenland Ice Sheet (e.g., Kahn et al., 2007). An obvious
675 drawback of these techniques is that spatial sampling of the response is limited because
676 of the difficulty of establishing high-quality GPS sites. In contrast, data from the Gravity
677 Recovery and Climate Experiment (GRACE) satellite mission are revealing ongoing
678 trends in gravity over the polar ice sheets (with a spatial resolution of ~400 km) from
679 which estimates of both regional and integrated mass flux are being obtained (e.g.,
680 Velicogna and Wahr, 2006). A general problem in all attempts to infer recent ice sheet
681 balance, whether from land-based or satellite gravity, GPS, or even altimetric
682 measurements of ice heights (e.g., Johannessen et al., 2005; Thomas et al., 2006), is that a

683 correction must be performed for the ongoing influence of glacial isostatic adjustments.
684 As discussed above (section 7.2.2c), this correction involves uncertainty associated with
685 both the ice sheet history and viscoelastic structure of the Earth.

686

687 Accurate glacial isostatic adjustment corrections are also central to non-local estimates
688 of ice-sheet mass balance. One of the primary means of inferring global sea-level change
689 over the last century has been to analyze long-term trends in records from a widely
690 distributed set of tide gauges (tide gauges are simple sea-level monitoring devices). In
691 this regard, most analyses of glacial isostatic adjustment-corrected (residual) tide-gauge
692 rates yield an average 20th century sea-level rise in the range 1.5-2 mm/yr (Douglas,
693 1997). Furthermore, geographic trends in the residual rates provide a potentially
694 important constraint on the sources of the meltwater. In particular, Mitrovica et al.
695 (2001) and Plag and Juttner (2001) have demonstrated that the rapid melting of different
696 ice sheets will have significantly different signatures, or fingerprints, in the spatial pattern
697 of sea-level change. These patterns are linked to the gravitational effects of the lost ice
698 (sea level is raised near an ice sheet because of the gravitational attraction of the ice mass
699 for the adjacent ocean water) and to the elastic (as opposed to viscoelastic) deformation
700 of the Earth driven by the rapid unloading. Some ambiguity in determining the source of
701 meltwater arises because of uncertainty in both the original glacial isostatic adjustment
702 correction and in the correction for the poorly known signature of ocean thermal
703 expansion, as well as from the non-uniform distribution of tide gauge sites.

704

705 A different set of geodetic indicators related to the Earth's rotational state also
706 constrains estimates of recent ice-sheet mass changes (Munk, 2002; Mitrovica et al.,
707 2006). The Earth's rotation is affected by any redistribution of mass on or inside the
708 planet. Transfer of mass from the poles to the equator slows the planet's rotation (like a
709 spinning ice skater extending her arms to slow her rotation). Moreover, any transfer of
710 mass that is not symmetric about the poles causes "wobble", or true polar wander (TPW)
711 (that is, the position of the north rotation pole moves relative to the surface of the planet).
712 True polar wander over the last century has been estimated using both astronomical and
713 satellite geodetic data. In contrast, changes in the rotation rate (or, as geodesists say,
714 "length-of-day"), have been determined over the last few decades using satellite
715 measurements, and for the last few millennia using observations of eclipses recorded by
716 ancient cultures. Specifically, the timing of ancient eclipses recorded by these cultures
717 differs from the timing one would expect by simply projecting the Earth-moon-sun
718 system back in time using the modern rotation rate of the Earth; the discrepancy indicates
719 a gradual slowing of the Earth's rotation rate (Munk, 2002). The difference in the
720 rotation-rate history over the last few millennia (after correcting for slowing of the
721 Earth's rotation associated with the "drag" of the tides) versus the last few decades
722 provides a measure of any anomalous recent melting of polar ice reservoirs. (This
723 difference does not uniquely constrain the individual sources of the meltwater because all
724 sources will be about equally efficient, for a given mass loss rate, at driving these
725 changes in rotation.) True polar wander, after correction for glacial isostatic adjustment,
726 serves as an important complement to this rotation-rate analysis because it does provide
727 source information. As an example, melting from the Antarctic, since it is located at the

728 pole, generates very little true polar wander, while melting from the Greenland Ice Sheet,
729 whose center of mass lies about 15 degrees off the Earth's rotation axis, is capable of
730 driving significant true polar wander (Munk, 2002; Mitrovica et al., 2006).

731

732 *7.2.2f Ice cores*

733

734 Ice cores provide information on many climatic variables that affect the ice sheet. Ice
735 cores also provide some insights to the history of the ice-sheet response to changes in
736 those climatic variables.

737

738 Interpretations of temperature history derived from ice cores are especially accurate.
739 Several indicators are used, as described next, including the isotopic ratios of
740 accumulated snow, ice-sheet temperature profiles (using borehole thermometry), and
741 various techniques using gas-isotopic indicators. Agreement among these different
742 indicators increases confidence in the results.

743

744 Looking first at isotopic ratios of the oxygen and hydrogen in accumulated snow (e.g.,
745 Jouzel et al., 1997), the ocean includes both normal and "heavy" water, with roughly one
746 molecule in 500 containing at least one extra neutron in the nucleus of an oxygen or
747 hydrogen atom. Evaporation is less likely, and condensation hence precipitation more
748 likely, for the heavier species. As an air mass carries water evaporated from the ocean
749 inland over an ice sheet, the heavy species preferentially rain or snow out; the colder the
750 air mass, the more vapor is removed, the more depleted of the heavy species is the

751 remaining vapor, and the lighter the isotopic ratios of the next precipitation. Hence, the
752 isotopic composition of precipitation is linked to temperature of the air mass, and over
753 polar ice sheets, the air-mass temperature is typically linked to the surface temperature.
754 Both oxygen- and hydrogen-isotope ratios are studied, and use of both provides
755 information on the source of precipitation, the evolution of air mass isotopic composition
756 as it moves (path effects), and on site temperature as well. For this review, with site
757 temperature most important, one species is sufficient. Results will be discussed here as
758 $\delta^{18}\text{O}$, the difference between the $^{18}\text{O}:^{16}\text{O}$ ratio of a sample and of standard mean ocean
759 water, normalized by the ratio of the standard and expressed not as percent but as per mil
760 (‰) (percent is parts per hundred, and per mil is parts per thousand).

761

762 Although linked to site temperature, $\delta^{18}\text{O}$ can be affected by many factors (Jouzel et
763 al., 1997; Alley and Cuffey, 2001), such as change in the ratio of summertime to
764 wintertime precipitation. Hence, additional means of determining past temperatures are
765 required. One of the most reliable is based on the physical temperature of the ice. Just as
766 a frozen turkey takes a long time in a hot oven to warm in the middle, intermediate depths
767 of the central Greenland Ice Sheet are colder than ice above or below because the center
768 of the ice sheet has not finished warming from the ice-age cold. If ice flow is understood
769 well at a site, the modern profile of the physical temperature of the ice over depth
770 provides a low-time-resolution history of the surface temperature over time. Joint
771 interpretation of the isotopic ratios and temperatures measured in boreholes (Cuffey et al.,
772 1995; Cuffey and Clow, 1997), or independent interpretation of the borehole
773 temperatures and then comparison to the isotopic ratios (Dahl-Jensen et al., 1998),

774 provides information on the history of temperature. Furthermore, the relation between
775 isotopic ratio and temperature (α ‰/°C) becomes a useful paleoclimatic indicator, and
776 changes in this ratio α over time can be used to test hypotheses for the overall changes in
777 seasonality of snowfall and other factors.

778

779 The isotopic composition of gases trapped in bubbles in the ice sheet provides an
780 additional indicator of temperature. Snow turns to ice without melting in central regions
781 of cold ice sheets through solid-state mechanisms that operate more rapidly under higher
782 temperature or higher load. The transformation of snow to ice in an ice sheet usually
783 occurs within the top few tens of meters; the intermediate material during transformation
784 is called firn, and the transformation is complete when bubbles are isolated so that the air
785 spaces are no longer interconnected to the surface. Wind moving over the ice sheet
786 typically mixes gases in the pore spaces of the firn only in the uppermost few meters or
787 less. **Diffusion** mixes the gases deeper than this. Gases are slightly separated by gravity
788 (Sowers et al., 1992), with the air trapped in bubbles slightly isotopically heavier than in
789 the free atmosphere, proportional to the thickness of the air column in which diffusion
790 dominates.

791 If a sudden temperature change occurs at the surface, the temperature change requires
792 typically about 100 years to penetrate to the depth of bubble trapping. However, when a
793 temperature gradient is applied across gases in diffusive equilibrium, the gases are
794 separated by thermal fractionation as well as by gravity, with the heavier gases moved
795 thermally to the colder end (Severinghaus et al., 1998). Equilibrium of gases is obtained
796 in a few years, far faster than the time for heat flow to remove the temperature gradient

797 across the firn. Within a few years after an abrupt temperature change at the surface,
798 newly forming bubbles will begin to trap air with very slight (but easily measured)
799 anomalies in gas-isotopic compositions, and this trapping of slightly anomalous air will
800 continue over a century or so. Because the relative sensitivities to temperature gradients
801 and gravity are different for different gases, measuring isotopic ratios of multiple gases
802 (such as argon and nitrogen) allows unique determination of the temperature difference
803 that existed across the firn at the time of bubble trapping, and of the thickness of firn in
804 which wind was not mixing the gas (Severinghaus et al., 1998). If the surface
805 temperature change was fast, the magnitude of the temperature difference across the firn
806 will peak at the magnitude of the surface-temperature change; if slow, the temperature
807 difference across the firn will always be less than the total temperature change at the
808 surface. If the climate was relatively steady before an abrupt temperature change, such
809 that the firn depth-density profile came into balance with the temperature and
810 accumulation rate, and if the accumulation rate is known independently (see below), the
811 number of years or amount of ice between the gas-phase and ice-phase indications of the
812 abrupt change provides information on the mean temperature before the abrupt change
813 (Severinghaus et al., 1998). With so many independent thermometers, highly confident
814 paleothermometry is possible.

815

816 Reconstructions of past accumulation rates are most readily obtained from measuring
817 annual-layer thickness in ice cores corrected for ice-flow thinning (e.g., Alley et al.,
818 1993), but indications of thickness of firn (old snow during transition to ice) from gas-
819 isotopic fractionation measurements or from bubble number-density measurements

820 (Spencer et al., 2006) can be combined with temperature estimates to constrain
821 accumulation rates as well. Aerosols (very small liquid and solid particles) of all types
822 fall with snow and are incorporated into the ice sheet; with knowledge of the
823 accumulation rate (hence dilution of the aerosols), time histories of atmospheric loadings
824 can be estimated (e.g., Alley et al., 1995a). Dust and volcanic fallout (e.g., Zielinski et
825 al., 1994) help constrain the cooling effects of aerosols (particles) blocking the sun.
826 Cosmogenic isotopes (beryllium-10 is most commonly measured) reflect cosmic-ray
827 bombardment of the atmosphere, which is modulated by the strength of the Earth's
828 magnetic field and by solar activity (e.g., Finkel and Nishiizumi, 1997). The observed
829 correlation in paleoclimatic records between climatic indicators and indicators of solar
830 activity (Stuiver et al., 1997; Muscheler et al., 2005; Bard and Frank, 2006), and the lack
831 of correlation with indicators of magnetic-field strength (Finkel and Nishiizumi, 1997;
832 Muscheler et al., 2005), help in understanding the climate changes.

833

834 Ages in ice cores are estimated by counting of annual layers (e.g., Alley et al., 1993;
835 Andersen et al., 2006), and by correlation to other records (Blunier and Brook, 2001).
836 Matching multiple indicators of atmospheric composition from Greenland ice cores to
837 longer similar records from Antarctica (Suwa et al., 2006) has allowed demonstration that
838 old ice exists in central Greenland (Suwa et al., 2006; Chappellaz et al., 1997) at depths
839 where flow processes have mixed the layers (Alley et al., 1997). In regions of continuous
840 and unmixed layers, other features in ice cores, such as the chemically “fingerprinted”
841 ash from particular volcanic eruptions, can be correlated to independently dated records

842 (e.g., Finkel and Nishiizumi, 1997; Zielinski et al. 1994). Flow models also can be used
843 to aid in dating.

844

845 Past ice-sheet elevation is indicated by the total gas content of the ice (Raynaud et al.,
846 1997) at a given depth and age. As noted above in this section, bubbles are pinched off
847 from interconnected air spaces in the firn (pore close-off) a few tens of meters down.
848 The density of the ice at this pore close-off is nearly constant, with a fairly well-known
849 and small correction for climatic conditions. Because air pressure varies with elevation,
850 which varies with ice thickness, the total number of trapped molecules of gas per unit
851 volume of ice is correlated to ice-sheet thickness. Detection of small elevation changes is
852 not possible because of additional fluctuations in total gas content likely linked to the
853 effects on bubble-trapping of changing layering in the firn, but elevation changes of >500
854 m are detectable with confidence (Raynaud et al., 1997).

855

856 Additional information on ice-sheet changes comes from the current distribution of
857 isochronous (equal-age) surfaces in the ice sheet. An explosive volcanic eruption
858 deposits an acidic layer of a single age on the surface of the ice sheet, and that layer can
859 be identified after burial using radar (Whillans, 1976). Ages of reflectors can be
860 determined at ice-core sites (e.g., Eisen et al., 2004), and the layers can then be mapped
861 over broad areas (Jacobel and Welch, 2005). Any hypothesis for the combined history of
862 climatic forcing (primarily accumulation rate affecting burial, and temperature) and ice-
863 sheet flow (including changes in surface elevation and extent) can be converted using a
864 model into a prediction of the current distribution of isochronous surfaces (e.g., Clarke et

865 al., 2005), as well as some other properties such as temperature in the ice. Optimal
866 histories can be estimated in this way.

867

868

869 **7.3 History of the Greenland Ice Sheet**

870

871 **7.3.1 Ice-Sheet Onset and Early Fluctuations**

872

873 Prior to 65 Ma (million years ago), dinosaurs lived on a high-CO₂, warm world that at
874 least usually was lacking permanent ice at sea level, and with indications of high-latitude
875 warmth (such as crocodylians along near-polar coastlines, suggesting coldest-month
876 temperatures above 5°C and mean annual temperatures above 14°C; Markwick, 1998).
877 Sluijs et al. (2006) showed ocean-surface warming near the North Pole from ~18°C to
878 peak temperatures of 23°C during the short-lived Paleocene-Eocene Thermal Maximum
879 about 55 Ma. Such temperatures preclude existence of permanent ice near sea level, and
880 indeed, no evidence of such ice is found (Moran et al., 2006).

881

882 Cooling following the Paleocene-Eocene Thermal Maximum may have allowed ice to
883 reach sea level fairly quickly; sand and coarser materials found in a core from the Arctic
884 Ocean sea floor dated as old as ~46 Ma (Moran et al. 2006; St. John, 2008) is most easily
885 interpreted as indicating ice rafting linked to glaciers, although one cannot absolutely rule
886 out other explanations. Ice-rafted debris (IRD) likely traceable at least in part to glaciers
887 rather than sea ice is found in a core from ~75°N latitude in the Norwegian-Greenland

888 Sea off east Greenland between about 38 and 30 Ma (late Eocene into the Oligocene).
889 Fingerprinting of the characteristics of the material in this debris points to east Greenland
890 as the source and excludes Svalbard, the next-nearest land mass (Eldrett et al., 2007). No
891 information is available on whether this represents isolated mountain glaciers or more-
892 extensive ice-sheet cover.

893

894 The central Arctic Ocean sediment core of Moran et al. (2006) shows a highly
895 condensed record that is difficult to read, suggesting erosion or little deposition, across
896 this interval of ice rafting off Greenland studied by Eldrett et al. (2007) and until ~16 Ma.
897 Ice-rafted debris, interpreted as representing iceberg as well as sea-ice transport, was
898 actively delivered to the open-ocean site of Moran et al. (2006) at 16 Ma, and increased at
899 ~14 Ma and again at ~3.2 Ma (also see Shackleton et al., 1984; Thiede et al., 1998;
900 Kleiven et al., 2002). St. John and Krissek (2002) suggested onset of sea-level glaciation
901 in southeastern Greenland at about 7.3 Ma, based on occurrence of ice-rafted debris near
902 Greenland in the Irminger Basin. Based on its observed geographical pattern, the
903 increase in ice-rafted debris at ~3.2 Ma is interpreted as involving ice on Greenland,
904 Scandinavia, and the North American landmass (Laurentide ice sheet). However,
905 fingerprinting of the debris to particular source rocks (e.g., Hemming et al., 2002) is in
906 general not available. There is also no direct evidence that would reveal whether this
907 debris was supplied to the ocean by an extensive ice sheet or by vigorous glaciers
908 draining coastal mountains, with ice absent from the central lowlands of Greenland.
909 Despite the lack of conclusive evidence, the available data seem to indicate at least some
910 glaciation on Greenland since at least 38 Ma, with more evidence of glaciation since

911 approximately 14 Ma (mid-Miocene). Initiation of Greenland glaciation thus occurred in
912 concert with the cooling from the “hothouse” conditions at the time of the dinosaurs to
913 the more-recent cooler conditions.

914

915 Following the establishment of ice in Greenland, a notable warm time about 2.4 Ma is
916 recorded by the Kap København Formation of North Greenland. This formation is a 100-
917 m thick unit of sand, silt and clay deposited primarily in shallow marine conditions.
918 Fossils in the deposit record a warming trend, with biota switching from arctic to
919 subarctic to boreal assemblages during the depositional interval. The unit was deposited
920 rapidly, perhaps in 20,000 years or less. Funder et al. (2001) interpreted the available data
921 as indicating complete deglaciation of Greenland at this time, primarily based on the
922 great summertime warmth indicated at this far-northern site, although there clearly is not
923 a comprehensive record of the whole ice sheet.

924

925

926 **7.3.2 The Most Recent Million Years**

927

928 The combination of fragmented records on land, and lack of unequivocal indicators in
929 the ocean, complicates ice-sheet reconstructions. Nonetheless, many additional
930 indications of ice-sheet change are available between the time of the Kap København
931 Formation and the last 100,000 years, with continuing indications of ice expansion during
932 colder times and ice retreat during warmer times, but with no comprehensive overviews
933 of the ice sheet.

934

935 Detailed studies of glacial-interglacial cycles have been made over the past few
936 decades by examining the oxygen isotope composition of foraminifera in deep-sea cores.
937 Results of these studies have given a fairly detailed picture of how glacial ice has grown
938 and retreated over the past 2 million years or so (the Quaternary period). In **Figure 7.4**,
939 the four most recent glacial-interglacial cycles are shown, with peaks indicating
940 interglacial periods (relatively high sea levels) and troughs indicating glacial periods
941 (relatively low sea levels). Glacial periods in the oxygen isotope record are called
942 “stages,” and numbered back in time with even numbers; interglacial stages are given odd
943 numbers. Thus, the present interglacial is Marine Isotope Stage (MIS) 1 and the
944 preceding glacial period is MIS 2.

945

946

947 ***7.3.2a Far-field sea-level indications***

948

949 In the absence of clear and well-dated records proximal to the Greenland Ice Sheet,
950 indications of global sea level that may be related to Greenland changes are of interest.
951 The most likely times that sea level would have been as high as or higher than present in
952 the past several glacial cycles are during previous interglacial times (MIS 5, 7, 9, and 11;
953 **Figure 7.4**). Under the assumption that any glacial-isostatic-adjustment contributions to
954 these relative highstands of sea level were small and thus that highstands of sea level are
955 primarily related to changes in ice volume, the amplitudes of the various highstands of

956 sea level provide a measure of the long-term mass balance of the Greenland Ice Sheet
957 together with other ice masses.

958

959 There are scattered localities far from the Greenland Ice Sheet where fragmentary and
960 poorly dated deposits indicate a possible higher-than-present sea-level stand during MIS
961 11, about 400 ka. Sea-level history of MIS 11 [~362 to 420 ka] is of particular interest to
962 paleoclimatologists because the Earth-sun orbital geometry during that interglacial period
963 was similar to the configuration during the current interglacial. (Berger and Loutre,
964 1991).

965

966 Hearty et al. (1999) proposed that marine deposits found in a cave on the tectonically
967 stable island of Bermuda date to the MIS 11 interglacial period. These marine deposits
968 are ~21 m above modern sea level, and contain coral pebbles that were dated by U-series
969 techniques. Hearty et al. (1999) interpreted the deposits to date to ~400 ka, although the
970 coral pebbles were dated older than 500 ka. Their interpretation is based primarily on an
971 overlying deposit that dates to ~400 ka. Although the deposit appears to record an old
972 sea stand significantly higher than present, the chronology is still uncertain, but additional
973 study might narrow that uncertainty.

974

975 A marine deposit, representing what has been called the “Anvilian marine
976 transgression”, occurs extensively along the Seward Peninsula and Arctic Ocean coast of
977 Alaska. This part of Alaska is tectonically stable. It is landward of Pelukian (MIS 5,
978 [~74–130 ka]) marine deposits and is found at altitudes of up to 22 m (Kaufman et al.,

979 1991), similar to that of the cave deposit on Bermuda. Amino-acid ratios in mollusks
980 presented by Kaufman and Brigham-Grette (1993) show that the Anvilian deposit is
981 easily distinguishable from last-interglacial (locally called Pelukian) deposits, but it is
982 younger than deposits thought to be of Pliocene age [$\sim 1.8\text{--}5.3$ Ma]. Kaufman et al.
983 (1991) reported that basaltic lava overlies deposits of the Nome River glaciation, which
984 in turn overlie Anvilian marine deposits. An average of several analyses on the lava
985 yields an age of 470 ± 190 ka. Within the broad limits permitted by this age, and using
986 reasonable rates of changes in the amino-acid ratios of marine mollusks, Kaufman et al.
987 (1991) proposed that the Anvilian marine transgression dates to ~ 400 ka, and correlates
988 with MIS 11.

989

990 Other far-field evidence supports the concept that MIS 11 had a sea level higher than
991 present. Oxygen-isotope and faunal data from the Cariaco Basin off Venezuela provide
992 independent evidence of a higher-than-present sea level during MIS 11 (Poore and
993 Dowsett, 2001). If the Bermudan cave deposits and the Anvilian marine deposits of
994 Alaska prove to be genuine manifestations of a ~ 400 ka-old high sea stand, the
995 implication for climate history is that all of the Greenland Ice Sheet (Willerslev et al.,
996 2007; see section 7.3.2b, below), all of the West Antarctic ice sheet, and part of the East
997 Antarctic ice sheet would have disappeared at this time (these being generally accepted as
998 the most vulnerable ice masses); preservation of the Greenland Ice Sheet would require
999 much more loss from the East Antarctic ice sheet, which is widely considered to be
1000 relatively stable (e.g., Huybrechts and de Wolde, 1999).

1001

1002 Until recently, there were no reliably dated emergent marine deposits from MIS 9
1003 [~303–331 ka] found on tectonically stable coasts, although coral reefs of this age have
1004 been recognized for some time on the tectonically rising island of Barbados (Bender et
1005 al., 1979). Stirling et al. (2001) reported that well-preserved fringing reefs are found on
1006 Henderson Island, in the southeastern Pacific Ocean. They found reef elevations on this
1007 tectonically stable island as high as ~29 m above sea level, and U-series dating indicates
1008 ages between ~334±4 and 293±5 ka, correlative with MIS 9. Despite the good
1009 preservation of the corals and the reefs they are found in, and the reliable U-series ages,
1010 there are uncertainties about how high sea level was at this time. Although Henderson
1011 Island is geologically stable, it is experiencing slow uplift of <0.1 m/1,000 yr, due to
1012 volcanic loading by the emplacement of nearby Pitcairn Island. Using a maximum uplift-
1013 rate-correction, therefore, could put the MIS 9 ancient level estimate below present sea
1014 level. Multer et al. (2002) reported U-series ages of ~370 ka for a coral (*Montastrea*
1015 *annularis*) from a fossil reef drilled at a locality called Pleasant Point in Florida Bay.
1016 This coral showed clear evidence of open-system conditions (i.e., it was not completely
1017 chemically isolated from its surroundings since formation, a requirement for the
1018 measured age to be accurate), and the age is probably closer to 300-340 ka, using the
1019 correction scheme of Gallup et al. (1994). If so, the age suggests that sea level was close
1020 to present during MIS 9, but perhaps not significantly above present.

1021

1022 As with MIS 9, there are several MIS 7 [~190–241 ka] reef or terrace records on
1023 tectonically rising coasts (Bender et al., 1979; Gallup et al., 1994; Edwards et al., 1997),
1024 but far fewer on tectonically relatively stable coasts. However, two recent reports show

1025 evidence of MIS 7 sea-level high stands on tectonically stable islands. One is a pair of U-
1026 series ages of ~200 ka from coral-bearing marine deposits ~2 meters above sea level on
1027 Bermuda (Muhs et al., 2002). The other is a single coral age from the Florida Keys,
1028 reported by Muhs et al. (2004). They collected samples of near-surface *Montastrea*
1029 *annularis* corals in quarry spoil piles on Long Key. Analysis of a single sample shows an
1030 apparent age of 235±4 ka. The higher-than-modern initial $^{234}\text{U}/^{238}\text{U}$ value indicates a
1031 probable bias to an older age by ~7 ka; thus, the true age may be closer to ~220-230 ka,
1032 using the Gallup et al. (1994) correction scheme. If valid, these data suggest that sea
1033 level may have stood close to its present level during the interglacial period MIS 7.
1034 Much more study is needed to confirm these preliminary ages, however.

1035

1036 Taken together, these data point to MIS 1 as a time that likely had sea level notably
1037 higher than present, although the data are sufficiently sparse that stronger conclusions are
1038 not warranted. If so, involvement of Greenland seems likely, based mostly on a process
1039 of elimination (Greenland is believed capable of supplying much of the sea-level rise
1040 needed to explain the observations, and the alternative—extracting an additional 7 m of
1041 sea-level rise from East Antarctica—is not considered as likely). Stages 9 and 7 seem to
1042 have had sea levels similar to modern.

1043

1044

1045 **7.3.2b Ice-sheet indications**

1046

1047 The cold MIS 6 ice age [~ 130 – 188 ka]) may have produced the most extensive ice in
1048 Greenland (Wilken and Meinert, 2006). Recently described glacial deposits in East
1049 Greenland support this view (Adriellsson and Alexanderson 2005), although at least
1050 locally-more-extensive, older deposits are known (Funder et al., 2004). Funder et al.
1051 (1998) reconstructed thick ice (>1000 m) during MIS 6 in areas of Jameson Land (east
1052 Greenland) that now are ice-free. However, no confident ice-sheet-wide reconstructions
1053 based on paleoclimatic data are available for the MIS 6 ice.

1054

1055 Both northwest and east Greenland preserve widespread marine deposits from early in
1056 the MIS 5 interglacial [~ 74 – 130 ka], and particularly from the warmest subdivision of
1057 MIS 5, called MIS 5e [~ 123 ka]. Depression of the land from the weight of the MIS 6 ice
1058 allowed marine incursion as the ice melted during the transition to MIS 5e. The resulting
1059 deposits were not reworked by the subsequent marine incursion during the transition from
1060 the most recent glaciation (MIS 2, [peaking at ~ 12 – 24 ka]) to the modern interglacial
1061 (MIS 1, [<11 ka]). Thus, a greater marine incursion occurred during the transition from
1062 MIS 6 to MIS 5 than during the transition from MIS 2 to MIS 1.

1063

1064 Several hypotheses can explain this difference. Perhaps most simply, there may have
1065 been more ice on Greenland causing greater isostatic depression during MIS 6 than
1066 during MIS 2. However, if some or all of the older deposits survived being overridden by
1067 cold-based ice of MIS 2, additional possibilities exist. Because isostatic uplift occurs
1068 while ice is thinning but before the ice pulls back to allow marine incursion, perhaps the
1069 MIS 6 ice melted faster to allow marine incursion over more-depressed land than for the

1070 MIS 2 ice. Additionally, at the time the ice in Greenland pulled back to allow marine
1071 incursion, global sea level might have been higher for MIS 6 than for MIS 2 because of
1072 relatively earlier melting of MIS 6 ice on North America or elsewhere beyond Greenland.
1073 More-detailed glacial isostatic adjustment modeling will be required to test these
1074 hypotheses. Nonetheless, more-extensive ice in MIS 6 than in MIS 2 seems to be the
1075 leading hypothesis.

1076

1077 A particularly interesting new result comes from analysis of materials found in ice
1078 cores from the deepest part of the ice sheet. Willerslev et al. (2007) attempted to amplify
1079 DNA from silty-ice samples at the base of the Greenland Ice Sheet from the Dye 3 drill
1080 site (on the southern dome of the ice sheet) and the GRIP drill site (at the crest of the
1081 main dome of the ice sheet), from “clean” ice just above the silty ice of these sites, and
1082 from the Kap København formation. The Kap København, clean-ice, and GRIP silty
1083 samples did not yield identifiable quantities of DNA (probably indicating post-
1084 depositional changes for Kap København perhaps during room-temperature storage
1085 following collection, and showing that long-distance transport is not important for
1086 supplying large quantities of DNA to the ice of the central part of the sheet). However, it
1087 was possible to prepare extensive materials from the Dye 3 silty ice. These materials
1088 indicate a northern boreal forest, compared to the tundra environment that exists in
1089 coastal sites at the same latitude and lower elevation today. The taxa indicate mean July
1090 temperatures then above 10°C, and minimum winter temperatures above -17°C, at an
1091 elevation of about 1 km above sea level (allowing for isostatic rebound following ice
1092 melting). Dating is problematic, but suggests an age of 450 to 800 ka for occurrence of

1093 this warm, reduced-ice time. Considering the uncertainties, this is probably consistent
1094 with the indications of high sea level in MIS 11.

1095

1096 Possibly relevant is the report (presented at a scientific meeting and in an abstract, but
1097 not in a refereed scientific paper, and thus subject to lower confidence than for other
1098 evidence discussed in this report) from Nishiizumi et al. (1996) of radioactive
1099 cosmogenic isotopes in the rock core collected from beneath the ice at the GISP2 site,
1100 central Greenland, 28 km west of the GRIP site at the Greenland summit. Joint analysis
1101 of beryllium-10 and aluminum-26 indicated a few-millennia-long interval of exposure to
1102 cosmic rays (hence ice cover of thickness less than 1 m or so) $\sim 500 \pm 200$ ka. This
1103 information is consistent with, and thus provides further support for, the DNA results of
1104 Willerslev et al. (2007).

1105

1106 No long, continuous climate records from Greenland itself are available for the time
1107 interval indicated by Willerslev et al. (2007) for existence of the boreal forest at Dye 3.
1108 Marine-sediment records from around the north Atlantic point toward MIS 11, at about
1109 440 ka, as the most likely time of anomalous warmth. Owing to the orbital forcing
1110 factors (reviewed in Droxler et al., 2003), this interglacial seems to have been
1111 anomalously long compared to those before and after. As discussed above, indications of
1112 sea level above modern level exist for this time (Kindler and Hearty, 2000), but much
1113 uncertainty remains (see Rohling et al., 1998; Droxler et al., 2003). The sea-surface-
1114 temperature records of the north Atlantic indicate that MIS 11 temperatures were similar
1115 to those from the current interglacial/Holocene within 1-2°C, with slightly cooler, similar,

1116 or slightly warmer conditions reported (e.g., Bauch et al., 2000; de Abreu et al. 2005;
1117 Helmke et al., 2003; McManus et al., 1999, Kandiano and Bauch, 2003). The longer of
1118 these records show no other anomalously warm times within the age interval most
1119 consistent with the Willerslev et al. (2007) dating. (Notice, however, that local indicators
1120 in Greenland from MIS 5e show more warmth than seen in the far-field sea-surface
1121 temperatures, so the lack of strong warmth far from the ice sheet does not guarantee lack
1122 of strong warming close to the ice sheet; see 7.3.3, below.) The independent indications
1123 of high global sea level during MIS 11, as discussed above in section 7.3.2a, and of major
1124 Greenland Ice Sheet shrinkage or loss at that time, are mutually consistent.

1125

1126 Because the Greenland Ice Sheet is believed to be capable of completing most of its
1127 response to a step forcing in climate within a few millennia (e.g., Alley and Whillans,
1128 1984; Cuffey and Clow, 1997), any of the interglacials over the last 420,000 years was
1129 long enough for the ice sheet to have completed most of its response to the end-of-the-
1130 ice-age forcings , although ongoing but smaller forcings during the interglacials may
1131 have caused the ice sheet to fail to reach a completely steady state. Thus, it is not
1132 obvious how a longer-yet-not-warmer interglacial, as suggested from MIS 11 indications
1133 in the north Atlantic away from Greenland, would have caused notable or even complete
1134 loss of the Greenland Ice Sheet, although this cannot be ruled out completely. Many
1135 possible interpretations remain (greater Greenland warming in MIS 11 than indicated by
1136 marine records from well beyond the ice sheet, large age error in the Willerslev et al.,
1137 2007 estimates, great warmth at Dye 3 yet persistence of a reduced Greenland Ice Sheet
1138 nearby, and others), but a possible interpretation is that the threshold for notable

1139 shrinkage or loss of Greenland ice is just 1-2°C above the level reached during MIS 5e,
1140 thus falling within the error bounds of the available data.

1141

1142 The data strongly indicate that Greenland's ice was notably reduced, or lost, sometime
1143 after ice coverage became extensive and large ice ages began, while temperatures
1144 surrounding Greenland were not grossly higher than they have been recently. The rate of
1145 mass loss within the warm period is unconstrained; the long interglacial at MIS 11 allows
1146 the possibility of very slow loss or much faster loss. If the cosmogenic isotopes in the
1147 GISP2 rock core are interpreted at face value, then the time over which ice was absent
1148 was only a few millennia.

1149

1150

1151 **7.3.3 Marine Isotope Stage 5e**

1152

1153 ***7.3.3a Far-field sea-level indications***

1154

1155 Sea level during the last interglacial, MIS 5 [~71–122 ka] and specifically MIS 5e
1156 [~123 ka] , has received the most attention by investigators studying sea-level history.
1157 Muhs (2002) reviewed the evidence of past sea level during MIS 5e from tectonically
1158 stable coasts, summarized here. The best estimates for the magnitude of the sea-level
1159 high stand during MIS 5e are from coral reef and marine deposits now standing above sea
1160 level in Australia, the Bahamas, Bermuda, and the Florida Keys.

1161

1162 On the coast and islands of tectonically stable Western Australia, emergent coral reefs
1163 and marine deposits now standing 2 – 4 m above sea level are widespread and well-
1164 preserved. U-series ages of the fossil corals range from 128 ± 1 to 116 ± 1 ka from
1165 mainland localities and Rottneest Island (Stirling et al., 1995, 1998). Stirling et al. (1995,
1166 1998) emphasized that the main period of last-interglacial coral growth was a restricted
1167 interval from ~ 128 to 121 ka. Because the highest corals are ~ 4 m above sea level at
1168 present but grew at some unknown depth below sea level, this figure is a minimum for
1169 the amount of last-interglacial sea-level rise, depending on the typical water depths for
1170 the dated species of corals.

1171

1172 The islands of the Bahamas are tectonically stable, although there may be a slow,
1173 long-term subsidence due to continued carbonate loading on the Bahamian platform.
1174 Fossil reefs in the Bahamas are well preserved (Chen et al., 1991). Reefs have elevations
1175 up to 5 m above sea level, and many corals are in growth position. On San Salvador
1176 Island, ages range from 130.3 ± 1.3 to 119.9 ± 1.4 ka. The sea level record of the Bahamas
1177 is particularly valuable, because many reefs contain the coral *Acropora palmata*, a
1178 species that almost always lives within the upper 5 m of the water column (Goreau,
1179 1959). Thus, fossil reefs containing this species place a fairly precise constraint on the
1180 former water depth.

1181

1182 As discussed above (section 7.3.2a), Bermuda is tectonically stable. Bermuda does
1183 not host MIS 5e fossil reefs, but does have numerous coral-bearing marine deposits that
1184 fringe the island. Muhs et al. (2002) reported a number of U-series ages of corals from

1185 Bermuda that range from ~119 to ~113 ka. The deposits are found 2–3 m above present
1186 sea level, although overlying wind-blown sand prevents precise estimates of where the
1187 former shoreline lay.

1188

1189 The Florida Keys, not far from the Bahamas, are also tectonically stable. Fruijtier et
1190 al. (2000) reported ages for corals from Windley Key, Upper Matecumbe Key and Key
1191 Largo that, when corrected for high initial $^{234}\text{U}/^{238}\text{U}$ values (Gallup et al., 1994), range
1192 from about ~130 to 121 ka. The last-interglacial, MIS 5 reef at Windley Key is 3–5 m
1193 above present sea level, on Grassy Key it is 1–2 m above sea level, and on Key Largo it
1194 is 3–4 m above modern sea level.

1195

1196 The collective evidence from Australia, Bermuda, the Bahamas, and the Florida Keys
1197 shows that sea level was above its present stand during MIS 5e. Based on measurements
1198 of the reefs themselves, sea level was at least 4–5 m higher than present. An additional
1199 correction should be applied for the water depth at which the various coral species grew.
1200 Most coral species found in Bermuda, the Bahamas, and the Florida Keys require water
1201 depths of at least a few meters for optimal growth, and many live at tens of meters depth.
1202 For example, *Montastrea annularis*, the most common coral found in MIS 5e reefs of the
1203 Florida Keys, has an optimum growth depth of 3–45 m and can live as deep as 80 m
1204 (Goreau, 1959). Thus, with fossil reefs 3 m above sea level at present, and using the
1205 most conservative growth-depth of 3 m, a minimum paleo-sea level 6 m higher than
1206 modern-day sea level is indicated (**Figures 7.5, 7.6**). A summary of additional sites led
1207 Overpeck et al. (2006) to indicate a sea-level rise of 4 to more than 6 m during MIS 5e.

1208

1209 Existing estimates generally presume that glacial isostatic adjustment effects have not
1210 notably affected the sites over the key times. The data set, and the accuracy of the dating
1211 (also see Thompson and Goldstein, 2005) are becoming sufficient to support improved
1212 glacial isostatic adjustment corrections in future work. The implications of a 4 to >6 m
1213 sea-level high-stand during the last interglacial are that: (1) all or most of the Greenland
1214 Ice Sheet would have been gone; or (2) all or most of the West Antarctic ice sheet would
1215 have been gone; or (3) some combination of parts of both would have disappeared. As
1216 pointed out by Overpeck et al. (2006), both ice sheets may indeed have been involved,
1217 but with greater confidence that Greenland was involved, as described in section 7.3.3c,
1218 below.

1219

1220

1221 ***7.3.3b Conditions in Greenland***

1222

1223 Paleoclimate data provide strong evidence for notable warmth on and around
1224 Greenland during MIS 5e, with peak temperatures occurring ~130 ka. As summarized by
1225 CAPE (2006), terrestrial data indicate peak temperatures ~4°C above recent in NW
1226 Greenland and ~5°C above recent in east Greenland (and thus 2–4°C above the mid-
1227 Holocene warmth [~6 ka]; Funder et al., 1998, and see below), with near-shore marine
1228 conditions 2–3°C above recent in east Greenland. Climate-model simulations by Otto-
1229 Bliesner et al. (2006) show that the strong summertime increase of sunshine (insolation)
1230 in MIS 5e as compared to now caused strong warming which was amplified by ice-

1231 albedo and other feedbacks. Simulated warming around Greenland exhibited local
1232 maxima of 4-5°C in those northwestern and eastern coastal regions for which terrestrial
1233 and shallow-marine data are available and show matching warmings; elsewhere over
1234 Greenland and surroundings, typical warmings of ~3°C were simulated.

1235

1236 The sea-level record in east Greenland (Scoresby Sund) indicates a two-step
1237 inundation at the start of MIS 5e. Of the possible interpretations, Funder et al. (1998)
1238 favored one in which early deglaciation of the coastal region of Greenland preceded
1239 much of the melting of non-Greenland land ice, so that early coastal flooding after
1240 deglaciation of isostatically depressed land was followed by uplift and then by flooding
1241 attributable to sea-level rise as that far-field land-ice melted. Additional testing of this
1242 idea would be very interesting, as it suggests that rapid Greenland Ice Sheet response to
1243 climate forcing has happened in the past.

1244

1245 Much of the evidence of climate change in Greenland comes from ice-core records.
1246 As discussed next, these changes cannot be estimated independent of a discussion of the
1247 ice sheet, because of the possibility of thickness change. Hence, the changes in the ice
1248 sheet are discussed before additional evidence bearing on forcing as well as response.

1249

1250

1251 ***7.3.3c Ice-sheet changes***

1252

1253 Compared to its modern configuration, the Greenland Ice Sheet in MIS 5e covered a
1254 smaller area. How much smaller is still not known with certainty. The most compelling
1255 evidence is the absence of pre-MIS 5e ice in the ice cores from south, northwest, and east
1256 Greenland (the locations Dye 3, Camp Century, and Renland, respectively); in all of these
1257 cores, the climate record extends through the entire last glacial period and then terminates
1258 at the bed in a layer of ice deposited in a much warmer climate (Koerner, 1989; Koerner
1259 and Fisher, 2002). This ice is most likely MIS 5e ice. Moreover, the composition of this
1260 ice is not an average of glacial and interglacial values, as would be expected if it were a
1261 mixture of ices from earlier cold and warm climates. Instead, the ice composition
1262 exclusively indicates a climate considerably warmer than that of the Holocene during
1263 deposition. (One cannot entirely eliminate the possibility that each core independently
1264 bottomed on a rock that had been transported up from the bed, with older ice beneath the
1265 rock in each case, but this seems highly improbable.)

1266

1267 More precisely, the oxygen isotopic composition of this basal ice layer at Dye 3 is
1268 $\delta^{18}\text{O} = -23\text{‰}$ (per mil, or -2.3%, meaning that it is 2.3% or 23‰ lighter than standard
1269 mean ocean water), compared to an estimated value of -30‰ for modern snowfall in the
1270 source region (up-flow from the site of Dye 3). The basal ice at Camp Century is -25‰,
1271 compared to a modern source region of approximately -31.5‰ (see Table 2 of Koerner,
1272 1989). These ~7‰ changes are much larger than the MIS 5e-to-MIS 1 climatic signal
1273 (about 3.3‰, according to the central Greenland cores; see below in this section). This
1274 means the MIS 5e ice at Dye 3 and Camp Century not only indicates a warmer climate

1275 but also a much reduced source elevation, thus showing that the ice sheet was re-growing
1276 when these MIS 5e ices were deposited.

1277

1278 In combination, these two observations (absence of pre-MIS 5e ice, and anomalously
1279 low-elevation sources for the basal ice) indicate that the Greenland margin had retreated
1280 considerably during MIS 5e. Of greatest importance is that retreat of the margin
1281 northward past Dye 3 implies that the southern dome of the ice sheet was completely
1282 gone, or nearly so.

1283

1284 It is very desirable in this context to understand the genesis of the basal ice layer at
1285 Dye 3 in particular. Unfortunately the picture is cloudy—not unlike the basal ice itself,
1286 which has a small amount of silt and sand particles dispersed through it, giving it an
1287 opaque appearance. This silty basal layer is ~25 m thick (Souchez et al. 1998).
1288 Overlying it is “clean” (not notably silty) ice that appears to be typical for polar ice
1289 sheets, with total gas content and gas composition indicating formation by normal
1290 densification of firn in a cold, dry environment. The oxygen isotope composition of this
1291 clean ice is -30.5‰. The bottom 4 m of the silty ice is radically different; its oxygen
1292 isotope value is -23‰, and its gas composition indicates substantial alteration by water.
1293 The total gas content of this basal silty ice is about half that for normal cold ice formed
1294 from solid-state transformation of firn, the carbon dioxide content is 100 times normal,
1295 and the oxygen/nitrogen ratio is less than 20% that of normal cold ice. This basal silty
1296 layer may be superimposed ice (ice formed by refreezing of meltwater in snow on a
1297 glacier or ice sheet, as Koerner, 1989, suggested for the entire silty layer), or may be non-

1298 glacial snowpack, or it may be a remnant of segregation ice in permafrost (permafrost
1299 often contains relatively “clean” although still impure lenses of ice, called segregation
1300 ice).

1301

1302 In any case, the upper 21 m of the silty ice may be explained as a mixture of these two
1303 end-members (Souchez et al. 1998). Mixing of deforming ice does occur, by small-scale
1304 structural folding (e.g., Alley et al., 1995b), by interactions between rock particles, by
1305 grain-boundary diffusion, and possibly by other processes. Unfortunately, there is no
1306 way to distinguish rigorously how much this ice really is a mixture of these end-member
1307 components and how much of it is warm-climate (presumably MIS 5e) normal ice-sheet
1308 ice. The difficulty is that the bottom layer is not itself well-mixed (the gas composition is
1309 highly variable), so a mixing model for the middle layer has an essentially arbitrary
1310 composition for one end-member. Souchez et al. (1998) used the composition at the top
1311 of the bottom layer for their mixing calculations, but it could just as well be argued that
1312 the composition here is determined by exchange with the overlying layer and is not a
1313 fixed quantity.

1314

1315 As discussed in section 7.3.2b, above, in a recent study, Willerslev et al. (2007)
1316 examined biological molecules in the silty ice from Dye 3, including DNA and amino
1317 acids. They concluded that organic material contained in that Dye 3 ice originated in a
1318 boreal forest environment (remnants of diagnostic plants and insects were identified).
1319 This environment implies a very much warmer climate than at the present margin in
1320 Greenland (e.g., July temperatures at 1 km elevation above 10°C), and hence it also

1321 suggests a great antiquity for this material; there is no evidence that MIS 5e in Greenland
1322 was nearly this warm. Indeed, Willerslev et al. (2007) also inferred the age of the organic
1323 material, and the age of exposure of the rock particles, using several methods. They
1324 concluded that a 450-800 ka age is most likely, although uncertainties in all four of their
1325 dating techniques prevented a definitive statement. This conclusion suggests that the
1326 bottom ice layer (the source of rock material to the overlying mixed layer) is much older
1327 than MIS 5e.

1328

1329 There are two leading interpretations of this evidence. One is that this material
1330 survived the MIS 5e deglaciation by being contained in permafrost. The second is that
1331 the MIS 5e deglaciation did not extend as far north as Dye 3, and that local topography
1332 allowed persistence of the ice through isolation from the large-scale flow. This latter
1333 hypothesis (while apparently favored by Willerslev et al., 2007) does not explain the
1334 several hundred thousand year hiatus within the ice, however, or the purely interglacial
1335 composition of the entire basal ice, both of which favor the permafrost interpretation.
1336 (Both hypotheses can be modified slightly to allow short-distance ice-flow transport to
1337 the Dye 3 site; e.g., Clarke et al., 2005.)

1338

1339 Marginal regions of the Greenland ice sheet are thawed at the bottom and slide over
1340 the materials beneath (e.g., Joughin et al., 2008a), across a thin film of water, or possibly
1341 thicker water or soft sediments. During a time of cooling, sliding allows faster advance
1342 of the ice margin than would occur if the ice were frozen to the bed. Furthermore, the
1343 sliding will bring to a place ice that was deposited elsewhere and at higher elevation;

1344 subsequently, freezing to the bed may occur. As discussed below (section 7.3.5b),
1345 widespread evidence shows a notable advance of the ice-sheet margin over the last few
1346 millennia. Regions near the ice-sheet margin, and icebergs calving from that margin,
1347 now contain ice that was deposited somewhere in the accumulation zone at higher
1348 elevation, and that slid into position (e.g., Petrenko et al., 2006). Were sliding not
1349 present, one might expect that re-glaciation of a site such as Dye 3 would have required
1350 cooling until the site became an accumulation zone, followed by slow buildup of the ice
1351 sheet, with the basal ice

1352

1353 In contrast to all the preceding information from south-, northwest-, and east-
1354 Greenland ice cores, the ice cores from central Greenland (the GISP2 and GRIP cores;
1355 Suwa et al., 2006) and north-central Greenland (the NGRIP core) do contain MIS 5e ice
1356 that is normal cold-environment ice-sheet ice. Unfortunately, none of these cores
1357 contains a complete or continuous MIS 5e chronology; the GISP2 and GRIP cores have
1358 had their layering disrupted by ice-flow processes (Alley et al., 1995b), and the NGRIP
1359 core site has been experiencing basal melting that has removed ice from the early part of
1360 MIS 5e and any older ice (Dahl-Jensen et al., 2003). The central Greenland cores do
1361 reveal two important facts: MIS 5e was warmer than MIS 1 (oxygen isotope ratios were
1362 3.3‰ higher than modern ones), and the elevation in the center of the ice sheet was
1363 similar to that of the modern ice sheet although the ice sheet was probably slightly
1364 thinner in MIS 5e (within a few hundred meters of elevation, based on the total gas
1365 content). Thus, considering also the evidence from the other cores, the climate was warm

1366 enough to shrink the ice sheet substantially at the edges, but it persisted in a narrower,
1367 steeper form.

1368

1369 What climate conditions were responsible for driving the ice sheet into this
1370 configuration? There is no clear answer to this, partly because none of the paleoclimate
1371 proxy information is continuous over time, partly because both precipitation and
1372 temperature changes are important, and partly because there are poorly constrained
1373 factors related to ice flow. Cuffey and Marshall (2000; also see Marshall and Cuffey,
1374 2000) were the first to address this question using the information from the central
1375 Greenland cores as constraints. In particular, Cuffey and Marshall (2000) noted that
1376 oxygen isotope ratios were at least 3.3‰ higher during MIS 5e, and used this to constrain
1377 the climate forcing on an ice sheet model. Because the isotopic composition depends on
1378 ice-sheet surface elevation as well as “climate change” (temperature change at a constant
1379 elevation), these analyses generated both climate histories and ice sheet histories. Results
1380 depended critically on the isotopic sensitivity parameter relating isotopic composition to
1381 temperature, and on parameterizations of mass balance forcings, which have large
1382 uncertainties. Furthermore there was no attempt to model increased flow in response to
1383 changes of calving margins, or increased flow in response to production of surface
1384 meltwater (see Lemke et al., 2007). Thus, the ice sheet model was conservative; a given
1385 climatic temperature change produced a smaller response of the model ice sheet than is
1386 expected in nature.

1387

1388 In the reconstruction favored by Cuffey and Marshall (isotopic sensitivity
1389 $\alpha=0.4\%/^{\circ}\text{C}$), complete melt of the southern dome of Greenland occurred after a sustained
1390 (for at least 2,000 years) climate warming of approximately 7°C relative to present. In a
1391 different scenario (sensitivity $\alpha=0.67\%/^{\circ}\text{C}$), a sustained warming of 3.5°C did not cause
1392 the southern ice sheet margin to retreat past Dye 3. Thus an intermediate scenario
1393 (sustained warming of $5\text{-}6^{\circ}\text{C}$) is required, in this view, to cause the margin to retreat just
1394 to Dye 3. Given the conservative representation of ice dynamics in the model, a smaller
1395 sustained warming would in fact be sufficient to accomplish such a retreat. How much
1396 smaller is not quantified, but the magnitude could be notable; observations have now
1397 shown that outflow of ice can increase by a factor of two in response to modest changes
1398 in air and ocean temperatures at the calving margins (see Lemke et al., 2007).

1399

1400 Mass balance depends on numerous variables that are not modeled, introducing much
1401 uncertainty. Examples of these variables are storm-scale weather controls on the
1402 warmest periods within summers, similar controls on annual snowfall, and enhanced
1403 warming due to exposure of dark ground as the ice sheet retreats. In contrast to the
1404 under-representation of ice dynamics, however, there are no major observations that
1405 show that the models are fundamentally in error with respect to mass-balance forcings. A
1406 hint of a serious error is, however, provided by the record of accumulation rate from
1407 central Greenland. Over the course of the past $\sim 11,000$ years (MIS 1) there is no
1408 consistent correlation between variations of accumulation and temperature, whereas most
1409 models assume snowfall (and hence accumulation) will increase with temperature. This
1410 lack of correlation suggests that models are over-predicting the extent to which increased

1411 snowfall will partly balance increased melt in a warmer climate. If this MIS 1 situation
1412 in central Greenland applied to much of the ice sheet in MIS 5e, then models would
1413 require less warming to match the reconstructed ice-sheet footprint; again, the real ice
1414 sheet appears to be more vulnerable than the model ones. We refer to this observation as
1415 only a “hint” of a problem, however, because snowfall on the center of Greenland may
1416 not be representative of snowfall over the whole ice sheet, for which other climatological
1417 influences come into play.

1418

1419 The climate forcing for the Cuffey and Marshall (2000) ice dynamics model, like that
1420 of most recent models that explore Greenland’s glacial history, is driven by a single
1421 paleoclimate record, the isotopically based surface temperature at the Summit ice core
1422 sites. From this information, temperature and precipitation fields are derived and then
1423 combined to obtain a mass balance forcing over space and time, which is applied to the
1424 entire ice sheet. This approach can be criticized for eliminating all local-scale climate
1425 variability, but there are few observations that would allow such variability to be
1426 adequately specified.

1427

1428 Recent efforts to estimate the minimum MIS 5e ice volume for Greenland have much
1429 in common with the Cuffey and Marshall (2000) approach, but focus on adding
1430 observational constraints that enable the model parameters to be optimized. For example,
1431 the ability to model the movement of materials passively entrained in ice sheets (Clarke
1432 and Marshall, 2002) is a major enhancement, which allows the predicted and observed
1433 isotopic profiles at ice core sites to be compared. With these capabilities, Tarasov and

1434 Peltier (2003) produced new estimates of MIS 5e ice volume that were constrained by the
1435 measured ice-temperature profiles at GRIP and GISP2, and by the $\delta^{18}\text{O}$ profiles at GRIP,
1436 GISP2, and NorthGRIP. Their conservative estimate is that the Greenland Ice Sheet
1437 contributed 2–5.2 m to MIS 5e sea-level rise, but with a more likely range of 2.7–4.5 m—
1438 lower than the 4–5.5 m estimate of Cuffey and Marshall (2000). Recognizing that sites
1439 closer to the ice sheet margins, such as Camp Century and Dye 3, provide a more
1440 stringent constraint on ice extent than do the central Greenland sites, Lhomme et al.
1441 (2005) added a tracer transport capability to the model used by Marshall and Cuffey
1442 (2000) and attempted to optimize the model fit to the isotopic profiles at GRIP, GISP2,
1443 Dye 3 and Camp Century. For now, their estimate of a 3.5–4.5 m maximum MIS 5e sea-
1444 level contribution stands as the best available based on this technique.

1445

1446 The discussion just above rested on interpretation of paleoclimatic data from the
1447 central Greenland ice cores to drive a model to match the inferred ice-sheet “footprint”
1448 (and sometimes other indicators) and thus learn volume changes in relation to
1449 temperature changes. An alternative approach is to use knowledge of known climate
1450 forcings to drive a coupled ocean-atmosphere climate model, test the output of that model
1451 against the available paleoclimatic data from around the ice sheet, and if the model is
1452 successful, use the modeled conditions over the ice sheet to drive an ice-sheet model to
1453 match the reconstructed ice-sheet footprint and learn volume changes in response to
1454 forcing changes. This latter approach avoids the difficulty of inferring the “ α ” parameter
1455 relating isotopic composition of ice to temperature, and of assuming a relation between
1456 temperature and snow accumulation, although this latter approach obviously raises other

1457 issues. The latter approach was conducted by Otto-Bliesner et al. (2006; also see
1458 Overpeck et al., 2006).

1459

1460 The primary forcings of Arctic warmth during MIS 5e are the seasonal and latitudinal
1461 changes in solar insolation at the top of the atmosphere associated with periodic, cyclical
1462 changes in the Earth's orbit. (Berger, 1978). The combined effects of obliquity (the
1463 inclination of the Earth's spin axis to the orbital plane, which peaked at ~130 ka), high
1464 eccentricity (the out-of-roundness of the Earth's elliptical orbit around the sun), and
1465 precession (the timing of closest approach to the sun on the elliptical orbit relative to
1466 hemispheric seasons) produced anomalously high Northern Hemisphere summer
1467 insolation during the first half of this interglacial (~130–123 ka) (Otto-Bliesner et al.,
1468 2006; Overpeck et al., 2006). Atmosphere-Ocean General Circulation Models of the
1469 climate (AOGCMs) have used the MIS 5e seasonal and latitudinal insolation changes to
1470 calculate both the seasonal temperatures and precipitation of the atmosphere, as well as
1471 changes to sea ice and ocean temperatures. These models simulate approximately correct
1472 sensitivity to the MIS 5e orbital forcing, reproducing the proxy-derived summer warmth
1473 for the Arctic of up to 5°C, with this warming largest over northern Greenland, northeast
1474 Canada, and Siberia (CAPE, 2006; Jansen et al., 2007).

1475

1476 In one of the models that has been analyzed extensively, the NCAR CCSM (National
1477 Center for Atmospheric Research Community Climate System Model), loss of snow and
1478 sea ice caused by the orbitally induced warmth of MIS 5e results in positive albedo
1479 feedbacks, reducing reflection of sunlight (Otto-Bliesner et al., 2006). The insolation

1480 anomalies result in increased sea-ice melting early in the northern spring and summer
1481 seasons, with reduced Arctic sea ice extending from April into November. The simulated
1482 reduced summer sea ice allows the North Atlantic to warm, with extensive warming
1483 along coastal regions of the Arctic and the surrounding waters of Greenland. Feedbacks
1484 associated with the reduced sea ice around Greenland and decreased snow depths over
1485 Greenland act to enhance the warming over Greenland during the summer months. In
1486 combination with simulated precipitation rates, which overall were not significantly
1487 different from present, the simulated mass balance of the Greenland Ice Sheet resulting
1488 from the model was negative. Then, as now, melting of the surface of the ice sheet
1489 occurred primarily in the summer, with winter too cold for widespread melting.

1490

1491 Temperatures and precipitation produced by the NCAR CCSM (which has a mid-
1492 range climate sensitivity among comprehensive atmosphere-ocean models; that is, this
1493 model exhibits mid-range warming in response to doubling of CO₂ or other specified
1494 forcing; Kiehl and Gent, 2004) for the time-slice at 130 ka were then used to drive an ice-
1495 flow model (an updated version of that used by Cuffey and Marshall, 2000, and thus also
1496 lacking representations of some physical processes that would accelerate ice-sheet
1497 response and increase sensitivity to climate change) to simulate the likely configuration
1498 of the MIS 5e Greenland Ice Sheet, for comparison to the available paleoclimatic data on
1499 ice-sheet configuration. In this model, the Greenland Ice Sheet proved sensitive to the
1500 warmer summer temperatures when melting is taking place. Increased melting
1501 outweighed the increase in snowfall. Over all but the summit of Greenland and isolated
1502 coastal sites, increased melt rates and the extended ablation season led to a negative

1503 mass-balance in response to the orbitally induced changes in temperature and snowfall.
1504 As the simulated ice sheet retreated over several millennia, the loss of ice mass led to a
1505 surface lowering of the Greenland Ice Sheet, an amplification of the negative mass-
1506 balance, and accelerated retreat. The Greenland Ice Sheet responded to the seasonal
1507 orbital forcings because it is particularly sensitive to warming in summer and autumn,
1508 rather than in winter when temperatures are too cold for melting. The modeled
1509 Greenland Ice Sheet melted due to both the direct effect of warmer atmospheric
1510 temperatures, and indirectly due to the reduction of altitude and size of the Greenland Ice
1511 Sheet.

1512

1513 The simulated MIS 5e Greenland Ice Sheet was a steep-sided ice sheet in central and
1514 northern Greenland (Otto-Bliesner et al., 2006) (**Figure 7.7**). The model did not
1515 incorporate feedbacks associated with the exposure of the bedrock as the ice sheet
1516 retreated, potential meltwater-driven or ice-shelf-driven ice-dynamical processes, or time-
1517 evolving orbital forcing, so the model was probably less sensitive and more slowly
1518 responsive to warming than the real ice sheet, as noted just above. The lateral extent of
1519 the modeled minimal Greenland Ice Sheet was constrained by available ice core data (see
1520 above). If the Greenland Ice Sheet's southern dome did not survive the peak interglacial
1521 warmth, as suggested by those data (Koerner and Fisher, 2002; Lhomme et al., 2005),
1522 then the model suggests that the Greenland Ice Sheet contributed 1.9–3.0 m of sea-level
1523 rise (with another 0.3-0.4 m from ice on Arctic Canada and Iceland) over several
1524 millennia during the last interglacial. The time evolution of the Greenland Ice Sheet
1525 retreat and rate of this sea level rise cannot be constrained by paleoclimatic observational

1526 data or currently available ice-sheet models. Furthermore, because the ice-sheet model
1527 was forced by conditions appropriate for 130 ka rather than being forced by more
1528 realistic, slowly time-varying conditions, the details of the modeled time-evolution of the
1529 Greenland Ice Sheet would not be expected to exactly match reality. Sensitivity studies
1530 with the Greenland Ice Sheet melting occurring at a more rapid rate than suggested by the
1531 ice sheet model indicate that the meltwater added to the North Atlantic was not sufficient
1532 to induce oceanic and other climate changes that would have inhibited meltback of the
1533 Greenland Ice Sheet (Otto-Bliesner et al., 2006).

1534

1535 The atmosphere-ocean modeling driven by known forcings produces reconstructions
1536 that match many data from around Greenland and the Arctic. The earlier work of Cuffey
1537 and Marshall (2000) had found that a very warm and snowy MIS 5e, or a more modest
1538 warming with less increase in snowfall, could be consistent with the data, and the
1539 atmosphere-ocean model favors the more modest temperature change. (The results of the
1540 different approaches, while broadly compatible, are not in detailed agreement, however.)
1541 The Otto-Bliesner et al. (2006) modeling leads to a somewhat smaller sea-level rise from
1542 melting of the Greenland Ice Sheet than does the earlier work of Cuffey and Marshall
1543 (2000). A temperature rise of 3–4°C and a sea-level rise of 3–4 m may be consistent
1544 with the data, with notable uncertainties.

1545

1546 Considering all of the efforts summarized above, as little as 1–2 m or as much as 4–5
1547 m of ice may have been removed from the Greenland Ice Sheet during MIS 5e relative to
1548 today, in response to climatic temperature changes of perhaps 2–7°C, but with at least the

1549 higher numbers for the warming based on estimates that include the feedbacks from
1550 melting of the ice sheet. Central values in the 3–4 m and 3–4°C range may be
1551 appropriate.

1552

1553

1554 **7.3.4 Post-MIS 5e Cooling to the Last Glacial Maximum (LGM, or MIS 2)**

1555

1556 ***7.3.4a Climate forcing***

1557

1558 Both climatic and ice-sheet reconstructions become more confident for times younger
1559 than MIS 5e. The climatic records derived from ice cores are especially good. The
1560 Greenland ice-core records primarily from the GRIP, NGRIP, and GISP2 cores, but also
1561 from Camp Century, Dye 3, and Renland cores, provide what are probably the most
1562 reliable paleoclimatic records of any sites on Earth (e.g., Cuffey et al., 1995; Dahl-Jensen
1563 et al., 1998; Johnsen et al., 2001; Jouzel et al., 1997; Severinghaus et al., 1998).

1564

1565 The paleoclimate information derived from near-field marine records is less robust.
1566 Because of the relatively high rates of sediment accumulation in depositional centers
1567 adjacent to glaciated margins, relatively few cores have been recovered that span all of
1568 the last 130,000 years. In core HU90-013 (**Figure 7.8**) from the Erik Drift (Stoner et al.,
1569 1995), rapid sedimentation has buried the sediments from MIS 5e to about 13 m depth.
1570 At that site, a strong change in $\delta^{18}\text{O}$ of planktonic foraminiferal shells from MIS 5e to 5d
1571 is observed, of close to 1.5‰, consistent with cooling as well as ice growth on land, and

1572 is associated with a rapid increase in magnetic susceptibility that indicates delivery of
1573 glacially derived sediments.

1574

1575 The broad picture, based on ice-core, far-field and near-field marine records, and
1576 more, indicates the following: a general cooling trend from MIS 5e (~123 ka) to MIS 2
1577 (with coldest conditions at ~24 ka; Alley et al., 2002), warming to the mid-Holocene/MIS
1578 1 a few millennia ago, cooling into the Little Ice Age of one to a few centuries ago, and
1579 then a bumpy warming (see section 7.3.5b, below). The cooling trend from MIS 5e
1580 involved temperature minima in MIS 5d, 5b and 4 before reaching the coldest of these
1581 minima in MIS 2, with maxima in MIS 5c, 5a, and 3.

1582

1583 Throughout the cooling from MIS 5e to MIS 2, and the subsequent warming into MIS
1584 1 (the Holocene), shorter-lived “millennial” events occurred. These events involved
1585 abrupt warmings that in central Greenland were often roughly 10°C in a few years to
1586 decades, gradual cooling, more abrupt cooling, slight gradual warming, and then repeat
1587 (**Figure 7.9**). Spacings between the abrupt coolings were often about 1500 years,
1588 although longer intervals are often observed (e.g., Alley et al., 2001; Braun et al., 2005).

1589

1590 Marine sediment cores from around the north Atlantic and beyond show temperature
1591 histories closely tied to those recorded in Greenland (Bond et al., 1993), and indeed, the
1592 Greenland ice cores appear to have recorded quite clearly the template for millennial
1593 climate oscillations around much of the planet (although the far-southern realization of
1594 that template involves a modified seesaw; **Figure 7.9**, and Stocker and Johnsen, 2003).

1595

1596 Closer to the ice sheet, marine cores display strong oscillations that correlate in time
1597 with that template, but with more complexity in the response (Andrews, 2008). **Figure**
1598 **7.10**, panel A shows data from a transect of cores (Andrews, 2008), and compares the
1599 marine near-surface isotopic variations with the $\delta^{18}\text{O}$ data from the Renland ice core, just
1600 inland from Scoresby Sund (Johnsen et al., 1992a; 2001) (**Figure 7.8**). The complexity
1601 observed in this comparison likely arises because of the rich nature of the marine
1602 indicators. As noted in section 7.2.1c, above, the oxygen isotope composition of surface-
1603 dwelling foraminiferal shells becomes lighter when the temperature increases, and also
1604 when meltwater supply is increased to the system (or meltwater removal is reduced). If
1605 cooling is caused by freshwater-induced reduction in deepwater formation, then one may
1606 observe either heavier or lighter isotopic ratios, depending on whether the core is
1607 primarily reflecting the temperature change or the freshwater change. Some of the
1608 signals in **Figure 7.10**, panel A likely involve additional delivery of meltwater (which
1609 could have various sources including melting of icebergs) to the vicinity of the core
1610 during colder times.

1611

1612 The slower tens-of-millennial cycling of the climate records is well explained by
1613 features of Earth's orbit and by associated influences of Earth-system response to the
1614 orbital features (especially changes in atmospheric carbon-dioxide and other greenhouse
1615 gases, ice-albedo feedbacks, and effects of changing dust loading), with strong
1616 modulation by the response of the large ice sheets (e.g., Broecker, 1995). The faster
1617 changes are rather clearly linked to switches in the behavior of the north Atlantic, with

1618 colder intervals during times of more-extensive wintertime sea ice, and with warmth
1619 when such sea ice was reduced (Denton et al., 2005), coupled to changes in deepwater
1620 formation in the north Atlantic and thus to the “**conveyor-belt**” **circulation** (e.g.,
1621 Broecker, 1995; Alley, 2007).

1622

1623 Of particular interest relative to the ice sheets is the observation that iceberg-rafted
1624 debris is much more abundant across the north Atlantic during some of the cold intervals,
1625 called **Heinrich events (Figure 7.9)**. This debris is compositionally largely tied to
1626 sources in Hudson Bay and Hudson Strait at the mouth of Hudson Bay, and thus to the
1627 North American Laurentide Ice Sheet, but additional materials from almost everywhere
1628 around the north Atlantic are observed (Hemming, 2004).

1629

1630

1631 ***7.3.4b Ice-sheet changes***

1632

1633 With certain qualifications, the ice-sheet behavior of the Greenland Ice Sheet during
1634 this interval was closely tied to the climate, expanding with cooling and retreating with
1635 warming. Records are generally inadequate to assess response to millennial changes, and
1636 dating is typically sufficiently uncertain that lead/lag relations cannot be determined with
1637 high confidence, but the colder conditions were accompanied by more-extensive ice.

1638

1639 Furthermore, with some uncertainty, the larger Greenland Ice Sheet footprint during
1640 colder times corresponded to a larger ice volume. This conclusion emerges both from the

1641 limited data on total gas content of ice cores (Raynaud et al., 1997) indicating small
1642 changes in thickness, and from physical understanding of the ice-flow response to
1643 changing temperature, accumulation rate, ice-sheet extent and other changes in the ice.
1644 As described in section 7.1.2, above, ice-sheet marginal retreat tends to thin central
1645 regions whereas marginal advance tends to thicken central regions, and the relative
1646 insensitivity of the ice thickness in central regions to changes in accumulation rate or
1647 other factors means that the marginal changes largely dominate the ice-volume changes.

1648

1649 The best records of ice-sheet response during the cooling into MIS 2 are probably
1650 those from the Scoresby Sund region of east Greenland (Funder et al., 1998). These
1651 records indicate ice advances during the coolings of MIS 5d and 5b that did not fully fill
1652 the Scoresby Sund fjord, retreats during the relatively warmer MIS 5c and 5a (although
1653 5c and 5a were colder than MIS 5e or MIS 1; e.g., Bennike and Bocher, 1994) and then
1654 advance to the mouth of Scoresby Sund, probably during MIS 4, and remaining there into
1655 MIS 2, building the extensive moraine at the mouth of the Sund.

1656

1657 Whether the ice advanced beyond the mouth of the Sund during this interval remains
1658 unclear. Most reconstructions place the ice edge very close to the mouth (e.g.,
1659 Dowdeswell et al., 1994a; Mangerud and Funder, 1994). However, the recent work of
1660 Hakansson et al. (2007) indicates wet-based ice on the south side of the mouth of the
1661 Sund 250 m above modern sea level at the Last Glacial Maximum (MIS 2), almost
1662 certainly requiring ice advance past the mouth. Seismic studies and cores on the
1663 Scoresby Sund trough-mouth fan offshore indicate that debris flows have been deposited

1664 fairly recently on the southern portion of the fan, whereas on the northern portion this
1665 activity pre-dates MIS 5 (O'Cofaigh et al., 2003); it is not clear how such debris flow
1666 activity occurred unless the ice had advanced well onto the shelf (O'Cofaigh et al., 2003).

1667

1668 To the south of Scoresby Sund, at Kangerdlugssuaq, Andrews et al. (1997, 1998a) and
1669 Jennings et al. (2002a) provided evidence of the ice extending to the edge of the
1670 continental shelf from about 31-19 ka. These data, combined with widespread
1671 geomorphic evidence of ice reaching the shelf break around south Greenland, are then the
1672 primary evidence for extensive ice cover of this age in southern Greenland (Funder et al.,
1673 2004; Weidick et al., 2004).

1674

1675 In the Thule region of northwestern Greenland, the available data are consistent both
1676 with the broad climatic picture (the MIS 5e to 2 sequence) and with ice-sheet response as
1677 in Scoresby Sund (advances in colder MIS 5d, 5b, 4 [\sim 59–73 ka] and especially 2,
1678 retreats in warmer 5c and 5a, possibly in MIS 3 [\sim 24–59 ka] , and surely in MIS 1, see
1679 Figure 7.6 for general chronology) (Kelly et al., 1999). However, the dating is really not
1680 secure enough to insist on much beyond the warmth of MIS 5e with retreated ice, the
1681 cold of MIS 2 with notably advanced ice, and the subsequent retreat.

1682

1683 The extent of ice at the glacial maximum also remains in doubt in the northwest of the
1684 Greenland ice sheet. The submarine moraines at the edge of the continental shelf are
1685 poorly dated. Ice from Greenland did merge with that from Ellesmere Island, thus
1686 joining the great Greenland Ice Sheet with the Innuitian sector of the North American

1687 Laurentide ice sheet (England, 1999; Dyke et al., 2002). However, whether ice advanced
1688 to the edge of the continental shelf in widespread regions to the north and south of the
1689 merger zone is poorly constrained (Blake et al., 1996; Kelly et al., 1999). A recent
1690 reconstruction (Funder et al., 2004) favors advance to the shelf edge in the northwest, but
1691 with ice shelves rather than further grounded advance to the north and south of the
1692 merger zone with North American ice. The lack of a high marine limit just south of
1693 Smith Sund in the northwest is prominent in that interpretation—more-extensive ice
1694 would have pushed the land down more and allowed the ocean to advance farther inland
1695 following deglaciation, with subsequent isostatic response raising the marine deposits
1696 higher. But, a trade-off does exist between slow retreat and small retreat in controlling
1697 the marine limit. This trade-off has been explored by some workers (e.g., Huybrechts,
1698 2002; Tarasov and Peltier, 2002), but the relative sea-level data are not as sensitive to the
1699 earlier part (~24 ka) as to the later, and so strong conclusions are not available.

1700

1701 Thus, the broad picture of ice advancing in cooling conditions, and retreating in
1702 warming, is quite clear. Remaining issues include the extent of advance onto the
1703 continental shelf (and if limited, why), and the rates and times of response.

1704

1705 Looking first at extent, the generally accepted picture has been one of expansion to the
1706 edge of the continental shelf in the south, much more limited expansion in the north, with
1707 the switch somewhere between Kangerdlugssuaq and Scoresby Sund on the east coast
1708 (Dowdeswell et al., 1996). On the west coast, the moraines that typically occur 30-50 km
1709 beyond the modern coastline (and more extended along troughs) are usually identified

1710 with MIS 2, and the shelf-edge moraines (often called Hellefisk moraines, and often
1711 roughly twice as far from the modern coastline as the presumably-stage-2 moraines) with
1712 MIS 6, although few solid dates are available (Funder and Larsen, 1989). On the east
1713 coast, the evidence from the mouth of Scoresby Sund and the trough-mouth fan, noted
1714 above in this section, opens the possibility of more-extensive ice there than indicated by
1715 the generally accepted picture, with termination mid-shelf or at the shelf edge possible.
1716 Similarly, the work of Blake et al. (1996) from the far northwest may indicate ice
1717 reaching the shelf edge. The indications from Blake et al. (1996) are geomorphically
1718 consistent with wet-based ice. The increasing realization that cold-based ice is
1719 sometimes extensive yet geomorphically inactive further complicates interpretations.
1720 Strong evidence is not available that would overturn the conventional view of expansion
1721 to the shelf-edge in the south, expansion to merge with North American ice in the
1722 northwest, and expansion onto the continental shelf but not to the shelf-edge elsewhere.
1723 Thus, this is probably the favored interpretation, but additional data would clearly be of
1724 interest.

1725

1726 Glaciological understanding indicates that ice sheets are almost always responsive to
1727 climatic or other environmental forcings (including sufficiently large sea-level change).
1728 The most prominent exception may exist if advance occurs to the edge of the continental
1729 shelf under conditions that would allow further advance were the huge topographic step
1730 in the sea floor not present. (Similar situations of ice being unresponsive to relatively
1731 small climate changes can exist, such as during the advance stage of the tidewater-glacier
1732 cycle [Meier and Post, 1987].) If this assessment is accurate, and if the Greenland Ice

1733 Sheet at the time of the Last Glacial Maximum terminated somewhere on the continental
1734 shelf rather than at the shelf edge around part of the coastline, then glaciological
1735 understanding indicates that the ice sheet should have responded to short-lived climate
1736 changes.

1737

1738 The near-field marine record is consistent with the occurrence of such fluctuations, as
1739 discussed next. However, unambiguous interpretations are not possible owing to the
1740 complexity of the controls on the paleoclimatic indicators.

1741

1742 Marine sediment cores from Baffin Bay, the Erik Drift off southwestern Greenland,
1743 the Irminger and Blosseville Basins (e.g. cores SU90-24 & PS2264, **Figure 7.8**), and
1744 from the Denmark Strait (**Figure 7.8**) have been recovered and extend back through MIS
1745 3 and occasionally into MIS 4. Many cores display large variations in the $\delta^{18}\text{O}$ of near-
1746 surface planktic foraminifera during MIS 3. These variations were initially documented
1747 by Fillon and Duplessy (1980) in cores HU75-041 & -042 from south of Davis Strait
1748 (**Figures 7.8 and 7.10**, panel B), and this documentation preceded the recognition of the
1749 large millennial oscillations (**Dansgaard-Oeschger or D-O events**; Johnsen et al.,
1750 1992b, Dansgaard et al., 1993) in the Greenland ice core records. In addition, Fillon and
1751 Duplessy (1980) also contributed information on the down-core numbers of volcanic-ash
1752 (tephra) shards in these two cores. These authors identified “Ash Zone B” in core HU75-
1753 042, which is correlated with the North Atlantic Ash Zone II with a current best-estimate
1754 age of ~54 ka (**Figure 7.10B**; it is associated with the end of interstadial 15 as identified
1755 by Dansgaard et al., 1993). Subsequent work, especially north and south of Denmark

1756 Strait, has also shown significant oscillations in planktonic foraminiferal $\delta^{18}\text{O}$ (Elliott et
1757 al., 1998; Hagen, 1999; van Kreveld et al., 2000; Hagen and Hald, 2002). As noted in
1758 section 7.3.4a, above, and shown in **Figure 7.10A**, the transect of cores appears to show
1759 both climatic forcing and ice-sheet response in the millennial oscillations, although strong
1760 conclusions are not possible.

1761

1762 Cores from the Scoresby Sund and Kangerdlugssuaq trough mouth fans, two of the
1763 major outlets from the eastern Greenland Ice Sheet, also have distinct layers that are rich
1764 in ice-rafted debris (Stein et al., 1996; Andrews et al., 1998a; Nam and Stein, 1999).
1765 Cores HU93030-007 and MD99-2260 from the Kangerdlugssuaq trough-mouth fan
1766 (Dunhill, 2005) (**Figure 7.8**) consist of alternating layers with more and less ice-rafted
1767 debris, overlying a massive debris flow. Dates above the debris flow are ~35 ka. The
1768 debris-rich layers have radiocarbon dates that indicate they are approximately coeval with
1769 **Heinrich events** 3 and 2. On the Scoresby Sund trough-mouth fan, Stein et al (1996)
1770 also recorded ice-rafted debris -rich intervals that they quantified by counting the number
1771 of clasts > 2mm as observed on x-radiographs. Although these cores are not as well
1772 dated as many from sites south of the Scotland-Greenland Ridge, they do indicate that
1773 such debris was delivered to the fan in pulses that may be approximately coeval with the
1774 | North Atlantic Heinrich events.

1775

1776 Although several papers have invoked the Iceland Ice Sheet as a significant
1777 contributor to North Atlantic sediment archives (Bond and Lotti, 1995; Elliot et al., 1998;
1778 Grousset et al., 2001), Farmer et al (2003) and Andrews (2008) have questioned this

1779 assertion and argued that the eastern Greenland ice sheet has been an ignored source of
1780 ice-rafted debris in the eastern North Atlantic south of the Scotland-Greenland Ridge. In
1781 particular, Andrews (2008) argued that the data from Iceland and Denmark Strait
1782 precluded any Icelandic contribution for Heinrich event 3. As noted by Huddard et al
1783 (2006), the area of the Iceland Ice Sheet during the Last Glacial Maximum was only
1784 200,000 km² with an annual loss of ~600 km³, and only ~150 km³ of this loss was
1785 associated with calving. This is less than one-half the estimated calving rate of the
1786 present day Greenland Ice Sheet (Reeh, 1985).

1787

1788 The marine evidence from the western margin of the GIS for fluctuations of the ice
1789 sheet during MIS 3 is confounded by the fact that: there are no published chronologies
1790 from the trough-mouth fan off Disko Island; and, the stratigraphic record from Baffin
1791 Bay consists of glacially derived sediments from the Greenland Ice Sheet, plus the
1792 Laurentide ice sheet including its Innuitian section (Dyke et al., 2002). Certainly, there is
1793 abundant evidence for major ice-sheet events during MIS 3, as seen in the widespread
1794 occurrence throughout Baffin Bay of layers rich in carbonate clasts transported from
1795 adjacent continental rocks (Aksu, 1985; Andrews et al., 1998b; Parnell et al., 2007)
1796 **(Figure 7.11)**.

1797

1798 Core PS1230 from Fram Strait, which records the export of sediments from ice sheets
1799 around the Arctic Ocean (Darby et al., 2002), shows ice-rafted debris intervals associated
1800 with major contributions from north Greenland at ~32, 23 and 17 ka. These correspond

1801 closely in timing to ice-rafted debris events from the Arctic margins of the Laurentide Ice
1802 Sheet.

1803

1804 The fact that ice-rafted debris is not a direct indicator of ice-sheet behavior presents a
1805 continuing difficulty. Iceberg rafting of debris at an offshore site may increase owing to
1806 several possible factors: faster flow of ice from an adjacent ice sheet; flow of ice
1807 containing more clasts; loss of an ice shelf (most ice shelves experience basal melting,
1808 tending to remove debris in the ice, so ice-shelf loss would allow calving of bergs bearing
1809 more debris); cooling of ocean waters to allow survival of debris in icebergs to reach a
1810 site; loss of extensive coastal sea ice allowing icebergs to reach sites more rapidly (Reeh,
1811 2004); alterations in currents or winds affecting iceberg drift tracks; or other changes.

1812 The very large changes in sediment flux from the North American Laurentide ice sheet
1813 during Heinrich events (Hemming, 2004) are generally interpreted to be true indicators of
1814 ice-dynamical changes (e.g., Alley and MacAyeal, 1994), but even that is debated (e.g.,
1815 Hulbe et al., 2004). Thus, the marine-sediment record is consistent with Greenland
1816 fluctuations in concert with millennial variability during the cooling into MIS 2, and
1817 trained observers have interpreted the records as indicating millennial oscillations of the
1818 Greenland Ice Sheet in concert with climate, but those fluctuations cannot be
1819 demonstrated uniquely.

1820

1821

1822 **7.3.5 Ice-Sheet Retreat from the Last Glacial Maximum (MIS 2)**

1823

1824 **7.3.5a Climatic history and forcing**

1825

1826 As shown in **Figure 7.9** (also see Alley et al., 2002), the coldest conditions recorded in
1827 Greenland ice cores since MIS 6 were reached about 24 ka, which corresponds closely in
1828 time with the minimum in local midsummer sunshine and with Heinrich Event H2. The
1829 suite of sediment cores from Denmark Strait (**Figures 7.8 and 7.10A**) plus data from
1830 other sediment cores (VM28-14 and HU93030-007) indicate that the most extreme values
1831 indicating Last Glacial Maximum in $\delta^{18}\text{O}$ of marine foraminifera occurred ~18–20 ka
1832 (slightly younger than the Last Glacial Maximum values in the ice cores) with values of
1833 4.6‰ indicating cold, salty waters.

1834

1835 The “orbital” warming signal in ice-core records and other climate records is fairly
1836 weak until perhaps 19 ka or so (Alley et al., 2002). The very rapid onset of warmth about
1837 14.7 ka (with the warm interval called the Bølling interstadial) is quite prominent;
1838 however, more than a third of the total deglacial warming was achieved before that
1839 abrupt step, with that pre-14.7 ka orbital warming interrupted by Heinrich event H1.
1840 Following Bølling warmth, general cooling occurred (with two prominent but short-lived
1841 cold events, often called the Older Dryas and the Inter-Allerød cold period), before a
1842 faster cooling into the Younger Dryas about 12.8 ka. Gradual warming then occurred
1843 through the Younger Dryas, followed by a step warming at the end of the Younger Dryas
1844 ~11.5 ka. This was followed by a ramp warming to above recent values by 9 ka or so,
1845 punctuated by the short-lived cold event of the Preboreal Oscillation (PBO) ~11.2-11.4
1846 ka (Bjorck et al., 1997; Geirsdottir et al., 1997; Hald and Hagen, 1998; Fisher et al.,

1847 2002; Andrews and Dunhill, 2004; van der Plicht et al., 2004; Kobashi et al. in press),
1848 and followed by the short-lived cold event about 8.3-8.2 ka (the “8k event”; e.g., Alley
1849 and Agustsdottir, 2005).

1850

1851 The cold times of Heinrich events H2, H1, the Younger Dryas, the 8k event, and
1852 probably the other short-lived cold events including the Preboreal Oscillation are linked
1853 to greatly expanded wintertime sea ice in response to decreases in near-surface salinity
1854 and the strength of the overturning circulation in the north Atlantic (see review by Alley,
1855 2007). The cooling associated with these oceanic changes probably affected summers in
1856 and around Greenland (but see Bjorck et al., 2002 and Jennings et al., 2002a), but
1857 occurred primarily in wintertime (Denton et al., 2005).

1858

1859 Peak MIS 1/Holocene warmth before and after the 8.2-ka event was, for roughly
1860 millennial averages, $\sim 1.3^{\circ}\text{C}$ above late Holocene values in central Greenland, based on
1861 frequency of occurrence of melt layers in the GISP2 ice core (Alley and Anandakrishnan,
1862 1995), with mean-annual changes slightly larger although still smaller than $\sim 2^{\circ}\text{C}$ (and
1863 with correspondingly larger wintertime changes); other indicators are consistent with this
1864 interpretation (Alley et al., 1999). Indicators from around Greenland similarly show mid-
1865 Holocene warmth, although with different sites often showing peak warmth at slightly
1866 different times (Funder and Fredskild, 1989). Peak Holocene warmth was followed by
1867 cooling (with oscillations) into the Little Ice Age. The ice-core data indicate that the
1868 century- to few-century-long anomalous cold of the Little Ice Age was $\sim 1^{\circ}\text{C}$ or slightly
1869 more (Johnsen, 1977; Alley and Koci, 1990; Cuffey et al., 1994).

1870

1871

1872 *7.3.5b Ice-sheet changes*

1873

1874 The Greenland Ice Sheet lost about 40% of its area (Funder et al., 2004) and a notable
1875 fraction of its volume (see below; also Elverhoi et al., 1998) since the peak of the last
1876 glaciation ~24-19 ka, a much less than the loss from the warmer Laurentide and
1877 Fennoscandian ice sheets (essentially complete loss) and much more than for colder
1878 Antarctica.

1879

1880 In general, the timing of the onset of retreat from the Last Glacial Maximum is not
1881 well constrained, with most of the indications now below sea level. Funder et al. (1998)
1882 suggested that the ice was most extended in the Scoresby Sund area from ~24,000 to
1883 ~19,000 ka, based on a comparison of marine and terrestrial data. This interval starts at
1884 the coldest time in Greenland ice cores (which also corresponds to the millennial
1885 Heinrich Event H2) and extends to roughly the time when sea-level rise became notable
1886 as many ice masses around the world retreated (e.g., Peltier and Fairbanks, 2006).

1887

1888 Extensive deglaciation leaving clear records is often more recent. For example, a core
1889 from Hall Basin (core 79, **Figure 7.8**), the northernmost of a series of basins that lie
1890 between northwest Greenland and Ellesmere Island, has a date on hand-picked
1891 foraminifera of ~16.2 ka, implying that the outlet to the Arctic Ocean had retreated by
1892 this time (Mudie et al., 2006). At Sermilik Fjord in southwest Greenland, retreat from the

1893 shelf preceded ~16 ka (Funder, 1989c). The ice was at the modern coastline or back into
1894 the fjords along much of the coast by approximately Younger Dryas time (13-11.5 ka, but
1895 with no implication that this is directly linked to the climatic anomaly of the Younger
1896 Dryas) (Funder, 1989c; Marienfeld, 1992b; Andrews et al., 1996; Jennings et al., 2002b;
1897 Lloyd et al., 2005; Jennings et al., 2006). In the Holocene, the marine evidence of ice-
1898 rafted debris from the east-central Greenland margin (Marienfeld, 1992a; Andrews et al.,
1899 1997; Jennings et al., 2002a; Jennings et al., 2006) shows a tripartite record with early
1900 debris inputs, a middle-Holocene interval with very little such debris, and a late Holocene
1901 (neoglacial) period that spans the last 5-6 ka of steady delivery of such debris (**Figure**
1902 **7.12**).

1903

1904 Along most of the Greenland coast, radiocarbon dates significantly older than the end
1905 of Younger Dryas time are rare, likely because of persistent cover by the Greenland Ice
1906 Sheet. Radiocarbon dates become common near the end of the Younger Dryas and
1907 especially during the Preboreal, and remain common for all younger ages, indicating
1908 deglaciation (Funder, 1989a; b; c). The term “Preboreal” typically refers to the
1909 millennium-long interval following the Younger Dryas; the Preboreal Oscillation (PBO)
1910 is a shorter-lived cold event within this interval, but the terminology has sometimes been
1911 used loosely in the literature. Owing to uncertainty about radiocarbon “reservoir” age of
1912 the waters in which mollusks lived, and other issues, it typically is not possible to assess
1913 whether a given date traces to the Preboreal Oscillation or the longer Preboreal, and often
1914 the uncertainties preclude identification of a particular date with Preboreal versus
1915 Younger Dryas.

1916

1917 Given the prominence of the termination of the Younger Dryas cold event in ice-core
1918 records (temperature increase of $\sim 10^{\circ}\text{C}$ in ~ 10 years; Severinghaus et al., 1998), it may
1919 seem surprising at first that widespread moraines abandoned in response to that warming
1920 have not been identified with confidence. Data-quality issues may figure in this, but it
1921 raises an interesting question. Part of the difficulty is solved by the hypothesis of Denton
1922 et al. (2005), who argued that most of the warming occurred in winter. Bjorck et al.
1923 (2002) and Jennings et al. (2002a) argued for notable summertime warmth in Greenland
1924 during the Younger Dryas, but from Denton et al. (2005) and Lie and Paasche (2006), at
1925 least some warming or lengthening of the melt season probably occurred at the end of the
1926 Younger Dryas. The terminal Younger Dryas warming then would be expected to have
1927 affected glacier and ice-sheet behavior.

1928

1929 All available ice-core records from Greenland show clearly that the temperature drop
1930 into the Younger Dryas was followed by a millennium of slow warming before the rapid
1931 warming at the end (Johnsen et al., 2001; North Greenland Ice Core Project Members,
1932 2004), with the slow warming perhaps reflecting orbitally rising mid-summer insolation
1933 during that time. The Younger Dryas was certainly long enough for coastal mountain
1934 glaciers to reflect both the cooling into the event and the warming during the event before
1935 the terminal step; as discussed in section 7.3.4b, above, and in this section below, the ice-
1936 sheet margin probably would have been influenced by these changes as well. If the
1937 margin did advance with the cooling into the Younger Dryas, and then retreat during the
1938 Younger Dryas and its termination, moraine sets would be expected from near the start of

1939 the Younger Dryas and from the cooling of the Preboreal Oscillation after the Younger
1940 Dryas (perhaps with minor moraines marking small events during the latter-Younger
1941 Dryas retreat). Because so much of the ice-sheet margin was marine at the start of the
1942 Younger Dryas, events of that age would not be recorded well.

1943

1944 Much study has focused on the spectacular late-glacial moraines of the Scoresby Sund
1945 region of east Greenland (Funder et al., 1998; Denton et al., 2005). Funder et al. (1998)
1946 suggested that the last resurgence of glaciers in the region, known as the Milne Land
1947 Stade, was correlated with the PBO, although a YD age for at least some of the moraines,
1948 perhaps with both YD and PBO present, cannot be excluded (Funder et al., 1998; Denton
1949 et al., 2005). Data and modeling remain sufficiently sketchy that strong conclusions do
1950 not seem warranted, but the available results are consistent with rapid response of the ice
1951 to forcing, with warming causing retreat.

1952

1953 Retreat of the ice sheet from the coastline passed the position of the modern ice
1954 margin ~8 ka and continued well inland, perhaps more than 10 km in west Greenland
1955 (Funder, 1989c), up to 20 km in north Greenland (Funder, 1989b), and perhaps as much
1956 as 60 km in parts of south Greenland (Tarasov and Peltier, 2002). Reworked marine
1957 shells and other organic matter of ages 7-3 ka found on the ice surface and in younger
1958 moraines document this (Weidick et al., 1990; Weidick, 1993). For west Greenland, the
1959 general retreat from the coast was interrupted by intervals of moraine formation,
1960 especially at ~9.5-9 ka and 8.3 ka (Funder, 1989c); these moraines are not all of the same
1961 age and are not in general directly traceable to the short-lived 8k cold event ~8.3-8.2 ka

1962 (Long et al., 2006). Timing of the onset of late Holocene readvance is not tightly
1963 constrained. Funder (1989c) suggested ~3 ka for west Greenland, the approximate time
1964 when relative sea-level fall from isostatic rebound of the land switched to begin a relative
1965 sea-level rise of ~5 m, perhaps in part responding to depression of the land by the
1966 advancing ice load. Similar considerations would place the onset of readvance somewhat
1967 earlier in the south, where relative sea-level fall switched to relative rise of ~10 m
1968 beginning ~8-6 ka (Sparrenbom et al., 2006a; 2006b).

1969

1970 The late-Holocene advance culminated in different areas at different times, especially
1971 in the mid-18th century, 1850-1890, and near 1920 (Weidick et al., 2004). Retreat from
1972 this maximum has occurred since.

1973

1974 Indications from relative sea-level changes are consistent with this history (Funder,
1975 1989d; Tarasov and Peltier, 2002; 2003; Fleming and Lambeck, 2004). Flights of raised
1976 beaches or other marine indicators are observed on many coasts of Greenland, reaching
1977 up to 160 m above modern sea level in west Greenland.

1978

1979 Fleming and Lambeck (2004) used an iterative technique to reconstruct the ice-sheet
1980 volume over time to match relative sea-level curves. They obtained an ice-sheet volume
1981 at the time of the Last Glacial Maximum about 42% larger than modern (3.1 m of
1982 additional sea-level equivalent in the ice sheet, compared to the modern value of 7.3 m of
1983 sea-level equivalent; interestingly, Huybrechts (2002) obtained a model-based estimate of
1984 3.1 m of excess ice at the Last Glacial Maximum). Fleming and Lambeck (2004)

1985 estimated that 1.9 m of the 3.1 m of excess ice during the Last Glacial Maximum
1986 persisted at the end of the Younger Dryas. They reconstructed the Last-Glacial-
1987 Maximum ice terminating on the continental shelf in most places, but extending to or
1988 near the shelf edge in parts of southern Greenland, northeast Greenland, and where the
1989 Greenland Ice Sheet coalesced with the Innuitian ice from North America in the far
1990 northwest. Ice thicknesses over much of the modern coastline were more than 500 m,
1991 with more than 1500 m thickness in some places. Mid-Holocene retreat of ~40 km
1992 behind the present margin before late-Holocene advance was also indicated. Rigorous
1993 error limits are not available, and the modeling for the Last Glacial Maximum did not
1994 include the effects of the Holocene retreat behind the modern margin, so additional
1995 uncertainty is introduced.

1996

1997 In the ICE5G model, Peltier (2004) (with a Greenland Ice Sheet history based on
1998 Tarasov and Peltier, 2002) found that the relative sea-level data were inadequate to
1999 constrain Greenland ice-sheet volume accurately. In particular, these constraints provide
2000 only a partial history of the ice-sheet footprint and no information on the small-but-
2001 nonzero changes inland. Thus, Tarasov and Peltier (2002; 2003) and Peltier (2004) chose
2002 to combine ice-sheet and glacial isostatic adjustment modeling with relative-sea-level
2003 observations to derive a model of the ice-sheet geometry extending back to the Eemian
2004 (MIS 5e, ~125–130 ka). The previous ICE4G reconstruction had been characterized by
2005 an excess ice volume during the Last Glacial Maximum, relative to the present, of 6 m;
2006 this volume is reduced to 2.8 m in ICE5G. Later shrinkage of the Greenland Ice Sheet
2007 largely occurred in the last 10 ka in the ICE5G reconstruction, and proceeded to a mid-

2008 Holocene (7-6 ka) volume about 0.5 m less than at present, before regrowth to the
2009 modern volume.

2010

2011 The 20th century included warming from the Little Ice Age to about 1930, sustained
2012 warmth into the 1960s, cooling, and then warming since ~1990 (e.g., Box et al., 2006).
2013 The earlier warming caused strong retreat in many places (e.g., Funder, 1989a; 1989b;
2014 1989c), and widespread retreat and mass loss are now occurring (e.g., Alley et al., 2005).
2015 Study of declassified satellite images shows that at least for Helheim Glacier in the
2016 southeast of Greenland, the ice was in a retreated position in 1965, advanced after that
2017 during a short-lived cooling, and has now switched to retreat (Joughin et al., 2008b). This
2018 latest phase of retreat is consistent with GPS--based inferences of rapid melting from the
2019 southeastern sector of the Greenland Ice Sheet (Khan et al., 2007), as well as GRACE
2020 satellite gravity observations, which indicate a mean mass loss in the period April 2002-
2021 April 2006 equivalent to 0.5 mm/yr of globally uniform sea-level rise (Velicogna and
2022 Wahr, 2006).

2023

2024 As discussed in section 7.2.2e, above, geodetic measurements of perturbations in the
2025 Earth's rotational state can also provide constraints on recent ice mass balance. Munk
2026 (2002) suggested that length-of-day and true polar wander (TPW) data were well fit by a
2027 model of ongoing glacial isostatic adjustment, and that this fit precluded a contribution
2028 from the Greenland Ice Sheet to recent sea-level rise. Mitrovica et al. (2006) reanalyzed
2029 the rotation data, and applied a new theory of glacial isostatic adjustment-induced true
2030 polar wander, and they found that an anomalous 20th-century contribution of up to ~1

2031 mm/yr of sea-level rise is consistent with the data; the partitioning of this value into
2032 signals from melting of mountain glaciers, Antarctic ice and the Greenland Ice Sheet is
2033 non-unique. Interestingly, Mitrovica et al. (2001) applied a fingerprinting analysis to a
2034 set of robust tide-gauge records and found that the geographic trends in the glacial
2035 isostatic adjustment-corrected rates suggested a mean 20th century melting of the
2036 Greenland Ice Sheet equivalent to ~0.4 mm/yr of sea-level rise.

2037

2038

2039 **7.4 Discussion**

2040

2041 Glaciers and ice sheets are highly complex features, controlled by numerous climatic
2042 factors and by internal dynamics. Textbooks have been written on the controls, and no
2043 complete list is possible. Unique attribution of an ice-sheet change to a particular cause
2044 is generally difficult, and requires appropriate modeling and related studies.

2045

2046 It remains, however, that across the whole suite of observations, the behavior of the
2047 Greenland Ice Sheet has been more closely tied to temperature than to anything else.
2048 Greenland Ice Sheet reduction has occurred with warming, and growth with cooling.
2049 Because of the general positive relation between temperature and precipitation (e.g.,
2050 Alley et al., 1993), the ice sheet has tended to grow with reduced precipitation/snowfall
2051 and to shrink when the atmospheric mass supply increased, so precipitation changes
2052 cannot have controlled the ice-sheet behavior, although it remains possible that local or
2053 regional events have reflected precipitation control at certain times.

2054

2055 The hothouse world of the dinosaurs and into the Eocene occurred with no evidence of
2056 ice reaching sea level in Greenland. The long-term cooling that followed is correlated in
2057 time with appearance of ice in Greenland.

2058

2059 Once ice appeared, paleoclimatic archives record fluctuations that closely match not
2060 only local but also widespread records of temperature, because of close correlation
2061 between local and more-widespread temperatures. Because any ice-albedo feedback or
2062 other feedbacks from the Greenland Ice Sheet itself are too weak to have controlled
2063 temperatures far beyond Greenland, the arrow of causation cannot have run primarily
2064 from the ice sheet to the widespread climate.

2065

2066 One must consider the possibility that something has been controlling both the
2067 temperature and the ice sheet, but this appears unlikely. The only physically reasonable
2068 control would be through sea level, with warming causing melting of ice beyond
2069 Greenland, and with the resulting sea-level rise forcing retreat of the Greenland Ice Sheet
2070 by floating marginal regions and speeding iceberg calving and ice-flow spreading.
2071 However, available data point to times when this explanation is not sufficient. There at
2072 least is a suggestion at MIS 6 that Greenland deglaciation led strong global sea-level rise,
2073 as described in section 7.3.2b, above. The growth of ice from MIS 5e to 5d occurred
2074 from a reduced ice sheet, which would have had little contact with the sea. Much of the
2075 retreat from the MIS 2 maximum occurred in a terrestrial setting, although with fjord
2076 glaciers in contact with the sea. The regrowth of ice after the mid-Holocene warmth

2077 occurred against a baseline of very little change in sea level but in general with slight sea-
2078 level rise, opposite to expectations if sea-level control of the ice sheet is important.
2079 Similarly, the advance of Helheim Glacier after the 1960s occurred with a slightly rising
2080 global sea level, and probably a slightly rising local sea level.

2081

2082 There were many other times when the sign of change of ice-sheet size matched that
2083 expected from sea-level control as well as from temperature control, because trends in
2084 temperature and sea level were broadly correlated. Strictly from the available
2085 paleoclimatic record, it is not possible to disentangle the relative effects of sea-level rise
2086 and temperature on the ice sheet at these times. However, it is notable that terminal
2087 positions of the ice are marked by sedimentary deposits; while the erosion of Greenland
2088 is not nearly so fast as in some mountain belts such as coastal Alaska, notable sediment
2089 supply to grounding lines continues. And, as shown by Alley et al. (2007), such
2090 sedimentation tends to stabilize an ice sheet against the effects of relative rise in sea level.
2091 Although a sea-level rise of tens of meters could overcome this stabilizing effect, the ice
2092 would need to be unaffected by other environmental forcings such as changing
2093 temperature for many millennia to allow that much sea-level rise to occur (Alley et al.,
2094 2007). Strong temperature control on the ice sheet is observed for recent events (e.g.,
2095 Zwally et al., 2002; Thomas et al., 2003; Hanna et al., 2005; Box et al., 2006), and is
2096 modeled (e.g., Huybrechts and de Wolde, 1999; Huybrechts, 2002; Toniazzo et al., 2004;
2097 Ridley et al., 2005; Gregory and Huybrechts, 2006).

2098

2099 Thus, it is clear that many of the changes in the ice sheet were forced by temperature.
2100 In general, the ice-sheet response has been inverse to that expected from changes in
2101 precipitation, retreating with increasing precipitation. Events explainable by sea-level
2102 forcing but not by temperature change have not been identified. Sea-level forcing might
2103 yet prove to have been important during cold times of extensively advanced ice; however,
2104 the warm-time evidence of Holocene and MIS 5e changes that cannot be explained by
2105 sea-level forcing indicates that temperature control was dominant.

2106

2107 Temperature change may affect ice sheets in many ways, as discussed in section 7.1.2.
2108 Warming of summertime conditions increases meltwater production and runoff from the
2109 ice-sheet surface, and may increase basal lubrication to speed mass loss by iceberg
2110 calving into adjacent seas. Warmer ocean waters (or more-vigorous circulation of those
2111 waters) can melt the undersides of ice shelves, reducing friction from these and so
2112 increasing flow speed and mass loss by iceberg calving. In general, the paleoclimatic
2113 record is not yet able to separate these influences, motivating the broad use of
2114 “temperature” in discussing ice-sheet forcing. In detail, ocean temperature will not
2115 exactly correlate with atmospheric temperature, so the possibility may exist that
2116 additional studies could quantify the relative importance of changes in ocean and air
2117 temperature.

2118

2119 Most of the forcings of past ice-sheet behavior considered here have been applied
2120 slowly. Orbital changes in sunshine, greenhouse-gas forcing, and sea level have all
2121 varied on 10,000-year timescales. Based purely on paleoclimatic evidence, it is generally

2122 not possible to separate the ice-volume response to incremental forcing from the
2123 continuing response to earlier forcing. In a few cases, sufficiently high time resolution
2124 and sufficiently accurate dating are available to attempt this separation for ice-sheet area.
2125 At least for the most recent events during the last decades of the 20th century and into the
2126 21st century, ice-marginal changes have tracked forcing, with very little lag. The data on
2127 ice-sheet response to earlier rapid forcing, including the Younger Dryas and Preboreal
2128 Oscillation, remain sketchy and preclude strong conclusions, but results are consistent
2129 with rapid temperature-driven response.

2130

2131 A summary of many of the observations is given in **Figure. 7.13**, showing ice-sheet
2132 changes in ice-sheet volume and temperature forcing from an assumed “modern”
2133 equilibrium (before the warming of the last decade or two). Rigorous error bars cannot be
2134 placed with confidence. A discussion of the plotted values and error bars is given in the
2135 caption of **Figure 7.13**. It remains possible that some of the ice-sheet change was caused
2136 directly by temperature and some by sea-level effects correlated with temperature; the
2137 techniques used here do not allow separation of these (nor do modern models allow
2138 complete separation; Alley et al., 2007). However, as discussed above in this section,
2139 temperature likely dominated, especially for warmer times when contact with the sea was
2140 reduced because of ice-sheet retreat. Again, no rates of change are implied. The large
2141 error bars on **Figure. 7.13** remain disturbing, but general covariation of temperature
2142 forcing and sea-level change from Greenland is indicated. The decrease in sensitivity to
2143 temperature with decreasing temperature also is physically reasonable; if the ice sheet

2144 were everywhere cooled to well below the freezing point, then a small warming would
2145 not cause melting, and so the ice sheet would not exhibit any shrinkage with warming.

2146

2147

2148 **7.5 Synopsis**

2149

2150 Paleoclimatic data show that the Greenland Ice Sheet has changed greatly over
2151 time. Physical understanding indicates that many environmental factors can force
2152 changes in ice-sheet size. Comparison of the histories of important forcings and of ice-
2153 sheet size implicates cooling as causing ice-sheet growth, with warming causing
2154 shrinkage and sufficiently large much warming causing loss. The evidence for
2155 temperature control is clearest for temperatures similar to or warmer than those occurring
2156 recently (the last few millennia). The available evidence shows an inverse relation
2157 between snow accumulation rate and ice-sheet volume (less ice when snowfall is higher),
2158 showing that accumulation rate in general is not the leading control on ice-sheet change.
2159 Rising sea level tends to float marginal regions of ice sheets and force retreat, so the
2160 generally positive relation between sea level and temperature means that typically both
2161 have pushed the ice sheet in the same direction. However, for some small changes over
2162 the most recent millennia, marginal fluctuations in the ice sheet have been opposed to
2163 those expected from local relative sea-level forcing but in the direction expected from
2164 temperature forcing. This, plus the tendency for shrinkage to pull ice-sheet margins out
2165 of the ocean, indicate that sea-level change is not the dominant forcing at least for
2166 temperatures similar to or above those of the last few millennia. High-time-resolution

2167 histories of the ice-sheet volume are not available, but the limited paleoclimatic data are
2168 at least consistent that short-term and long-term response to temperature change have the
2169 same sign. The best estimate from paleoclimatic data is thus that warming will cause
2170 shrinkage of the Greenland Ice Sheet, with warming of a few degrees sufficient to cause
2171 ice-sheet loss. Tightly constrained numerical estimates of the threshold warming for ice-
2172 sheet loss are not available, nor are rigorous error bounds, and rate of loss is very poorly
2173 constrained by the available data. Numerous opportunities exist for additional data
2174 collection and analyses that would reduce the uncertainties.
2175

2175 **FIGURE CAPTIONS**

2176

2177 **Figure 7.1.** Satellite image (SeaWiFS) of the Greenland Ice Sheet and surroundings,
2178 from July 15, 2000 (<http://www.gsfc.nasa.gov/gsfcr/earth/pictures/earthpic.htm>).

2179

2180 **Figure 7.2.** Recently published estimates of the mass balance of the Greenland Ice
2181 Sheet through time (modified from Alley et al., 2007). A Total Mass Balance of 0
2182 indicates neither growth nor shrinkage, and -180 Gt yr^{-1} indicates ice-sheet shrinkage
2183 contributing to sea-level rise of 0.5 mm/yr, as indicated. Each box extends from the
2184 beginning to the end of the time interval covered by the estimate, with the upper and
2185 lower lines indicating the uncertainties in the estimates. A given color is associated with a
2186 particular technique, and the different letters identify different studies. Two estimates
2187 have arrows attached, because those authors indicated that the change is probably larger
2188 than shown. The dotted box in the upper right is a frequently-cited study that applies only
2189 to the central part of the ice sheet, which is thickening, and misses the faster thinning in
2190 the margins.

2191

2192 **FIGURE 7.3.** Cross-sections showing idealized geomorphic and stratigraphic
2193 expression of coastal landforms and deposits found on low-wave-energy carbonate coasts
2194 of Florida and the Bahamas (upper) and high-wave-energy rocky coasts of Oregon and
2195 California (lower). Redrawn from Muhs et al. (2004) and references therein. (Vertical
2196 elevations are greatly exaggerated.)

2197

2198 **FIGURE 7.4.** Relations of oxygen isotope records in foraminifera of deep-sea
2199 sediments to emergent reef or wave-cut terraces on an uplifting coastline (upper) and a
2200 tectonically stable or slowly subsiding coastline (lower). Emergent marine deposits
2201 record interglacial periods. Oxygen isotope data shown are from the SPECMAP record
2202 (Imbrie et al., 1984). Redrawn from Muhs et al. (2004).

2203

2204 **FIGURE 7.5.** Photographs of last-interglacial (MIS 5e) reef and corals on Key Largo,
2205 Florida, their elevations, probable water depths, and estimated paleo-sea level.
2206 Photographs by D.R. Muhs.

2207

2208 **FIGURE 7.6.** . Oxygen isotope data from the SPECMAP record (Imbrie et al., 1984),
2209 with indications of sea-level stands for different interglacials, assuming minimal glacial
2210 isostatic adjustments to the observed reef elevations.

2211

2212 **Figure 7.7.** Modeled configuration of the Greenland Ice Sheet today (left) and in MIS
2213 5e (right), from Otto-Bliesner et al. (2006).

2214

2215 **Figure 7.8.** Location map with core locations discussed in the text. Full core identities
2216 are as follows: 79=LSSLL2001-079; 75-41 and -42=HU75-4,-42; 77-017=HU77-017; 76-
2217 033=HU76-033; 90-013=HU90-013; 1230=PS1230; 2264=PS2264; 1225 and
2218 1228=JM96-1225,-1228; 007=HU93-007; 2322=MD99-2322; 90-24=SU90-24.
2219 HS=Hudson Strait, source for major Heinrich events; R = location of the Renland Ice
2220 Cap.

2221

2222 **Figure 7.1** Ice-isotopic records ($\delta^{18}\text{O}$, a proxy for temperature, with less-negative
2223 values indicating warmer conditions) from GISP2, Greenland (Grootes and Stuiver,
2224 1997) (scale on right) and Byrd Station, Antarctica (scale on left), as synchronized by
2225 Blunier and Brook (2001), with various climate-event terminology indicated. Ice age
2226 terms are shown in blue (top); the classical Eemian/Sangamonian is slightly older than
2227 shown here, as is the peak of marine isotope stage (MIS, shown in purple) 5, known as
2228 5e. Referring specifically to the GISP2 curve, the warm Dansgaard-Oeschger events or
2229 stadial events, as numbered by Dansgaard et al. (1993), are indicated in red; Dansgaard-
2230 Oeschger event 24 is older than shown here. Occasional terms (L = Little Ice Age, 8 = 8k
2231 event, P=Preboreal Oscillation (PBO), Y = Younger Dryas, B = Bolling-Allerod, and
2232 LGM = Last Glacial Maximum) are shown in pink. Heinrich events are numbered in
2233 green just below the GISP2 isotopic curve, as placed by Bond et al. (1993). The Antarctic
2234 warm events A1–A7, as identified by Blunier and Brook (2001), are indicated for the
2235 Byrd record. Modified from Alley (2007).

2236

2237 **Figure 7.10.** A) Variations in $\delta^{18}\text{O}$ from a series of cores north to south of Denmark
2238 Strait (see Fig. 7.8), namely: PS2264, JM96-1225 and 1228 plotted against the $\delta^{18}\text{O}$ from
2239 the Renland Ice Cap. B) $\delta^{18}\text{O}$ variations in cores HU75-42 (NW Labrador Sea). C) Stable
2240 oxygen variations in cores HU77-017 from north of Davis Strait.

2241

2242 **Figure 7.11.** Variations in detrital carbonate (pieces of old rock) in core HU76-033
2243 from Baffin Bay (Fig. 7.8) showing down-core variations in magnetic susceptibility and
2244 $\delta^{18}\text{O}$.

2245

2246 **Figure 7.12.** Holocene ice-rafted debris concentrations from MD99-2322 off
2247 Kangerdlugssuaq Fjord, East Greenland (Fig. 7.8) showing log values of the percent of
2248 sediment > 1 mm and the weight % of quartz in the < 2mm sediment fraction.

2249

2250 **Figure 7.13.** A best-guess representation of the dependence of the volume of the
2251 Greenland Ice Sheet on temperature. Large uncertainties should be understood, and any
2252 ice-volume changes in response to sea-level changes correlated with temperature changes
2253 are included (although, as discussed in the text, temperature changes probably dominated
2254 forcing, especially at warmer temperatures when the reduced ice sheet had less contact
2255 with the sea). Recent values of temperature and ice volume (perhaps appropriate for
2256 1960 or so) are assigned 0,0. The Last Glacial Maximum was probably $\sim 6^{\circ}\text{C}$ colder than
2257 modern for global average (e.g., Cuffey and Brook, 2000; data and results summarized in
2258 Jansen et al., 2007). Cooling in central Greenland was $\sim 15^{\circ}\text{C}$ (with peak cooling
2259 somewhat more; Cuffey et al., 1995). Some of the central-Greenland cooling was
2260 probably linked to strengthening of the temperature inversion that lowers near-surface
2261 temperatures relative to the free troposphere (Cuffey et al., 1995). A cooling of $\sim 10^{\circ}\text{C}$ is
2262 thus plotted. The ice-volume-change estimates of Peltier (2004; ICE5G) and Fleming
2263 and Lambeck (2004) are used, with the upper end of the uncertainty taken to be the
2264 ICE4G estimate (see Peltier, 2004), and somewhat arbitrarily set as 1 m on the lower

2265 side. The arrow indicates that the ice sheet in MIS 6 was more likely than not slightly
2266 larger than in MIS 2, and that some (although inconsistent) evidence of slightly colder
2267 temperatures is available (e.g., Bauch et al., 2000). The mid-Holocene result from
2268 ICE5G (Peltier, 2004) of an ice sheet smaller than modern by ~0.5 m of sea-level
2269 equivalent is plotted; the error bars reflect the high confidence that the mid-Holocene ice
2270 sheet was smaller than modern, with similar uncertainty assumed for the other side. Mid-
2271 Holocene temperature is taken from the Alley and Anandakrishnan (1995) summertime
2272 melt-layer history of central Greenland, with their 0.5°C uncertainty on the lower side,
2273 and a wider uncertainty on the upper side to include larger changes from other indicators
2274 (which are probably weighted by wintertime changes that have less effect on ice-sheet
2275 mass balance, and so are not used for the best estimate; Alley et al., 1999). As discussed
2276 in 7.3.3b and c, MIS 5e (the Eemian) is plotted with a warming of 3.5°C and a sea-level
2277 rise of 3.5 m. The uncertainties on sea-level change come from the range of data-
2278 constrained models discussed in 7.3.3c. The temperature uncertainties reflect the results
2279 of Cuffey and Marshall (2000) on the high side, and the lower values simulated over
2280 Greenland by Otto-Bliesner et al. (2006). Loss of the full ice sheet is also plotted, to
2281 reflect the warmer conditions that may date to MIS 11 if not earlier, and perhaps also to
2282 the Pliocene times of the Kap København Formation. Very large warming is indicated by
2283 the paleoclimatic data from Greenland, but much of that warming probably was a
2284 feedback from loss of the ice sheet itself (Otto-Bliesner et al., 2006). Data from around
2285 the North Atlantic for MIS 11 and other interglacials do not show significantly higher
2286 temperatures than during MIS 5e, allowing the possibility that sustaining MIS 5e levels
2287 for a longer time led to loss of the ice sheet. Slight additional warming is indicated here,

2288 within the error bounds of the other records, based on assessment that MIS 5e was
2289 sufficiently long for much of the ice-sheet response to have been completed, so that
2290 additional warmth was required to cause additional retreat. The volume of ice possibly
2291 persisting in highlands even after loss of central regions of the ice sheet is poorly
2292 quantified; 1 m is indicated.
2293

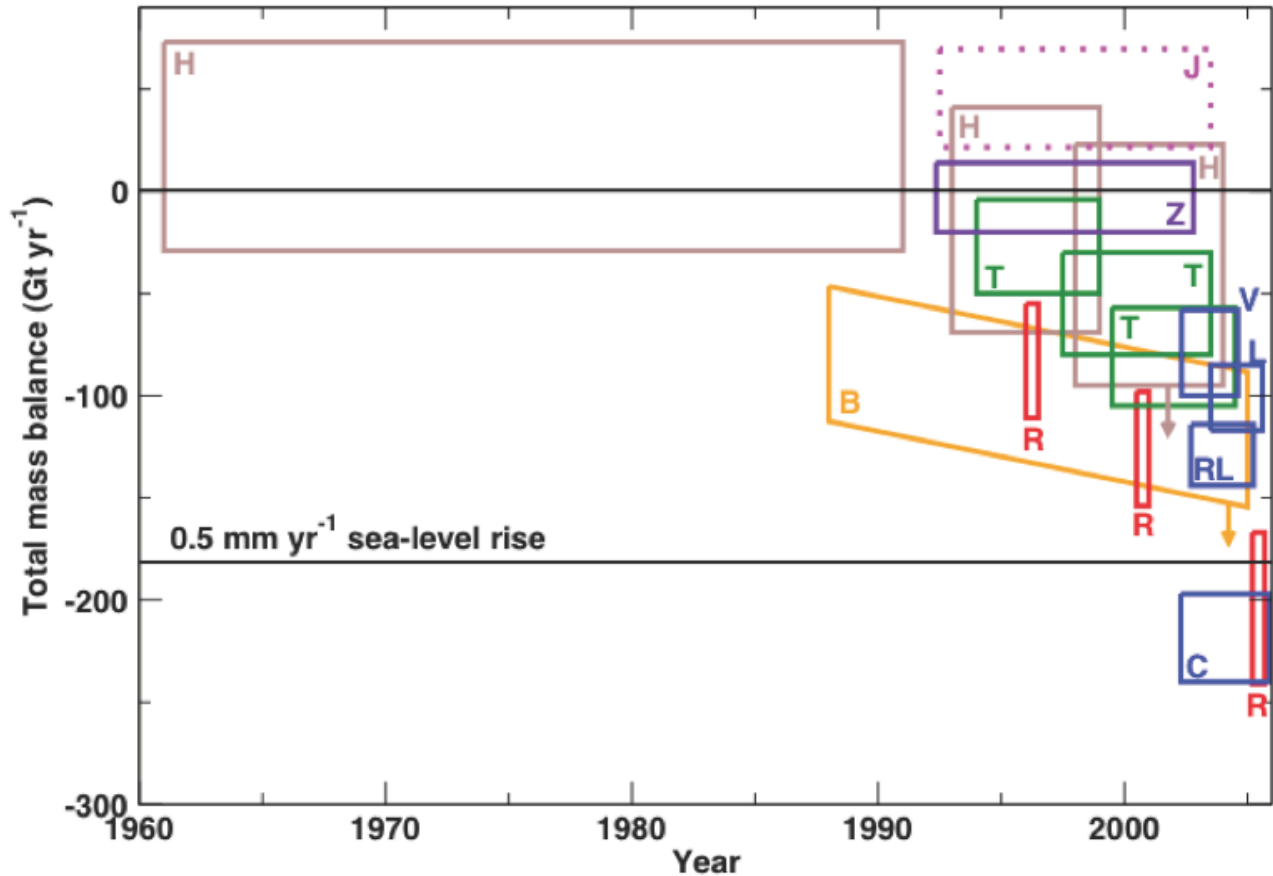
2293



2294

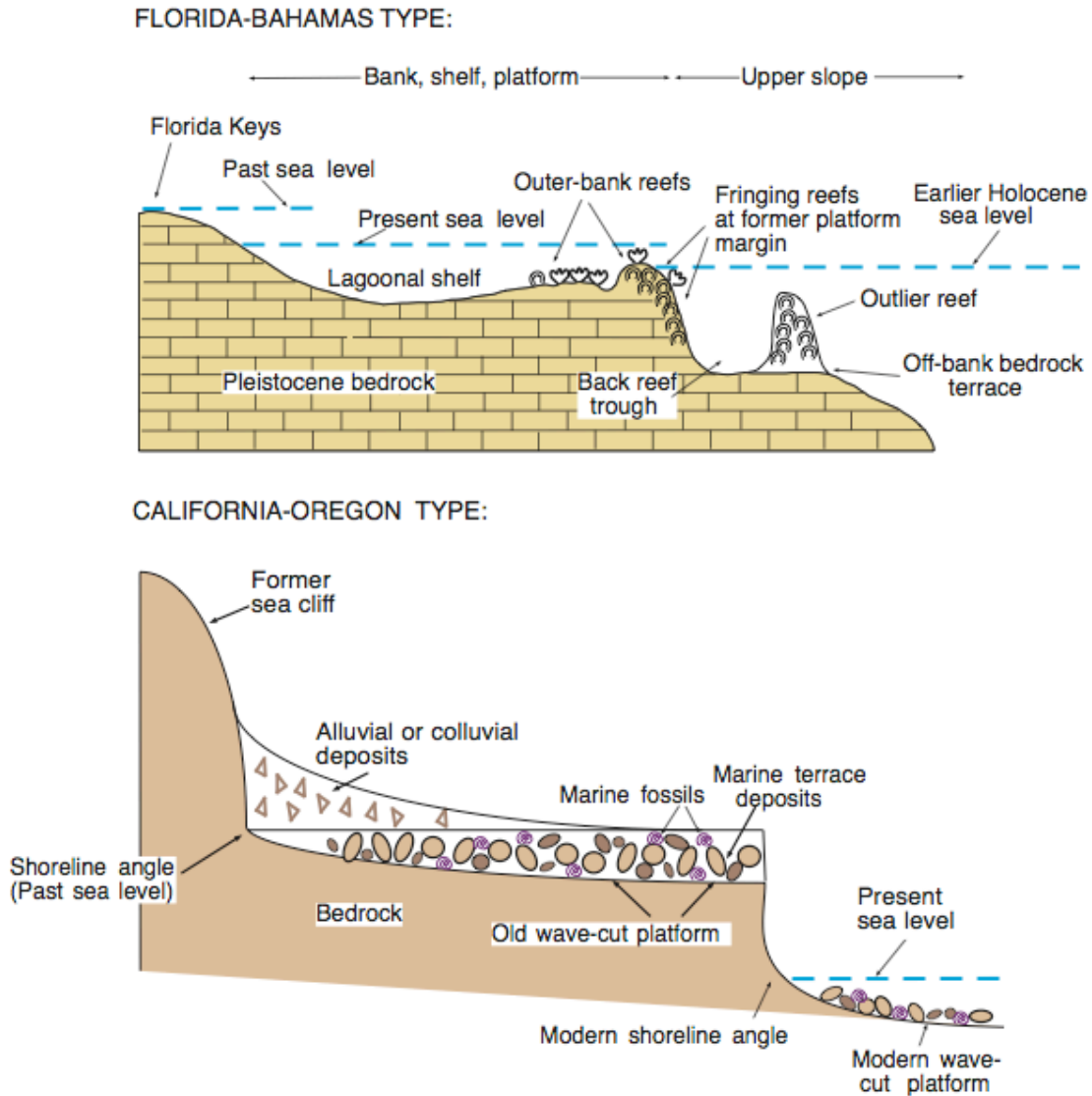
2295 **Figure 7.1** Satellite image (SeaWiFS) of the Greenland Ice Sheet and surroundings,
2296 from July 15, 2000 (<http://www.gsfc.nasa.gov/gsf/earth/pictures/earthpic.htm>).

2297

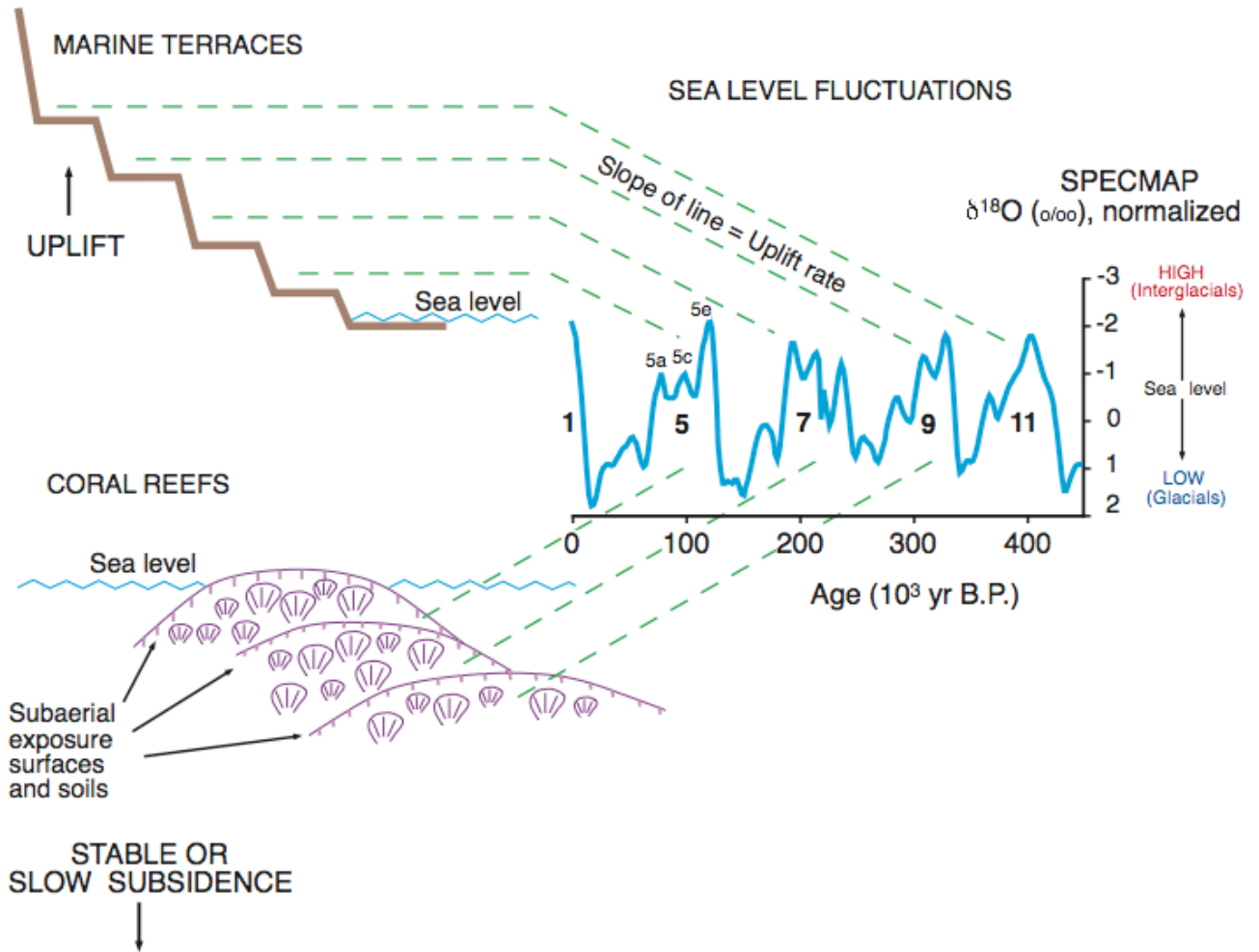


2297

2298 **Figure 7.2** Recently published estimates of the mass balance of the Greenland Ice
2299 **Sheet** through time (modified from Alley et al., 2007). A Total Mass Balance of 0
2300 **indicates** neither growth nor shrinkage, and -180 Gt yr⁻¹ indicates ice-sheet
2301 **shrinkage** contributing to sea-level rise of 0.5 mm/yr, as indicated. Each box extends
2302 **from** the beginning to the end of the time interval covered by the estimate, with the
2303 **upper** and lower lines indicating the uncertainties in the estimates. A given color is
2304 **associated** with a particular technique, and the different letters identify different
2305 **studies**. Two estimates have arrows attached, because those authors indicated that
2306 **the** change is probably larger than shown. The dotted box in the upper right is a
2307 **frequently-cited** study that applies only to the central part of the ice sheet, which is
2308 **thickening**, and misses the faster thinning in the margins.



2309 **Figure 7.3 Cross-sections showing idealized geomorphic and stratigraphic**
2310 **expression of coastal landforms and deposits found on low-wave-energy carbonate**
2311 **coasts of Florida and the Bahamas (upper) and high-wave-energy rocky coasts of**
2312 **Oregon and California (lower). (Vertical elevations are greatly exaggerated.)**
2313



2313

2314 **Figure 7.4 Relations of oxygen isotope records in foraminifera of deep-sea**
2315 **sediments to emergent reef or wave-cut terraces on an uplifting coastline (upper)**
2316 **and a tectonically stable or slowly subsiding coastline (lower). Emergent marine**
2317 **deposits record interglacial periods. Oxygen isotope data shown are from the**
2318 **SPECMAP record (Imbrie et al., 1984). Redrawn from Muhs et al. (2004).**

2319

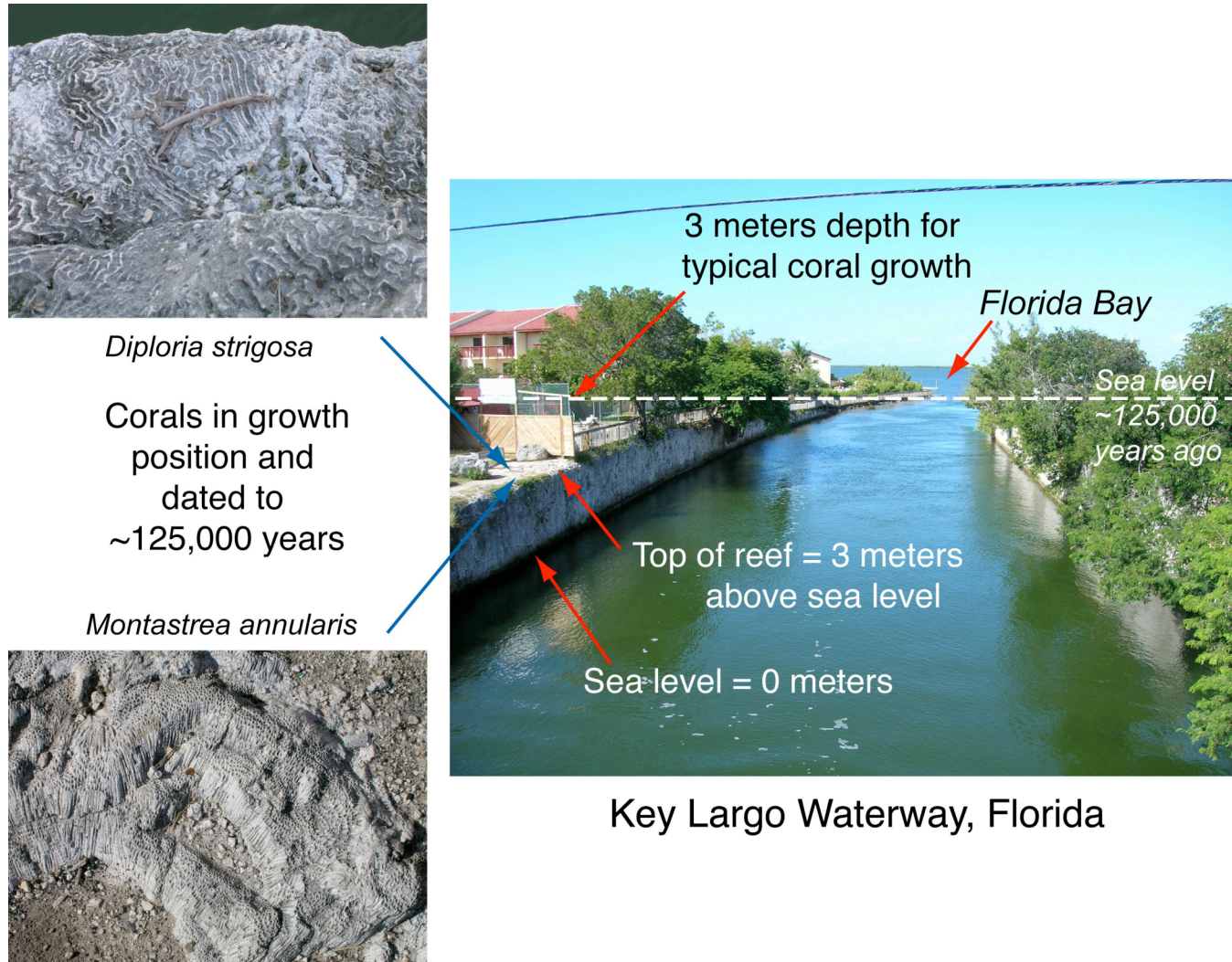


Figure 7.5 Photographs of last-interglacial (MIS 5e) reef and corals on Key Largo, Florida, their elevations, probable water depths, and estimated paleo-sea level. Photographs by D.R. Muhs.

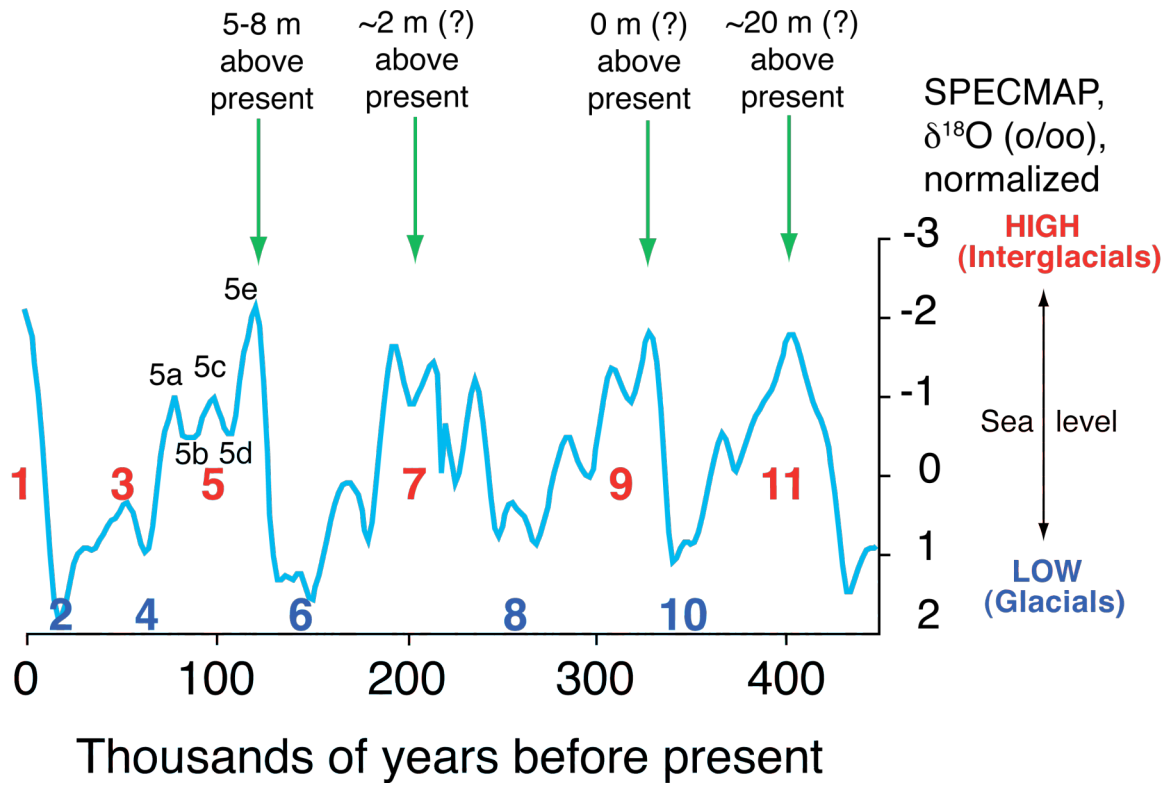


Figure 7.6 Oxygen isotope data from the SPECMAP record (Imbrie et al., 1984), with indications of sea-level stands for different interglacials, assuming minimal glacial isostatic adjustments to the observed reef elevations. Numbers identify Marine Isotope Stages (MIS) 1 through 11.

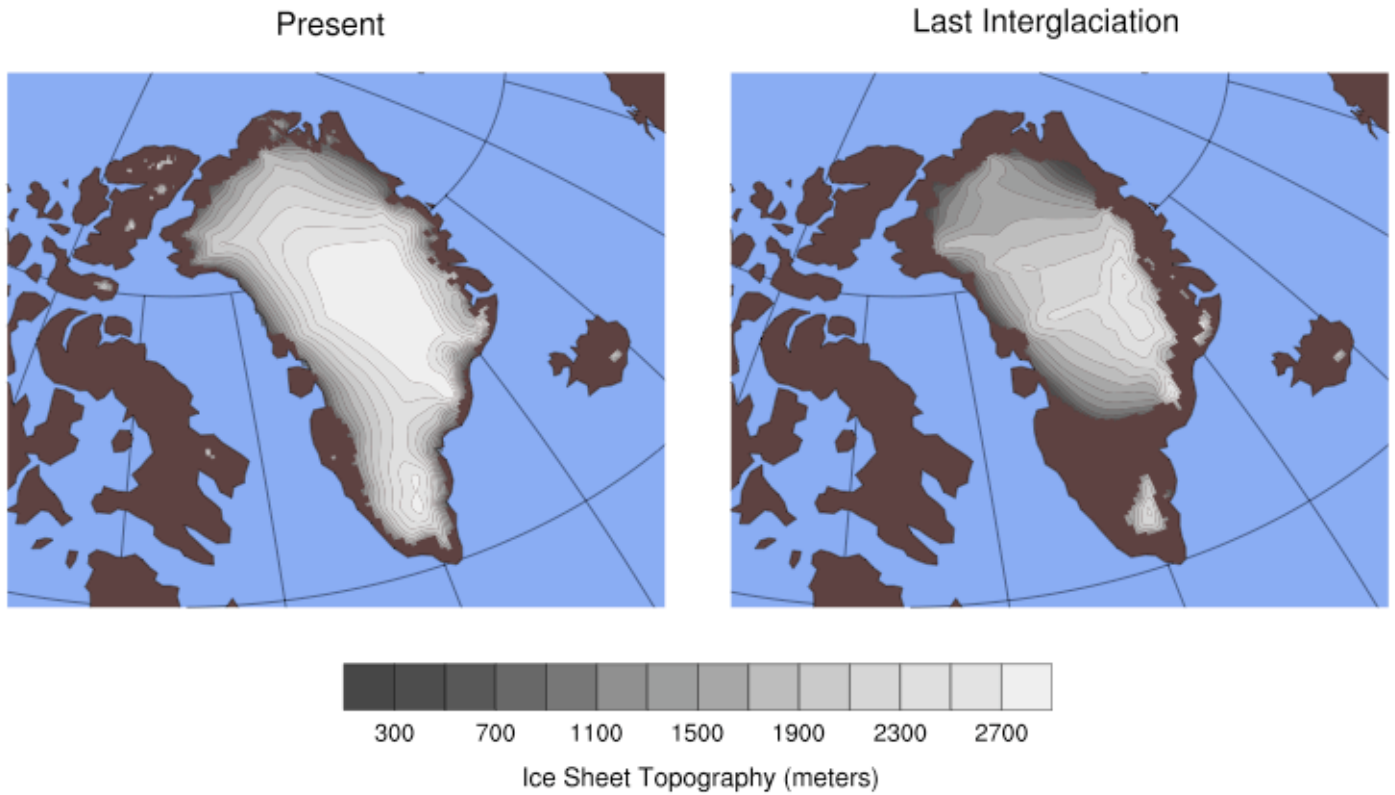


Figure 7.7 Modeled configuration of the Greenland Ice Sheet today (left) and in MIS 5e (right), from Otto-Bliesner et al. (2006).

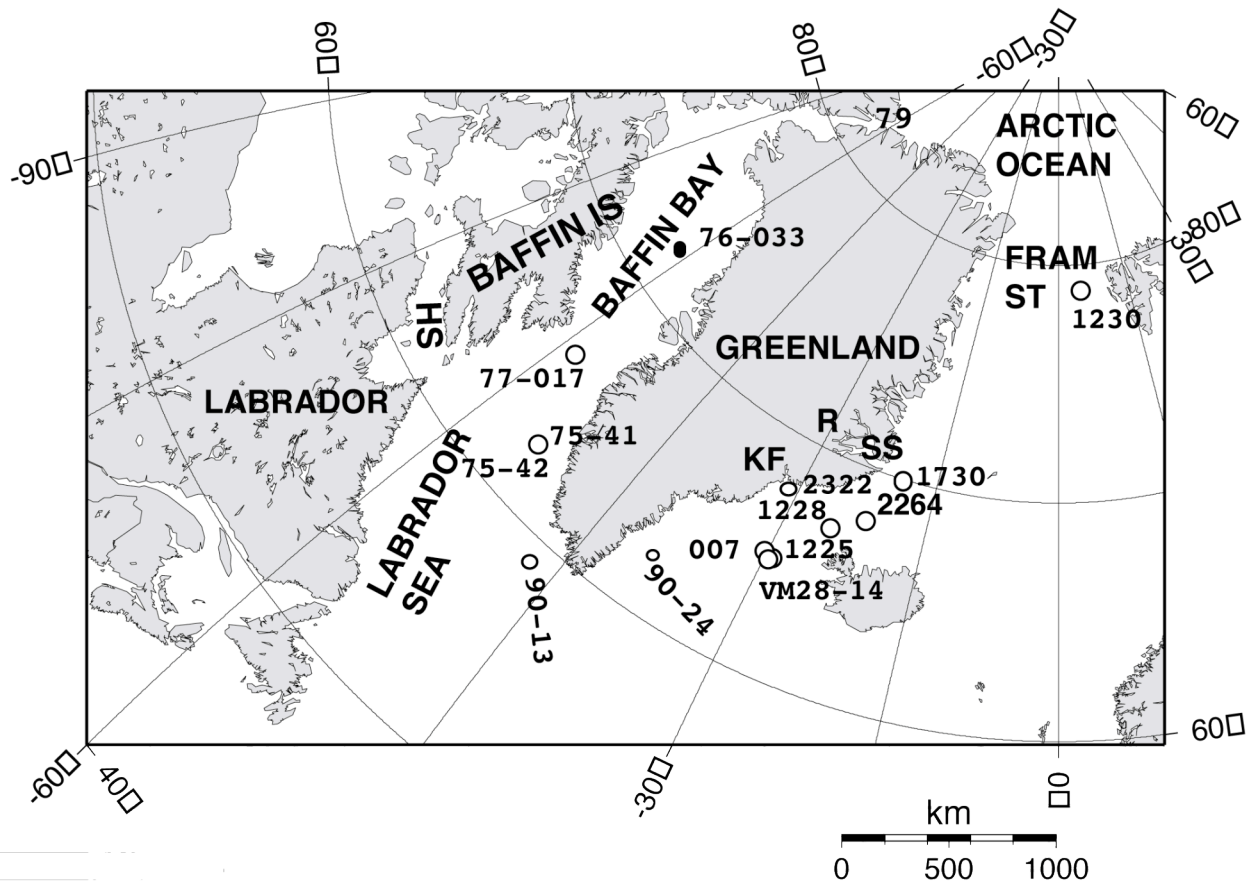


Figure 7.8 Location map with core locations discussed in the text. Full core identities are as follows: 79=LSSLL2001-079; 75-41 and-42=HU75-4,-42; 77-017=HU77-017; 76-033=HU76-033; 90-013=HU90-013; 1230=PS1230; 2264=PS2264; 1225 and 1228=JM96-1225,-1228; 007=HU93-007; 2322= MD99-2322; 90-24=SU90-24. HS=Hudson Strait, source for major Heinrich events; R = location of the Renland Ice Cap.

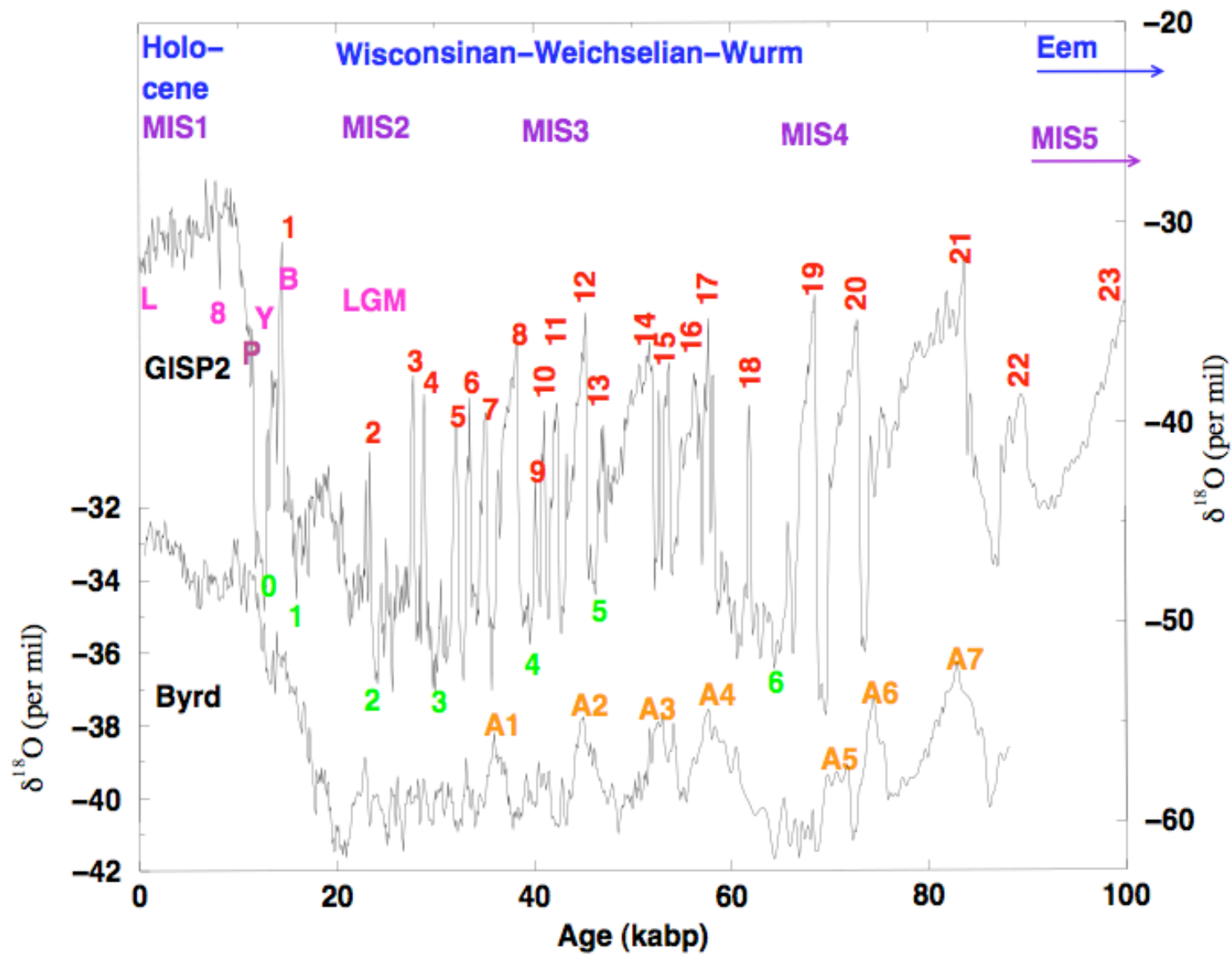


Figure 7.9 Ice-isotopic records ($\delta^{18}\text{O}$, a proxy for temperature, with less-negative values indicating warmer conditions) from GISP2, Greenland (Grootes and Stuiver, 1997) (scale on right) and Byrd Station, Antarctica (scale on left), as synchronized by Blunier and Brook (2001), with various climate-event terminology indicated. Ice age terms are shown in blue (top); the classical Eemian/Sangamonian is slightly older than shown here, as is the peak of marine isotope stage (MIS, shown in purple) 5, known as 5e. Referring specifically to the GISP2 curve, the warm Dansgaard-Oeschger events or stadial events, as numbered by Dansgaard et al. (1993), are indicated in red; Dansgaard-Oeschger event 24 is older than shown here. Occasional terms (L = Little Ice Age, 8 = 8k event, P=Preboreal Oscillation (PBO), Y = Younger Dryas, B = Bølling-Allerød, and LGM = Last Glacial Maximum) are shown in pink. Heinrich events are numbered in green just below the GISP2 isotopic curve, as placed by Bond et al. (1993). The Antarctic warm events A1–A7, as identified by Blunier and Brook (2001), are indicated for the Byrd record. Modified from Alley (2007).

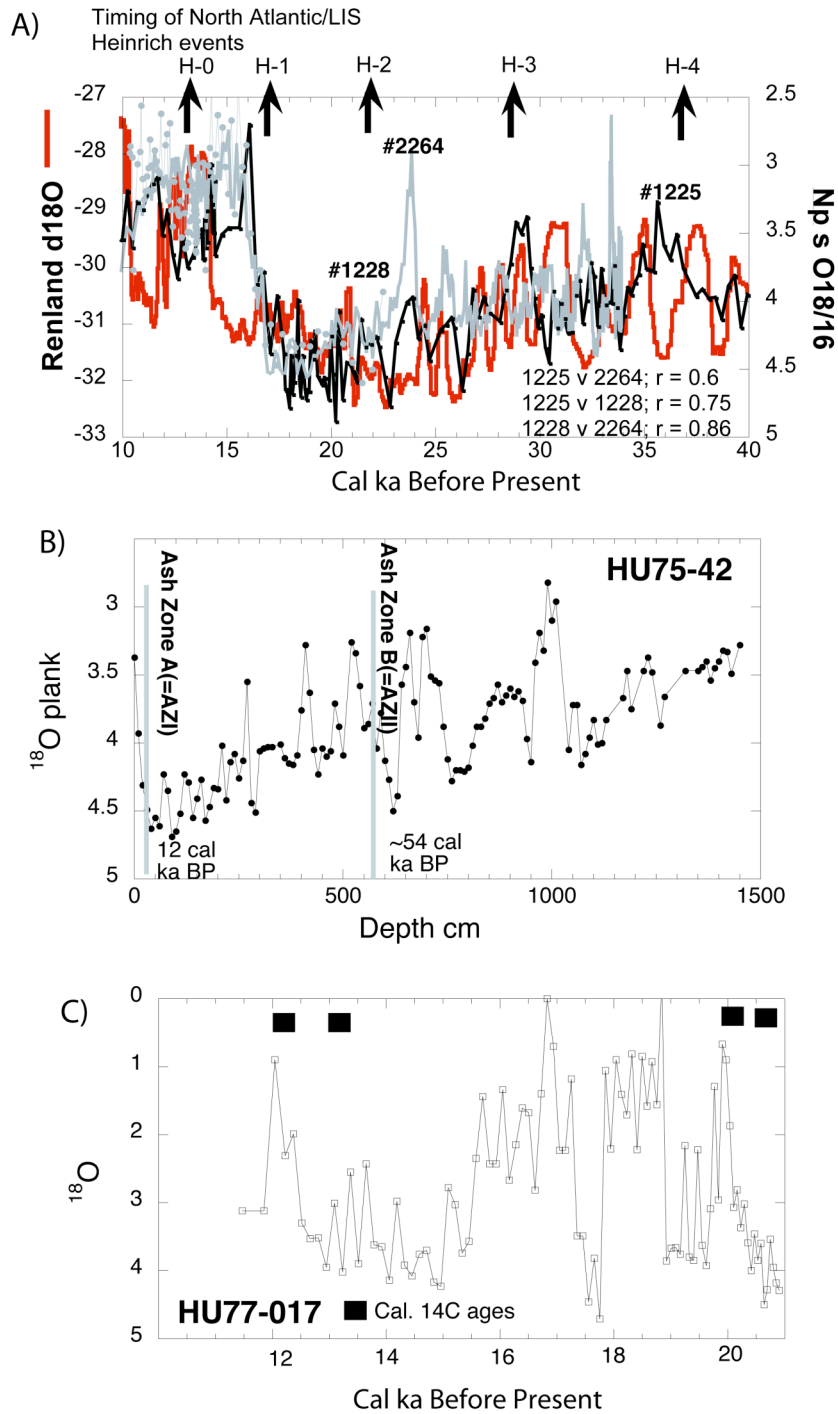


Figure 7.10 A) Variations in $\delta^{18}O$ from a series of cores north to south of Denmark Strait (see Fig. 7.8), namely: PS2264, JM96-1225 and 1228 plotted against the $\delta^{18}O$ from the Renland Ice Cap. B) $\delta^{18}O$ variations in cores HU75-42 (NW Labrador Sea). C) Stable oxygen variations in cores HU77-017 from north of the Davis Strait.

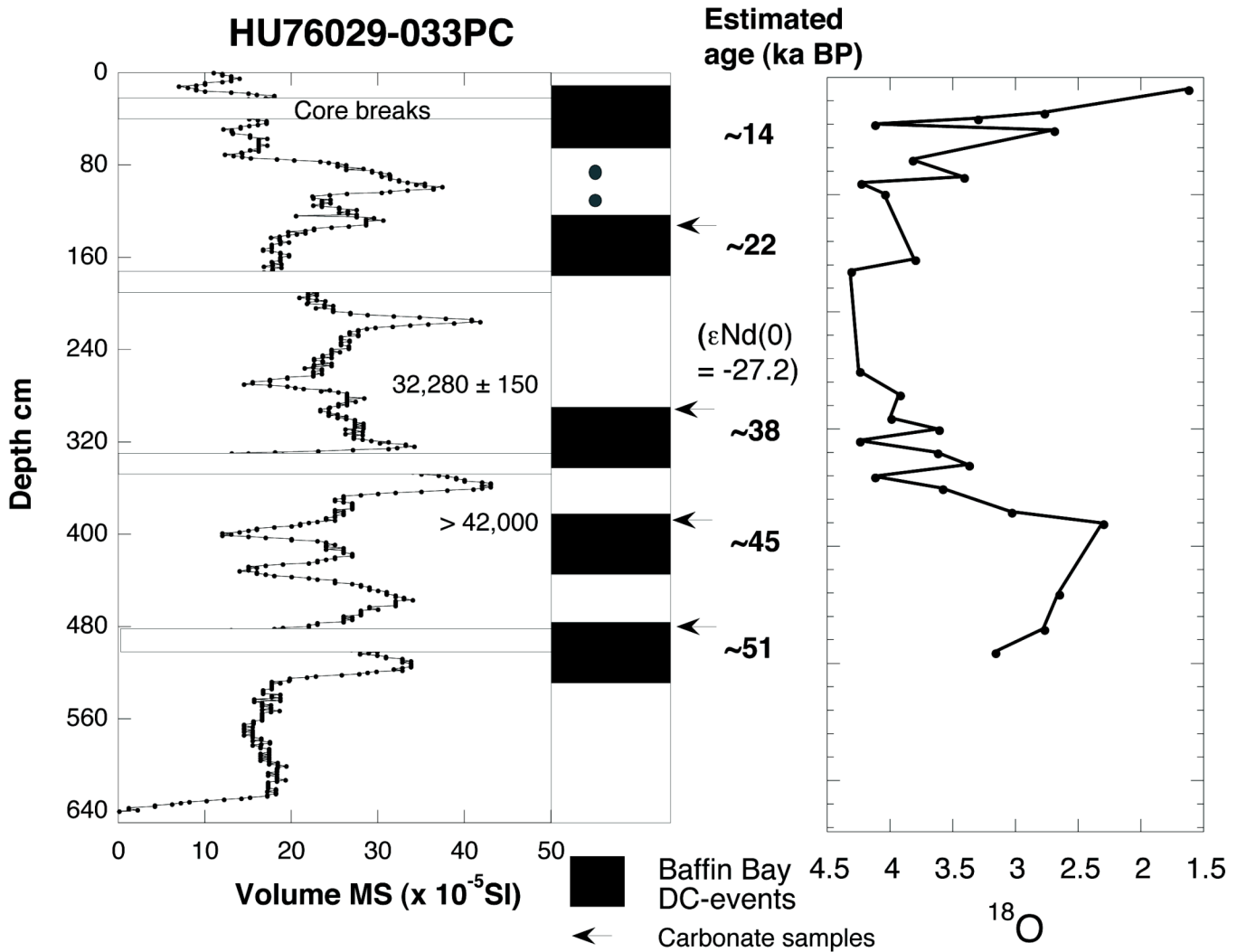


Figure 7.11 Variations in detrital carbonate (pieces of old rock) in core HU76-033 from Baffin Bay (Figure 7.8) showing down-core variations in magnetic susceptibility and $\delta^{18}O$.

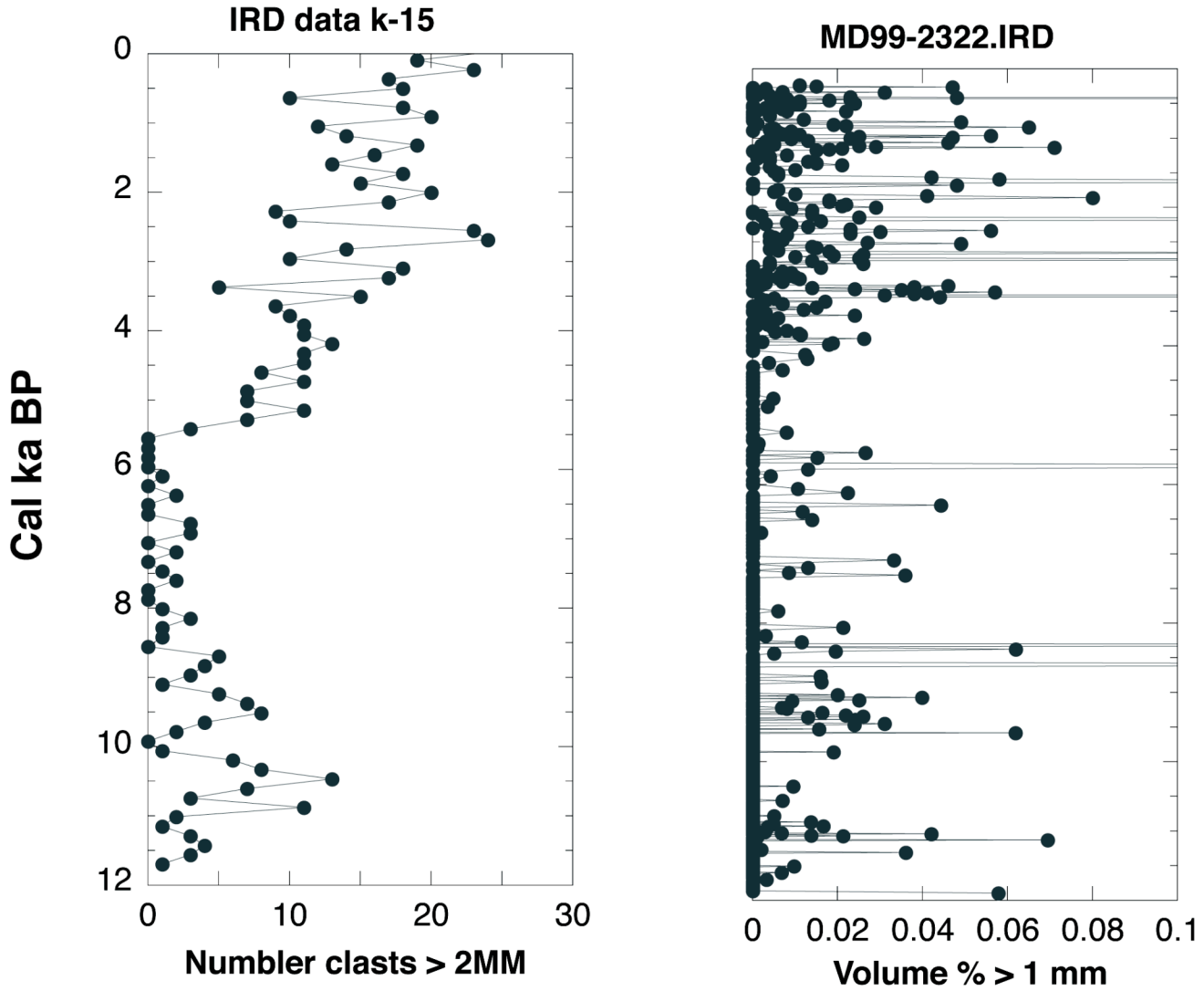
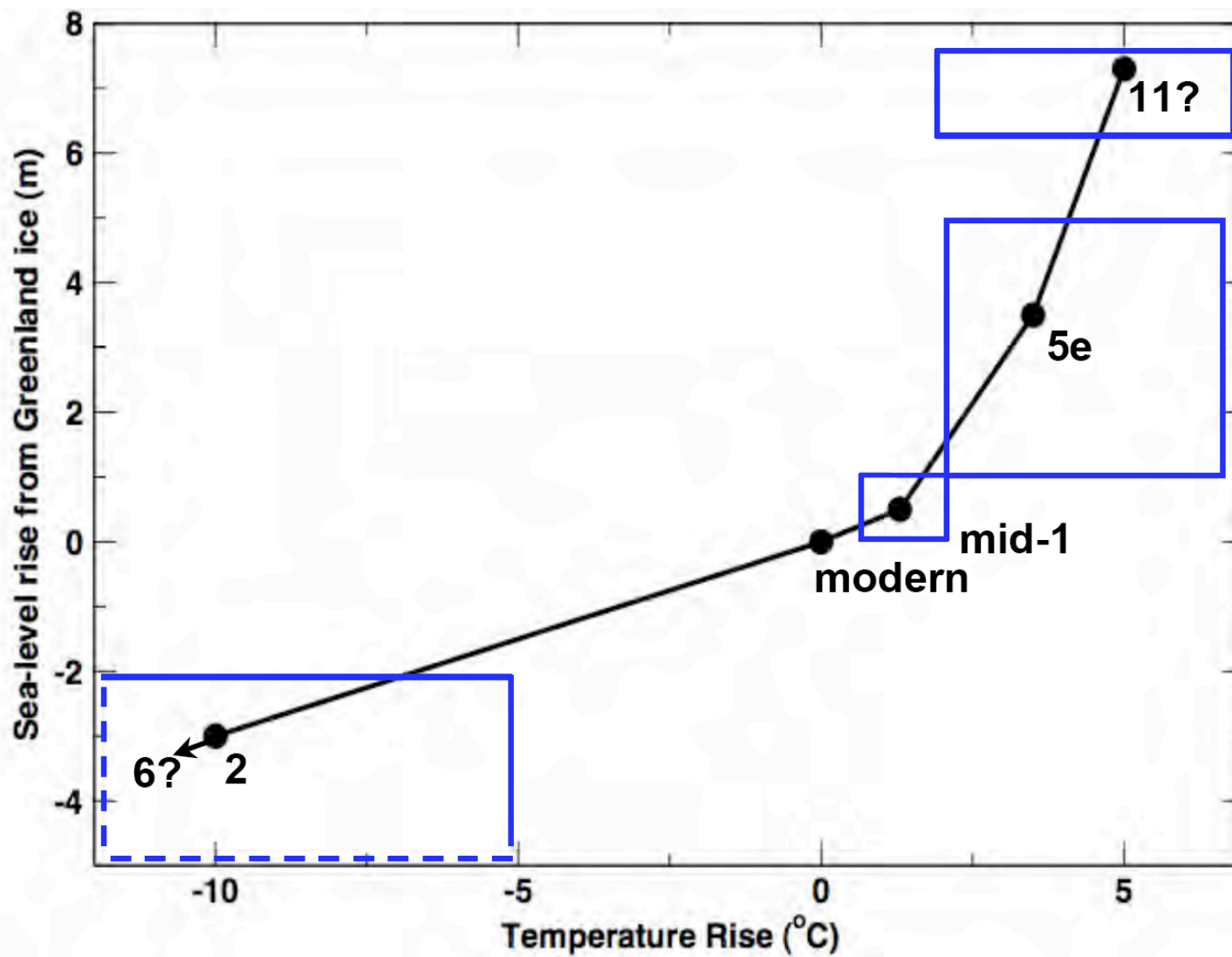


Figure 7.12 Holocene ice-rafted debris concentrations from MD99-2322 off Kangerdlugssuaq Fjord, East Greenland (Figure 7.8) showing log values of the percent of sediment > 1 mm and the weight % of quartz in the < 2mm sediment fraction.

1



2 **Figure 7.13** A best-guess representation of the dependence of the volume of the Greenland Ice Sheet on temperature. Large
3 **uncertainties should be understood, and any ice-volume changes in response to sea-level changes correlated with temperature**
4 **changes are included (although, as discussed in the text, temperature changes probably dominated forcing, especially at**
5 **warmer temperatures when the reduced ice sheet had less contact with the sea). Recent values of temperature and ice volume**
6 **(perhaps appropriate for 1960 or so) are assigned 0,0. The Last Glacial Maximum was probably $\sim 6^{\circ}\text{C}$ colder than modern for**
7 **global average (e.g., Cuffey and Brook, 2000; data and results summarized in Jansen et al., 2007). Cooling in central**
8 **Greenland was $\sim 15^{\circ}\text{C}$ (with peak cooling somewhat more; Cuffey et al., 1995). Some of the central-Greenland cooling was**
9 **probably linked to strengthening of the temperature inversion that lowers near-surface temperatures relative to the free**
10 **troposphere (Cuffey et al., 1995). A cooling of $\sim 10^{\circ}\text{C}$ is thus plotted. The ice-volume-change estimates of Peltier (2004;**
11 **ICE5G) and Fleming and Lambeck (2004) are used, with the upper end of the uncertainty taken to be the ICE4G estimate (see**
12 **Peltier, 2004), and somewhat arbitrarily set as 1 m on the lower side. The arrow indicates that the ice sheet in MIS 6 was more**
13 **likely than not slightly larger than in MIS 2, and that some (although inconsistent) evidence of slightly colder temperatures is**
14 **available (e.g., Bauch et al., 2000). The mid-Holocene result from ICE5G (Peltier, 2004) of an ice sheet smaller than modern**
15 **by ~ 0.5 m of sea-level equivalent is plotted; the error bars reflect the high confidence that the mid-Holocene ice sheet was**
16 **smaller than modern, with similar uncertainty assumed for the other side. Mid-Holocene temperature is taken from the Alley**
17 **and Anandakrishnan (1995) summertime melt-layer history of central Greenland, with their 0.5°C uncertainty on the lower**
18 **side, and a wider uncertainty on the upper side to include larger changes from other indicators (which are probably weighted**
19 **by wintertime changes that have less effect on ice-sheet mass balance, and so are not used for the best estimate; Alley et al.,**
20 **1999). As discussed in 7.3.3b and c, MIS 5e (the Eemian) is plotted with a warming of 3.5°C and a sea-level rise of 3.5 m. The**
21 **uncertainties on sea-level change come from the range of data-constrained models discussed in 7.3.3c. The temperature**
22 **uncertainties reflect the results of Cuffey and Marshall (2000) on the high side, and the lower values simulated over Greenland**
23 **by Otto-Bliesner et al. (2006). Loss of the full ice sheet is also plotted, to reflect the warmer conditions that may date to MIS**
24 **11 if not earlier, and perhaps also to the Pliocene times of the Kap København Formation. Very large warming is indicated by**
25 **the paleoclimatic data from Greenland, but much of that warming probably was a feedback from loss of the ice sheet itself**
26 **(Otto-Bliesner et al., 2006). Data from around the North Atlantic for MIS 11 and other interglacials do not show significantly**
27 **higher temperatures than during MIS 5e, allowing the possibility that sustaining MIS 5e levels for a longer time led to loss of**
28 **the ice sheet. Slight additional warming is indicated here, within the error bounds of the other records, based on assessment**
29 **that MIS 5e was sufficiently long for much of the ice-sheet response to have been completed, so that additional warmth was**
30 **required to cause additional retreat. The volume of ice possibly persisting in highlands even after loss of central regions of the**
31 **ice sheet is poorly quantified; 1 m is indicated.**

32

33

CHAPTER 7 CITED REFERENCES

34

35 **Adrielsson, L.** and H. Alexanderson, 2005: Interactions between the Greenland Ice Sheet
36 and the Liverpool Land coastal ice cap during the last two glaciation cycles. *Journal*
37 *of Quaternary Science*, **20**, 269-283.

38

39 **Aksu, A. E.**, 1985: Climatic and oceanographic changes over the past 400,000 years—
40 Evidence from deep-sea cores on Baffin Bay and David Strait. In: *Quaternary*
41 *Environments—Eastern Canadian Arctic, Baffin Bay and Western Greenland*
42 [Andrews, J.T. (ed.)]. Allen and Unwin, Boston, pp. 181-209.

43

44 **Alley, R.B.**, 2007. Wally was right—Predictive ability of the North Atlantic “conveyor
45 belt” hypothesis for abrupt climate change. *Annual Review of Earth and Planetary*
46 *Sciences*, **35**, 241-272.

47

48 **Alley, R.B.** and S. Anandakrishnan, 1995: Variations in melt-layer frequency in the
49 GISP2 ice core—Implications for Holocene summer temperatures in central
50 Greenland. *Annals of Glaciology*, **21**, 64-70.

51

52 **Alley, R.B.** and K.M. Cuffey. 2001. Oxygen- and hydrogen-isotopic ratios of water in
53 precipitation—Beyond paleothermometry. In: *Stable Isotope Geochemistry*, [Valle,
54 J.W. and D. Cole (eds.)]. Reviews in Mineralogy and Geochemistry, **43**, 527-553.

55

56 **Alley, R.B.** and B.R. Koci, 1990: Recent warming in central Greenland? *Annals of*
57 *Glaciology*, **14**, 6-8.

58

59 **Alley, R.B.** and I.M. Whillans, 1984: Response of the East Antarctic ice sheet to sea-level
60 rise. *Journal of Geophysical Research*, **89C**, 6487-6493.

61

- 62 **Alley, R.B., A.M. Agustsdottir, and P.J. Fawcett, 1999:** Ice-core evidence of late-
63 Holocene reduction in north Atlantic ocean heat transport. In: *Mechanisms of Global*
64 *Climate Change at Millennial Time Scales* [Clark, P.U., R.S. Webb and L.D. Keigwin
65 (eds.)]. Geophysical Monograph 112, American Geophysical Union, Washington,
66 DC, p. 301-312.
67
- 68 **Alley, R.B., S. Anandakrishnan, and P. Jung, 2001:** Stochastic resonance in the North
69 Atlantic. *Paleoceanography*, **16**, 190-198.
70
- 71 **Alley, R.B., E.J. Brook and S. Anandakrishnan, 2002:** A northern lead in the orbital
72 band—North-south phasing of ice-age events. *Quaternary Science Reviews*, 21, 431-
73 441 (2002).
74
- 75 **Alley, R.B., P.U. Clark, P. Huybrechts, and I. Joughin, 2005a:** Ice-sheet and sea-level
76 changes. *Science*, **310**, 456-460.
77
- 78 **Alley, R.B., T.K. Dupont, B.R. Parizek, and S. Anandakrishnan, 2005b:** Access of
79 surface meltwater to beds of sub-freezing glaciers—Preliminary insights. *Annals of*
80 *Glaciology*, **40**, 8-14.
81
- 82 **Alley, R.B., R.C. Finkel, K. Nishiizumi, S. Anandakrishnan, C.A. Shuman, G.R.**
83 **Mershon, G.A. Zielinski, and P.A. Mayewski, 1995a:** Changes in continental and sea-
84 salt atmospheric loadings in central Greenland during the most recent deglaciation.
85 *Journal of Glaciology*, **41(139)**, 503-514.
86
- 87 **Alley, R.B., A.J. Gow, S.J. Johnsen, J. Kipfstuhl, D.A. Meese, and Th. Thorsteinsson,**
88 **1995b:** Comparison of deep ice cores. *Nature*, **373**, 393-394.
89
- 90 **Alley, R.B., A.J. Gow, D.A. Meese, J.J. Fitzpatrick, E.D. Waddington, and J.F. Bolzan,**
91 **1997:** Grain-scale processes, folding, and stratigraphic disturbance in the GISP2 ice
92 core. *Journal of Geophysical Research*, **102(C12)**, 26,819-26,830.

93

94 **Alley, R.B., D.A. Meese, C.A. Shuman, A.J. Gow, K.C. Taylor, P.M. Grootes, J.W.C.**
95 **White, M. Ram, E.D. Waddington, P.A. Mayewski, and G.A. Zielinski, 1993: Abrupt**
96 **increase in snow accumulation at the end of the Younger Dryas event. *Nature*, **362**,**
97 **527-529.**

98

99 **Alley, R.B., M.K. Spencer, and S. Anandakrishnan, 2007: Ice-sheet mass balance:**
100 **assessment, attribution and prognosis. *Annals of Glaciology*, **46**, 1-7.**

101

102 **Andersen, K.K., A. Svensson, S.J. Johnsen, S.O. Rasmussen, M. Bigler, R.**
103 **Rothlisberger, U. Ruth, M.L. Siggaard-Andersen, J.P. Steffensen, D. Dahl-Jensen,**
104 **B.M. Vinther, and H.B. Clausen, 2006: The Greenland ice core chronology 2005, 15-**
105 **42 ka. Part 1—Constructing the time scale. *Quaternary Science Reviews*, **25**, 3246-**
106 **3257.**

107

108 **Andresen, C.S., S. Bjorck, O. Bennike, and G. Bond, 2004: Holocene climate changes in**
109 **southern Greenland—Evidence from lake sediments. *Journal of Quaternary Science*,**
110 ****19**, 783-795.**

111

112 **Andrews, J.T., 2008: The role of the Iceland Ice Sheet in sediment delivery to the North**
113 **Atlantic during the late Quaternary—How important was it? Evidence from the area**
114 **of Denmark Strait. *Journal of Quaternary Science*, **23**, 3-20.**

115

116 **Andrews, J.T. and G. Dunhill, 2004: Early to mid-Holocene Atlantic water influx and**
117 **deglacial meltwater events, Beaufort Sea slope, Arctic Ocean. *Quaternary Research*,**
118 ****61**, 14-21.**

119

120 **Andrews, J.T., T.A. Cooper, A.E. Jennings, A.B. Stein, and H. Erlenkeuser, 1998a: Late**
121 **Quaternary iceberg-rafted detritus events on the Denmark Strait/Southeast Greenland**
122 **continental slope (~65° N)—Related to North Atlantic Heinrich Events? *Marine***
123 ***Geology*, **149**, 211-228.**

124

125 **Andrews, J.T., Erlenkeuser, H., Tedesco, K., Aksu, A., and Jull, A.J.T., 1994:** Late
126 Quaternary (Stage 2 and 3) meltwater and Heinrich events, NW Labrador Sea.
127 *Quaternary Research*, **41**, 26-34.

128

129 **Andrews, J.T., Jennings, A.E., Cooper, T., Williams, K.M., and Mienert, J., 1996:** Late
130 Quaternary sedimentation along a fjord to shelf (trough) transect, East Greenland (ca.
131 68°N). In: *Late Quaternary Paleoceanography of North Atlantic Margins* [Andrews,
132 J.T., W. Austin, H. Bergsten, and A.E. Jennings (eds.)]. Geological Society, London,
133 pp. 153-166.

134

135 **Andrews, J.T., M.E. Kirby, A. Aksu, D.C. Barber, and D. Meese, 1998b:** Late
136 Quaternary detrital carbonate (DC-) events in Baffin Bay (67°–74° N)—Do they
137 correlate with and contribute to Heinrich Events in the North Atlantic? *Quaternary*
138 *Science Reviews*, **17**, 1125-1137.

139

140 **Andrews, J.T., L.M. Smith, R.Preston, T. Cooper, and A.E. Jennings, 1997:** Spatial and
141 temporal patterns of iceberg rafting (IRD) along the East Greenland margin, ca. 68 N,
142 over the last 14 cal.ka. *Journal of Quaternary Science*, **12**, 1-13.

143

144 **Bamber, J.L., R.L. Layberry, and S.P. Gogineni, 2001:** A new ice thickness and bed data
145 set for the Greenland Ice Sheet 1—Measurement, data reduction, and errors. *Journal*
146 *of Geophysical Research*, **106**, 33,773-33,780.

147

148 **Bamber, J.L., R.B. Alley, and I. Joughin, 2007:** Rapid Response of modern day ice
149 sheets to external forcing. *Earth and Planetary Science Letters*, **257**, 1-13.

150

151 **Bard, E. and M. Frank, 2006:** Climate change and solar variability—What's new under
152 the sun? *Earth and Planetary Science Letters*, **248**, 1-14.

153

- 154 **Bauch**, H.A., H. Erlenkeuser, J.P. Helmke, and U. Struck, 2000: A paleoclimatic
155 evaluation of marine oxygen isotope stage 11 in the high-northern Atlantic (Nordic
156 seas). *Global and Planetary Change*, **24**, 27-39.
- 157
- 158 **Bender**, M.L., R.G. Fairbanks, F.W. Taylor, R.K. Matthews, J.G. Goddard, and W.S.
159 Broecker, 1979: Uranium-series dating of the Pleistocene reef tracts of Barbados,
160 West Indies. *Geological Society of America Bulletin, Part I*, **90**, 577-594.
- 161
- 162 **Bennike**, O. and J. Bocher, 1994: Land biotas of the last interglacial-glacial cycle on
163 Jameson Land, East Greenland. *Boreas*, **23**, 479-487.
- 164
- 165 **Bennike**, O., S. Bjorck, and K. Lambeck, 2002: Estimates of South Greenland late-
166 glacial ice limits from a new relative sea level curve. *Earth and Planetary Science*
167 *Letters*, **197**, 171-186.
- 168
- 169 **Berger**, A.L., 1978: Long-term variations of caloric insolation resulting from the earth's
170 orbital elements. *Quaternary Research*, **9**, 139-167.
- 171
- 172 **Berger**, A. and Loutre, M.F., 1991: Insolation values for the climate of the last 10 million
173 years. *Quaternary Science Reviews*, **10**, 297-317.
- 174
- 175 **Bigg**, G.R., 1999: An estimate of the flux of iceberg calving from Greenland. *Arctic,*
176 *Antarctic, and Alpine Research*, **31**, 174-178.
- 177
- 178 **Bjorck**, S., M. Rundgren, O. Ingolfsson, and S. Funder, 1997: The Preboreal oscillation
179 around the Nordic Seas—Terrestrial and lacustrine responses. *Journal of Quaternary*
180 *Science*, **12**, 455-465.
- 181
- 182 **Bjorck**, S., O. Bennike, P. Rosen, C.S. Andresen, S. Bohncke, E. Kaas, and D. Conley,
183 2002: Anomalously mild Younger Dryas summer conditions in southern Greenland.
184 *Geology*, **30**, 427-430.

185

186 **Blake, W., Jr., H.R. Jackson, and C.G. Currie, 1996:** Seafloor evidence for glaciation,
187 northernmost Baffn Bay. *Bulletin of the Geological Survey of Denmark*, **43**, 157-168.

188

189 **Blunier, T. and E.J. Brook, 2001:** Timing of millennial-scale climate change in
190 Antarctica and Greenland during the last glacial period. *Science*, **291**, 109-112.

191

192 **Bond, G., W. Broecker, S. Johnson, J. McManus, L. Labeyrie, J. Jouzel, and G. Bonani,**
193 1993: Correlation between climate records from North Atlantic sediments and
194 Greenland ice. *Nature*, **365**, 507-508.

195

196 **Bond, G.C. and R. Lotti, 1995:** Iceberg discharges into the North Atlantic on millennial
197 time scales during the last glaciation. *Science*, **267**, 1005-1009.

198

199 **Box, J.E., D.H. Bromwich, B.A. Veenhuis, L.-S. Bai, J.C. Stroeve, J.C. Rogers, K.**
200 Steffen, T. Haran, and S.-H. Wang, 2006: Greenland ice-sheet surface mass balance
201 variability (1988-2004) from calibrated Polar MM5 output. *Journal of Climate*,
202 **19(12)**, 2783–2800.

203

204 **Bradley, R.S., 1999:** *Paleoclimatology—Reconstructing Climate of the Quaternary*.
205 Academic Press, San Diego, 613 pp.

206

207 **Braun, H., M. Christl, S. Rahmstorf, A. Ganopolski, A. Mangini, C. Kubatzki, K. Roth,**
208 and B. Kromer, 2005: Possible solar origin of the 1,470-year glacial climate cycle
209 demonstrated in a coupled model. *Nature*, **438**, 208-211.

210

211 **Brodersen, K.P. and O. Bennike, 2003:** Interglacial Chironomidae (Diptera) from Thule,
212 Northwest Greenland—Matching modern analogues to fossil assemblages. *Boreas*,
213 **32**, 560-565.

214

- 215 **Broecker, W.S.**, 1995: *The Glacial World According to Wally*. Eldigio Press, Palisades,
216 NY, 89 pp.
217
- 218 **CircumArctic PaleoEnvironments (CAPE)—Last Interglacial Project Members (P.**
219 Anderson, O. Bermike, N. Bigelow, J. Brigham-Grette, M. Duvall, M. Edwards, B.
220 Frechette, S. Funder, S. Johnsen, J. Knies, R. Koerner, A. Lozhkin, S. Marshall, J.
221 Matthiessen, G. Macdonald, G. Miller, M. Montoya, D. Muhs, B. Otto-Bliesner, J.
222 Overpeck, N. Reeh, H.P. Sejrup, R. Spielhagen, C. Turner and A. Velichko), 2006:
223 Last Interglacial Arctic warmth confirms polar amplification of climate change.
224 *Quaternary Science Reviews*, **25**, 1383-1400.
225
- 226 **Cazenave, A.**, 2006: How fast are the ice sheets melting? *Science*, **314**, 1250-1252.
227
- 228 **Chappellaz, J.**, E. Brook, T. Blunier, and B. Malaize, 1997: CH₄ and delta O-18 of O-2
229 records from Antarctic and Greenland ice—A clue for stratigraphic disturbance in the
230 bottom part of the Greenland Ice Core Project and the Greenland Ice Sheet Project 2
231 ice cores. *Journal of Geophysical Research*, **102(C12)**, 26,547-26,557.
232
- 233 **Chen, J.H.**, H.A. Curran, B. White, and G.J. Wasserburg, 1991: Precise chronology of
234 the last interglacial period—²³⁴U-²³⁰Th data from fossil coral reefs in the Bahamas:
235 *Geological Society of America Bulletin*, **103**, 82-97.
236
- 237 **Clarke, G.K.C.** and S.J. Marshall, 2002: Isotopic balance of the Greenland Ice Sheet—
238 Modeled concentrations of water isotopes from 30,000 BP to present. *Quaternary*
239 *Science Reviews*, **21**, 419-430.
240
- 241 **Clarke, G.K.C.**, N. Lhomme, and S.J. Marshall, 2005: Tracer transport in the Greenland
242 Ice Sheet—Three-dimensional isotopic stratigraphy. *Quaternary Science Reviews*, **24**,
243 155-171.
244

- 245 **Cronin, T.M.**, 1999: *Principles of Paleoclimatology*. Columbia University Press, New
246 York, 560 pp.
247
- 248 **Cuffey, K.M. and E.J. Brook**, 2000: Ice sheets and the ice-core record of climate change.
249 In: *Earth System Science—From Biogeochemical Cycles to Global Change*
250 [Jacobson, M.C., R.J. Charlson, H. Rodhe, and G.H. Orians (eds.)]. Academic Press,
251 New York, pp. 459-497.
252
- 253 **Cuffey, K.M. and G.D. Clow**, 1997: Temperature, accumulation, and ice sheet elevation
254 in central Greenland through the last deglacial transition. *Journal of Geophysical*
255 *Research*, **102(C12)**, 26,383-26,396.
256
- 257 **Cuffey, K.M. and S.J. Marshall**, 2000: Substantial contribution to sea-level rise during
258 the last interglacial from the Greenland Ice Sheet. *Nature*, **404**, 591-594.
259
- 260 **Cuffey, K.M., R.B. Alley, P.M. Grootes, J.F. Bolzan, and S. Anandakrishnan**, 1994:
261 Calibration of the d¹⁸O isotopic paleothermometer for central Greenland, using
262 borehole temperatures. *Journal of Glaciology*, **40(135)**, 341-349.
263
- 264 **Cuffey, K.M., G.D. Clow, R.B. Alley, M. Stuiver, E.D. Waddington, and R.W. Saltus**,
265 1995: Large Arctic temperature change at the glacial-Holocene transition. *Science*,
266 **270**, 455-458.
267
- 268 **Dahl-Jensen, D., K. Mosegaard, N. Gundestrup, G.D. Clow, S.J. Johnsen, A.W. Hansen,**
269 **and N. Balling**, 1998: Past temperatures directly from the Greenland Ice Sheet.
270 *Science*, **282**, 268-271.
271
- 272 **Dahl-Jensen, D., N. Gundestrup, S.P. Gogineni, and H. Miller**, 2003: Basal melt at
273 NorthGRIP modeled from borehole, ice-core and radio-echo sounded observations.
274 *Annals of Glaciology*, **37**, 207-212.
275

- 276 **Dansgaard, W.**, S.J. Johnsen, H.B. Clausen, D. Dahl-Jensen, N.S. Gundestrup, C.U.
277 Hammer, C.S. Hvidberg, J.P. Steffensen, A.E. Sveinbjorndottir, J. Jouzel, and G.
278 Bond, 1993: Evidence for general insatbility of past climate from a 250-kyr ice-core
279 record. *Nature*, **364**, 218-220.
280
- 281 **Darby, D.A.**, J. Bischof, R.F. Spielhagen, S.A. Marshall, and S.W. Herman, 2002: Arctic
282 ice export events and their potential impact on global climate suring the late
283 Pleistocene. *Palaeoceanography*, **17**, doi. 10.1029/2001PA000639, 000615-000631
284 to 000615-000617.
285
- 286 **De Abreu, C.**, F.F. Abrantes, N.J. Shackleton, P.C. Tzedakis, J.F. McManus, D.W.
287 Oppo, and M.A. Hall, 2005: Ocean climate variability in the eastern North Atlantic
288 during interglacial marine isotope stage 11—A partial analogue to the Holocene?
289 *Paleoceanography*, **20**, Art. No. PA3009.
290
- 291 **Denton, G.H.**, R.B. Alley, G.C. Comer, and W.S. Broecker, 2005: The role of seasonality
292 in abrupt climate change. *Quaternary Science Reviews*, **24**, 1159-1182.
293
- 294 **Dickinson, W.R.**, 2001: Paleoshoreline record of relative Holocene sea levels on Pacific
295 Islands. *Earth-Science Reviews*, **55**, 191-234.
296
- 297 **Dowdeswell, J.A.**, G. Uenzelmann-Neben, R.J. Whittington, P. and Marienfeld, 1994a:
298 The Late Quaternary sedimentary record in Scoresby Sund, East Greenland. *Boreas*,
299 **23**, 294-310.
300
- 301 **Dowdeswell, J.A.**, R.J. Whittington, and P. Marienfeld, 1994b: The origin of massive
302 diamicton facies by iceberg rafting and scouring, Scoresby Sund, East Greenland.
303 *Sedimentology*, **41**, 21-35.
304
- 305 **Dowdeswell, J.A.**, N.H. Kenyon, A. Elverhoi, J.S. Laberg, F.-J. Hollender, J. Mienert,
306 and M.J. Siegert, 1996: Large-scale sedimentation on the glacier-influenced Polar

- 307 North Atlantic margins—Long-range side-scan sonar evidence. *Geophysical*
308 *Research Letters*, **23**, 3535-3538.
- 309
- 310 **Dowdeswell, J.A., N.H. Kenyon, and J.S. Laberg, 1997:** The glacier-influenced Scoresby
311 Sund Fan, east Greenland continental margin—Evidence from GLORIA and 3.5 kHz
312 records. *Marine Geology*, **143**, 207-221.
- 313
- 314 **Droxler, A.W., R.B. Alley, W.R. Howard, R.Z. Poore, and L.H. Burckle, 2003:** Unique
315 and exceptionally long interglacial marine isotope stage 11—Window into Earth
316 future climate. In: *Earth's Climate and Orbital Eccentricity—The Marine Isotope*
317 *Stage 11 Question* [Droxler, A.W., R.Z. Poore and L.H. Burckle (eds.)]. *Geophysical*
318 *Monograph 137*, American Geophysical Union, p. 1-14.
- 319
- 320 **Dunhill, G., 2005:** Iceland and Greenland margins—A comparison of depositional
321 processes under different glaciological and oceanographic settings. PhD dissertation,
322 Geological Sciences, University of Colorado, Boulder.
- 323
- 324 **Dupont, T.K. and R.B. Alley, 2005:** Assessment of the importance of ice-shelf
325 buttressing to ice-sheet flow. *Geophysical Research Letters*, **32**, L04503, doi
326 10.1029/2004GL022024.
- 327
- 328 **Dupont, T.K. and R.B. Alley, 2006:** Role of small ice shelves in sea-level rise.
329 *Geophysical Research Letters*, **33**, L09503.
- 330
- 331 **Dyke, A.S., J.E. Dale, and R.N. McNeely, 1996:** Marine molluscs as indicators of
332 environmental change in glaciated North America and Greenland during the last
333 18,000 years. *Geographie Physique et Quaternaire*, **50**, 125-184.
- 334
- 335 **Dyke, A.S., J.T. Andrews, P.U. Clark, J.H. England, G.H. Miller, J. Shaw, and J.J.**
336 **Veillette, 2002:** The Laurentide and Innuitian ice sheets during the Last Glacial
337 Maximum. *Quaternary Science Reviews*, **21**, 9-31.

338

339 **Edwards, R.L., H. Cheng, M.T. Murrell, and S.J. Goldstein, 1997:** Protactinium-231
340 dating of carbonates by thermal ionization mass spectrometry—Implications for
341 Quaternary climate change: *Science*, **276**, 782-786.

342

343 **Eisen, O., U. Nixdorf, F. Wilhelms, and H. Miller, 2004:** Age estimates of isochronous
344 reflection horizons by combining ice core, survey, and synthetic radar data. *Journal*
345 *of Geophysical Research*, **109(B4)**, Art. No. B04106.

346

347 **Eldrett, J.S., I.C. Harding, P.A. Wilson, E. Butler, and A.P. Roberts, 2007:** Continental
348 ice in Greenland during the Eocene and Oligocene. *Nature*, **446**, 176-179.

349

350 **Elliot, M., L. Labeyrie, G. Bond, E. Cortijo, J.-L. Turon, N. Tiseray, and J.-C. Duplessy,**
351 1998: Millennial-scale iceberg discharges in the Irminger Basin during the last glacial
352 period—Relationship with the Heinrich events and environmental settings.
353 *Paleoceanography*, **13**, 433-446.

354

355 **Elverhoi, A., J.A. Dowdeswell, S. Funder, J. Mangerud, and R. Stein, 1998:** Glacial and
356 oceanic history of the polar North Atlantic margins—An overview. *Quaternary*
357 *Science Reviews*, **17**, 1-10.

358

359 **England, J., 1999:** Coalescent Greenland and Inuitian ice during the Last Glacial
360 Maximum—Revising the Quaternary of the Canadian High Arctic. *Quaternary*
361 *Science Reviews*, **18**, 421-456.

362

363 **Fairbanks, R.G., R.A. Mortlock, C. Tzu-Chien, L. Cao, A. Kaplan, T.P. Guilderson,**
364 T.W. Fairbanks, A.L. Bloom, P.M. Grootes, and M.-J. Nadeau, 2005: Radiocarbon
365 calibration curve spanning 0 to 50,000 years BP based on paired ²³⁰Th/²³⁴U/²³⁸U
366 and ¹⁴C dates on pristine corals. *Quaternary Science Reviews*, **24**, 1781-1796.

367

368 **Farmer, G.L. D.C., Barber, and J.T. Andrews, 2003:** Provenance of Late Quaternary ice-
369 proximal sediments in the North Atlantic—Nd, Sr and Pd isotopic evidence. *Earth*
370 *and Planetary Science Letters*, **209**, 227-243.

371

372 **Fillon, R.H. and J.C. Duplessy, 1980:** Labrador Sea bio-, tephro-, oxygen isotopic
373 stratigraphy and Late Quaternary paleoceanographic trends. *Canadian Journal Earth*
374 *Sciences*, **17**, 831-854.

375

376 **Finkel, R.C. and K. Nishiizumi, 1997:** Beryllium 10 concentrations in the Greenland Ice
377 Sheet Project 2 ice core from 3-40 ka. *Journal of Geophysical Research*, **102(C12)**,
378 26,699-26,706.

379

380 **Fisher, T.G., D.G. Smith, and J.T. Andrews, 2002:** Preboreal oscillation caused by a
381 glacial Lake Agassiz flood. *Quaternary Science Reviews*, **21**, 873-878.

382

383 **Fleming, K. and K. Lambeck, 2004:** Constraints on the Greenland Ice Sheet since the
384 Last Glacial Maximum from sea-level observations and glacial-rebound models.
385 *Quaternary Science Reviews*, **23**, 1053-1077.

386

387 **Fruijtier, C., T. Elliot, and W. Schlager, 2000:** Mass-spectrometric ^{234}U - ^{230}Th ages from
388 the Key Largo Formation, Florida Keys, United States—Constraints on diagenetic
389 age disturbance. *Geological Society of America Bulletin*, **112**, 267-277.

390

391 **Funder, S., 1989a:** Quaternary geology of east Greenland. In: Chapter 13 of *Quaternary*
392 *Geology of Canada and Greenland* [Fulton, R.J. (ed.)]. Geological Survey of Canada,
393 Geology of Canada, no. 1, 839 pp.; also Geological Society of America, the Geology
394 of North America, v. K-1, p. 756-763.

395

396 **Funder, S., 1989b:** Quaternary geology of north Greenland. In: Chapter 13 of
397 *Quaternary Geology of Canada and Greenland* [Fulton, R.J. (ed.)]. Geological

- 398 Survey of Canada, *Geology of Canada*, no. 1, 839 pp.; also Geological Society of
399 America, the *Geology of North America*, v. K-1, p. 763-769.
400
- 401 **Funder, S.**, 1989c: Quaternary geology of west Greenland. In: Chapter 13 of *Quaternary*
402 *Geology of Canada and Greenland* [R.J. Fulton (ed.)]. Geological Survey of Canada,
403 *Geology of Canada*, no. 1, 839 pp.; also Geological Society of America, the *Geology*
404 of North America, v. K-1, p. 749-756.
405
- 406 **Funder, S.**, 1989d: Sea level history. In: Chapter 13 of *Quaternary Geology of Canada*
407 *and Greenland* [R.J. Fulton (ed.)]. Geological Survey of Canada, *Geology of Canada*,
408 no. 1, 839 pp.; also Geological Society of America, the *Geology of North America*, v.
409 K-1, p. 772-774.
410
- 411 **Funder, S.** and B. Fredskild, 1989: Paleofaunas and floras. In: Chapter 13 of *Quaternary*
412 *Geology of Canada and Greenland* [Fulton, R.J. (ed.)]. Geological Survey of Canada,
413 *Geology of Canada*, no. 1; also Geological Society of America, the *Geology of North*
414 *America*, v. K-1, p. 775-783.
415
- 416 **Funder, S.** and H.C. Larsen, 1989: Quaternary geology of the shelves adjacent to
417 Greenland. In: Chapter 13 of *Quaternary Geology of Canada and Greenland* [Fulton,
418 R.J. (ed.)]. Geological Survey of Canada, *Geology of Canada*, no. 1; also Geological
419 Society of America, *The Geology of North America*, v. K-1, p. 769-772.
420
- 421 **Funder, S.**, C. Hjort, J.Y. Landvik, S.I. Nam, N. Reeh, and R. Stein, 1998: History of a
422 stable ice margin East Greenland during the Middle and Upper Pleistocene.
423 *Quaternary Science Reviews*, **17**, 77-123.
424
- 425 **Funder, S.**, O. Bennike, J. Böcher, C. Israelson, K.S. Petersen, and L.A. Simonarson,
426 2001: Late Pliocene Greenland—The Kap København Formation in North Greenland.
427 *Bulletin of the Geological Society of Denmark*, **48**, 117–134.
428

- 429 **Funder, S., A.E. Jennings, and M.J. Kelly, 2004:** Middle and late Quaternary glacial
430 limits in Greenland. In: *Quaternary Glaciations—Extent and Chronology, Part II*
431 [Ehlers, J. and P.L. Gibbard (eds.)]. Elsevier, New York, pp. 425-430.
432
- 433 **Gallup, C.D., R.L. Edwards, and R.G. Johnson, 1994:** The timing of high sea levels over
434 the past 200,000 years: *Science*, **263**, 796-800.
435
- 436 **Geirsdottir, A., H. Hardardottir, and J. Eirsson, 1997:** The depositional history of the
437 Younger Dryas–Preboreal Budi moraines in south-central Iceland. *Arctic and Alpine*
438 *Research*, **29**, 13-23.
439
- 440 **Geirsdottir, A., J. Hardardottir, and J.T. Andrews, 2000:** Late Holocene terrestrial
441 geology of Miki and I.C. Jacobsen Fjords, East Greenland. *The Holocene*, **10**, 125-
442 134.
443
- 444 **Gilbert, R., 1990:** Rafting in glacial marine environments. In: *Glacial Marine Environments—*
445 *Processes and Sediments* [Dowdeswell, J.A. and J.D. Scourse (eds.)]. Geological
446 Society, London, 105-120.
447
- 448 **Goreau, T.F., 1959:** The ecology of Jamaican coral reefs I—Species composition and
449 zonation. *Ecology*, **40(1)**, 67-90.
450
- 451 **Gosse, J.C. and F.M. Phillips, 2001:** Terrestrial in situ cosmogenic nuclides—Theory and
452 application. *Quaternary Science Reviews*, **20**, 1475-1560.
453
- 454 **Gregory, J.M. and P. Huybrechts, 2006:** Ice-sheet contributions to future sea-level
455 change. *Philosophical Transactions of the Royal Society A: Mathematical, Physical*
456 *and Engineering Sciences*, **364(1844)**, 1709-1731.
457

- 458 **Grootes**, P.M. and M. Stuiver, 1997: Oxygen 18/16 variability in Greenland snow and
459 ice with 10(-3)- to 10(5)-year time resolution. *Journal of Geophysical Research*,
460 **102C**, 26,455-26,470.
- 461
- 462 **Grousset**, F.E., E. Cortijo, S. Huon, L. Herve, T. Richter, D. Burdloff, J. Duprat, and O.
463 Weber, 2001: Zooming in on Heinrich layers. *Paleoceanography*, **16**, 240-259.
- 464
- 465 **Hagen**, S., 1999: North Atlantic paleoceanography and climate history during the last ~
466 70 cal. ka years. PhD dissertation, Department of Geology, University of Tromso,
467 Norway, 110 pp.
- 468
- 469 **Hagen**, S. and Hald, M., 2002: Variation in surface and deep water circulation in the
470 Denmark Strait, North Atlantic, during marine isotope stages 3 and 2.
471 *Paleoceanography*, **17**, 13-11 to 13-16 (10.1029/2001PA000632).
- 472
- 473 **Hakansson**, L., J. Briner, H. Alexanderson, A. Aldahan, and G. Possnert, 2007: ¹⁰Be
474 ages from central east Greenland constrain the extent of the Greenland Ice Sheet
475 during the Last Glacial Maximum. *Quaternary Science Reviews*, **26(19-21)** 2316-
476 **2321**, doi:10.1016/j.quascirev.2007.08.001
- 477
- 478 **Hald**, M. and S. Hagen, 1998: Early Preboreal cooling in the Nordic seas region triggered
479 by meltwater. *Geology*, **26**, 615-618.
- 480
- 481 **Hanna**, E., P. Huybrechts, I. Janssens, J. Cappelen, K. Steffens, and A. Stephens, 2005:
482 Runoff and mass balance of the Greenland Ice Sheet—1958-2003. *Journal of*
483 *Geophysical Research*, **110**, D13108, doi:10.1029/2004JD005641
- 484
- 485 **Hearty**, P.J., P. Kindler, H. Cheng, and R.L. Edwards, 1999: A +20 m middle
486 Pleistocene sea-level highstand (Bermuda and the Bahamas) due to partial collapse of
487 Antarctic ice: *Geology*, **27**, 375-378.
- 488

- 489 **Helmke, J.P., H.A. Bauch, and H. Erlenkeuser, 2003:** Development of glacial and
490 interglacial conditions in the Nordic seas between 1.5 and 0.35 Ma. *Quaternary*
491 *Science Reviews*, **22**, 1717-1728.
492
- 493 **Hemming, S.R., 2004:** Heinrich events—Massive late Pleistocene detritus layers of the
494 North Atlantic and their global climate imprint. *Reviews of Geophysics*, **42**, Art. No.
495 RG1005.
496
- 497 **Hemming, S.R., T.O. Vorren, and J. Kleman, 2002:** Provinciality of ice rafting in the
498 North Atlantic—Application of Ar-40/Ar-39 dating of individual ice rafted
499 hornblende grains. *Quaternary International*, **95**, 75-85.
500
- 501 **Hooke, R. LeB., 2005:** *Principles of Glacier Mechanics*. Cambridge University Press,
502 Cambridge, 429 pp.
503
- 504 **Hopkins, T.S., 1991:** The GIN Sea—A synthesis of its physical oceanography and
505 literature review 1972-1985. *Earth Science Reviews*, **30**, 175-318.
506
- 507 **Huddard, A., D. Sugden, A. Dugmore, H. Norddahl, and H.G. Petersson, 2006:** A
508 modelling insight into the Icelandic Last Glacial Maximum ice sheet. *Quaternary*
509 *Science Reviews*, **25**, 2283-2296.
510
- 511 **Hughes, T.J., 1998:** *Ice Sheets*. Oxford University Press, New York, 343 pp.
512
- 513 **Hulbe, C.L., D.R. MacAyeal, G.H. Denton, J. Kleman, and T.V. Lowell, 2004:**
514 Catastrophic ice shelf breakup as the source of Heinrich event icebergs.
515 *Paleoceanography*, **19**, Art. No. PA1004.
516
- 517 **Huybrechts, P., 2002:** Sea-level changes at the LGM from ice-dynamic reconstructions
518 of the Greenland and Antarctic ice sheets during the glacial cycles. *Quaternary*
519 *Science Reviews*, **21**, 203-231.

520

521 **Huybrechts, P.** and J. de Wolde, 1999: The dynamic response of the Greenland and
522 Antarctic ice sheets to multiple-century climatic warming. *Journal of Climate*, **12**,
523 2169-2188.

524

525 **Intergovernmental Panel on Climate Change (IPCC)**, 2007: Summary for
526 policymakers. In: *Climate Change 2007—The Physical Science Basis. Contribution*
527 *of Working Group I to the Fourth Assessment Report of the Intergovernmental Panel*
528 *on Climate Change* [Solomon, S., D. Qin, M. Manning, Z. Chen, M. Marquis, K.B.
529 Averyt, M.Tignor and H.L. Miller (eds.)]. Cambridge University Press, Cambridge
530 and New York, 18 pp.

531

532 **Jacobel, R.W.** and B.C. Welch, 2005: A time marker at 17.5 kyr BP detected throughout
533 West Antarctica. *Annals of Glaciology*, **41**, 47-51.

534

535 **Jansen, E., J. Overpeck, K.R. Briffa, J.-C. Duplessy, F. Joos, V. Masson-Delmotte, D.**
536 **Olago, B. Otto-Bliesner, W.R. Peltier, S. Rahmstorf, R. Ramesh, D. Raynaud, D.**
537 **Rind, O. Solomina, R. Villalba, and D. Zhang**, 2007: Palaeoclimate. In: *Climate*
538 *Change 2007: The Physical Science Basis. Contribution of Working Group I to the*
539 *Fourth Assessment Report of the Intergovernmental Panel on Climate Change*
540 [Solomon, S., D. Qin, M. Manning, Z. Chen, M. Marquis, K.B. Averyt, M. Tignor
541 and H.L. Miller (eds.)]. Cambridge University Press, Cambridge, United Kingdom
542 and New York, NY, USA.

543

544 **Jennings, A.E.** and N.J. Weiner, 1994: East Greenland climate change over the last 1300
545 years from foraminiferal evidence. *PaleoBios*, **16(Supplement to No. 2)**, 38

546

547 **Jennings, A.E., K. Gronvold, R. Hilberman, M. Smith, and M. Hald**, 2002a: High
548 resolution study of Icelandic tephtras in the Kangerlussuaq Trough, SE East
549 Greenland, during the last deglaciation. *Journal of Quaternary Science*, **17**, 747-757.

550

- 551 **Jennings, A.E., K.L. Knudsen, M. Hald, C.V. Hansen, and J.T. Andrews, 2002b:** A mid-
552 Holocene shift in Arctic sea ice variability on the East Greenland shelf. *The*
553 *Holocene*, **12**, 49-58.
554
- 555 **Jennings, A.E., M. Hald, L.M. Smith, and J.T. Andrews, 2006:** Freshwater forcing from
556 the Greenland Ice Sheet during the Younger Dryas—Evidence from Southeastern
557 Greenland shelf cores. *Quaternary Science Reviews*, **25**, 282-298.
558
- 559 **Johannessen, O.M., K. Khvorostovsky, M.W. Miles, and L.P. Bobylev, 2005:** Recent
560 ice-sheet growth in the interior of Greenland. *Science*, **310**, 1013-1016.
561
- 562 **Johnsen, S.J., 1977:** Stable isotope homogenization of polar firn and ice. In: *Proceedings*
563 *of a Symposium on Isotopes and Impurities in Snow and Ice, I.U.G.G. XVI, General*
564 *Assembly, Grenoble Aug. Sept. 1975*, IAHS-AISH Publ. 118, Washington D.C., pp.
565 210-219.
566
- 567 **Johnsen, S., H.B. Clausen, W. Dansgaard, N.S. Gundestrup, M. Hansson, P. Johnsson, P.**
568 **Steffensen, and A.E. Sveinbjornsdottir, 1992a:** A “deep” ice core from East
569 Greenland. *Meddelelser om Gronland, Geoscience*, **29**, 3-22
570
- 571 **Johnsen, S.J., H.B. Clausen, W. Dansgaard, K. Fuhrer, N. Gundestrup, C.U. Hammer, P.**
572 **Iversen, J. Jouzel, B. Stauffer, and J.P. Steffensen, 1992b:** Irregular glacial
573 interstadials recorded in a new Greenland ice core. *Nature*, **359**, 311-313.
574
- 575 **Johnsen, S.J., D. Dahl-Jensen, N. Gundestrup, J.P. Steffensen, H.B. Clausen, H. Miller,**
576 **V. Masson-Delmotte, A.E. Sveinbjornsdottir, and J. White, 2001:** Oxygen isotope and
577 palaeotemperature records from six Greenland ice-core stations: Camp Century, Dye-
578 3, GRIP, GISP2, Renland and NorthGRIP. *Journal of Quaternary Science*, **16**, 299-
579 307.
580

- 581 **Jones, G.A.** and L.D. Keigwin, 1988: Evidence from the Fram Strait (78 N) for early
582 deglaciation. *Nature*, **336**, 56-59.
583
- 584 **Joughin, I., S. Tulaczyk, M. Fahnestock, and R. Kwok**, 1996: A mini-surge on the Ryder
585 Glacier, Greenland, observed by satellite radar interferometry. *Science*, **274**, 228-230.
586
- 587 **Joughin, I., Das, S.B., King, M.A., Smith, B. E., Howat, I.M., and Moon, T.**, 2008a:
588 Seasonal Speedup Along the Western Flank of the Greenland Ice Sheet. *Science*,
589 published online, 10.1126/science.1153288 (Science Express Reports).
590
- 591 **Joughin, I., I. Howat, R.B. Alley, G. Ekstrom, M. Fahnestock, T. Moon, M. Nettles, M.**
592 **Truffer, and V.C. Tsai**, 2008b: Ice front variation and tidewater behavior on Helheim
593 and Kangerdlugssuaq Glaciers, Greenland. *Journal of Geophysical Research*, **113**,
594 F01004, doi:10.1029/2007JF000837.
595
- 596 **Jouzel, J., R.B. Alley, K.M. Cuffey, W. Dansgaard, P. Grootes, G. Hoffmann, S.J.**
597 **Johnsen, R.D. Koster, D. Peel, C.A. Shuman, M. Stievenard, M. Stuiver, and J.**
598 **White**, 1997: Validity of the temperature reconstruction from water isotopes in ice
599 cores. *Journal of Geophysical Research*, **102(C12)**, 26,471-26,487.
600
- 601 **Kahn, S.A., J. Wahr, L.A. Stearns, G.S. Hamilton, T. van Dam, K.M. Larson, and O.**
602 **Francis**, 2007: Elastic uplift in southeast Greenland due to rapid ice mass loss.
603 *Geophysical Research Letters*, **34**, L21701. doi:10.1029/2007GL031468.
604
- 605 **Kamb, B., C.F. Raymond, W.D. Harrison, H. Engelhardt, K.A. Echelmeyer, N.**
606 **Humphrey, M.M. Brugman, and T. Pfeffer**, 1985: Glacier Surge Mechanism: 1982-
607 1983 surge of Variegated Glacier, Alaska. *Science*, **227**, 469-479.
608
- 609 **Kandiano, E.S. and H.A. Bauch**, 2003: Surface ocean temperatures in the north-east
610 Atlantic during the last 500,000 years—Evidence from foraminiferal census data.
611 *Terra Nova*, **15**, 265-271.

612

613 **Kaufman**, D.S. and J. Brigham-Grette, 1993: Aminostratigraphic correlations and
614 paleotemperature implications, Pliocene–Pleistocene high sea level deposits,
615 northwestern Alaska. *Quaternary Science Reviews*, **12**, 21-33.

616

617 **Kaufman**, D.S., R.C. Walter, J. Brigham-Grette, and D.M. Hopkins, 1991: Middle
618 Pleistocene age of the Nome River glaciation, northwestern Alaska. *Quaternary*
619 *Research*, **36**, 277-293.

620

621 **Kelly**, M., S. Funder, M. Houmark-Nielsen, K.L. Knudsen, C. Kronborg, J. Landvik, and
622 L. Sorby, 1999: Quaternary glacial and marine environmental history of northwest
623 Greenland—A review and reappraisal. *Quaternary Science Reviews*, **18**, 373-392.

624

625 **Kiehl**, J.T. and P.R. Gent, 2004: The Community Climate System model, version two.
626 *Journal of Climate*, **17**, 3666-3682.

627

628 **Kindler**, P. and P.J. Hearty, 2000: Elevated marine terraces from Eleuthera (Bahamas)
629 and Bermuda: sedimentological, petrographic and geochronological evidence for
630 important deglaciation events during the middle Pleistocene. *Global and Planetary*
631 *Change*, **24**, 41-58.

632

633 **Kleiven**, H.F., E. Jansen, T. Fronval, and T.M. Smith, 2002: Intensification of Northern
634 Hemisphere glaciations in the circum Atlantic region (3.5-2.4 Ma) —Ice-rafted
635 detritus evidence. *Palaeogeography, Palaeoclimatology, Palaeoecology*, **184**, 213-
636 223.

637

638 **Kobashi**, T., J.P. Severinghaus, and J.-M. Barnola. In press. $4\pm 1.5^{\circ}\text{C}$ abrupt warming
639 11,270 years ago identified from trapped air in Greenland ice. *Earth and Planetary*
640 *Science Letters*.

641

642 **Koerner, R.M.**, 1989: Ice core evidence for extensive melting of the Greenland Ice Sheet
643 in the last interglacial. *Science*, **244**, 964-968.

644

645 **Koerner, R.M.** and D.A. Fisher, 2002: Ice-core evidence for widespread Arctic glacier
646 retreat in the last interglacial and the early Holocene. *Annals of Glaciology*, **35**, 19-
647 24.

648

649 **Kuijpers, A.**, N. Abrahamsen, G. Hoffmann, V. Huhnerbach, P. Konradi, H.
650 Kunzendorf, N. Mikkelsen, J. Thiede, and W. Weinrebe, scientific party of RV
651 Poseidon, surveyors of the Royal Danish Administration for Navigation, and
652 Hydrology, 1999: Climate change and the Viking-age fjord environment of the
653 Eastern Settlement, South Greenland. *Geology of Greenland Survey Bulletin*, **183**, 61-
654 67.

655

656 **Lambeck, K.**, C. Smither, and P. Johnston, 1998: Sea-level change, glacial rebound and
657 mantle viscosity for northern Europe. *Geophysical Journal International*, **134**, 102-
658 144.

659

660 **Lemke, P.**, J. Ren, R.B. Alley, I. Allison, J. Carrasco, G. Flato, Y. Fujii, G. Kaser, P.
661 Mote, R.H. Thomas, and T. Zhang, 2007: Observations: Changes in Snow, Ice and
662 Frozen Ground. In: *Climate Change 2007: The Physical Science Basis. Contribution*
663 *of Working Group I to the Fourth Assessment Report of the Intergovernmental Panel*
664 *on Climate Change* [Solomon, S., D. Qin, M. Manning, Z. Chen, M. Marquis, K.B.
665 Averyt, M. Tignor and H.L. Miller (eds.)]. Cambridge University Press, Cambridge
666 and New York, 996 pp.

667

668 **Lhomme, N.**, G.K.C. Clarke, and S.J. Marshall, 2005: Tracer transport in the Greenland
669 Ice Sheet—Constraints on ice cores and glacial history. *Quaternary Science Reviews*,
670 **24**, 173-194.

671

- 672 **Lisitzin, A.P.**, 2002: *Sea-Ice and Iceberg Sedimentation in the Ocean—Recent and Past*.
673 Springer-Verlag, Berlin, 563 pp.
674
- 675 **Lloyd, J. M.**, L.A. Park, A. Kuijpers, and M. Moros, 2005: Early Holocene
676 palaeoceanography and deglacial chronology of Disko Bugt, West Greenland.
677 *Quaternary Science Reviews*, **24**, 1741-1755.
678
- 679 **Lloyd, J.M.**, 2006: Late Holocene environmental change in Disko Bugt, west
680 Greenland— Interaction between climate, ocean circulation and Jakobshavn Isbrae.
681 *Boreas*, **35**, 35-49.
682
- 683 **Ljung, K.** and S. Bjorck, 2004: A lacustrine record of the Pleistocene-Holocene
684 boundary in southernmost Greenland. *GFF (Geological Society of Sweden)*, **126**, 273-
685 278, Part 3.
686
- 687 **Locke, W.W.I.**, J.T. Andrews, and P.J. Webber, 1979: *A Manual for Lichenometry*.
688 British Geomorphological Research Group, Technical Bulletin 26, 47 pp.
689
- 690 **Long, A.J.**, D.H. Roberts, and S. Dawson, 2006: Early Holocene history of the west
691 Greenland Ice Sheet and the GH-8.2 event. *Quaternary Science Reviews*, **25**, 904-
692 922.
693
- 694 **Mangerud, J.** and Funder, S., 1994: The interglacial-glacial record at the mouth of
695 Scoresby Sund, East Greenland. *Boreas*, **23**, 349-358.
696
- 697 **Marienfeld, P.**, 1992a: Recent sedimentary processes in Scoresby Sund, East Greenland.
698 *Boreas*, **21**: 169-186.
699
- 700 **Marienfeld, P.**, 1992b: Postglacial sedimentary history of Scoresby Sund, East
701 Greenland. *Polarforschung*, **60**, 181-195.
702

- 703 **Marshall**, S.J. and K.M. Cuffey, 2000: Peregrinations of the Greenland Ice Sheet divide
704 in the last glacial cycle—Implications for central Greenland ice cores. *Earth and*
705 *Planetary Science Letters*, **179**, 73-90.
- 706
- 707 **Marwick**, P.J., 1998: Fossil crocodylians as indicators of Late Cretaceous and Cenozoic
708 climates—Implications for using palaeontological data in reconstructing
709 palaeoclimate. *Palaeogeography, Palaeoclimatology, Palaeoecology*, **137**, 205-271.
- 710
- 711 **McCave**, I.N. and B.E. Tucholke, 1986: Deep current-controlled sedimentation in the
712 western North Atlantic. In: *The Geology of North America: The Western North*
713 *Atlantic Region* [Vogt, P.R. and B.E. Tucholke (eds.)]. Geological Society of
714 America, pp. 451-468.
- 715
- 716 **McManus**, J.F., D.W. Oppo, and J.L. Cullen, 1999: A 0.5-million-year record of
717 millennial-scale climate variability in the North Atlantic. *Science*, **283**, 971-975.
- 718
- 719 **Meier**, M.F. and A. Post, 1987: Fast tidewater glaciers. *Journal of Geophysical*
720 *Research*, **92(B9)**, 9051-9058.
- 721
- 722 **Mienert**, J., J.T. Andrews, and J.D. Milliman, 1992: The East Greenland continental
723 margin (65 N) since the last deglaciation—Changes in sea floor properties and ocean
724 circulation. *Marine Geology*, **106**: 217-238.
- 725
- 726 **Milne**, G.A., J.X. Mitrovica, H.G. Scherneck, J.L. Davis, J.M. Johansson, H. Koivula,
727 and M. Vermeer, 2004: Continuous GPS measurements of postglacial adjustment in
728 Fennoscandia— 2. Modeling results. *Journal of Geophysical Research*, **109(B2)**, Art.
729 No. B02412.
- 730
- 731 **Mitrovica**, J.X., 1996: Haskell [1935] Revisited. *Journal Geophysical Research*, **101**,
732 555-569.
- 733

- 734 **Mitrovica, J.X. and G.A. Milne, 2002:** On the origin of Late Holocene highstands within
735 equatorial ocean basins, *Quaternary Science Reviews*, **21**, 2179-2190.
736
- 737 **Mitrovica, J.X. and W.R. Peltier, 1991:** On post-glacial geoid relaxation over the
738 equatorial oceans. *Journal Geophysical Research*, **96**, 20,053-20,071.
739
- 740 **Mitrovica, J.X., M.E. Tamisiea, J.L. Davis, and G.A. Milne, 2001:** Recent mass balance
741 of polar ice sheets inferred from patterns of global sea-level change. *Nature*, **409**,
742 1026-1029.
743
- 744 **Mitrovica, J.X., J. Wahr, I. Matsuyama, A. Paulson, and M.E. Tamisiea, 2006:**
745 Reanalysis of ancient eclipse, astronomic and geodetic data—A possible route to
746 resolving the enigma of global sea-level rise. *Earth and Planetary Science Letters*,
747 **243**, 390-399.
748
- 749 **Moran, K., J. Backman, H. Brinkhuis, S.C. Clemens, T. Cronin, G.R. Dickens, F.**
750 **Eynaud, J. Gattacceca, M. Jakobsson, R.W. Jordan, M. Kaminski, J. King, N. Koc, A.**
751 **Krylov, N. Martinez, J. Matthiessen, D. McInroy, T.C. Moore, J. Onodera, M.**
752 **O'Regan, H. Palike, B. Rea, D. Rio, T. Sakamoto, D.C. Smith, R. Stein, K. St. John,**
753 **I. Suto, N. Suzuki, K. Takahashi, M. Watanabe, M. Yamamoto, J. Farrell, M. Frank,**
754 **P. Kubik, W. Jokat and Y. Kristoffersen, 2006:** The Cenozoic palaeoenvironment of
755 the Arctic Ocean. *Nature*, **441**, 601-605.
756
- 757 **Moros, M., K.G. Jensen, and A. Kuijpers, 2006:** Mid- to late-Holocene hydrological
758 variability and climatic variability in Disko Bugt, central West Greenland. *The*
759 *Holocene*, **16**, 357-367.
760
- 761 **Mudie, P.J., A. Rochon, M.A. Prins, D. Soenarjo, S.R. Troelstra, E. Levac, D.B. Scott, L.**
762 **Roncaglia, and A. Kuijpers, 2006:** Late Pleistocene-Holocene marine geology of
763 Nares Strait region—Palaeoceanography from foraminifera and dinoflagellate cysts,

- 764 sedimentology and stable isotopes. *Polarforschung*, **74(1/3)**, 169-183.
765 hdl:10013/epic.29931.d001
766
- 767 **Muhs, D.R.**, 2002: Evidence for the timing and duration of the last interglacial period
768 from high-precision uranium-series ages of corals on tectonically stable coastlines.
769 *Quaternary Research*, **58**, 36-40.
770
- 771 **Muhs, D.R.** and B.J. Szabo, 1994: New uranium-series ages of the Waimanalo
772 Limestone, Oahu, Hawaii—Implications for sea level during the last interglacial
773 period: *Marine Geology*, **118**, 315-326.
774
- 775 **Muhs, D.R.**, K.R. Simmons, and B. Steinke, 2002: Timing and warmth of the last
776 interglacial period—New U-series evidence from Hawaii and Bermuda and a new
777 fossil compilation for North America. *Quaternary Science Reviews*, **21**, 1355-1383.
778
- 779 **Muhs, D.R.**, J.F. Wehmiller, K.R. Simmons, and L.L. York, 2004: Quaternary sea level
780 history of the United States. In: *The Quaternary Period in the United States*
781 [Gillespie, A.R., S.C. Porter, and B.F. Atwater, (eds.)]. Elsevier, Amsterdam, pp. 147-
782 183.
783
- 784 **Multer, H.G.**, E. Gischler, J. Lundberg, K.R. Simmons, and E.A. Shinn, 2002: Key
785 Largo Limestone revisited—Pleistocene shelf-edge facies, Florida Keys, USA:
786 *Facies*, **46**, 229-272.
787
- 788 **Munk, W.**, 2002: Twentieth century sea level—An enigma. *Proceedings of the National*
789 *Academy of Sciences of the United States of America*, **99**, 6550-6555.
790
- 791 **Muscheler, R.**, R. Beer, P.W. Kubik, and H.A. Synal, 2005: Geomagnetic field intensity
792 during the last 60,000 years based on Be-10 and Cl-36 from the Summit ice cores and
793 C-14. *Quaternary Science Reviews*, **24**, 1849-1860.
794

- 795 **Nam, S. I.** and R. Stein, 1999: Late Quaternary variations in sediment accumulation rates
796 and their paleoenvironment implications: a case study from the East Greenland
797 continental margin. *GeoResearch Forum*, **5**, 223-240.
- 798 **Nishiizumi, K.**, R.C. Finkel, K.V. Ponganis, T. Graf, C.P. Kohl, and K. Marti, 1996: In
799 situ produced cosmogenic nuclides in GISP2 rock core from Greenland Summit
800 (Abstract, Fall Meeting 1996). *Eos, Transactions of the American Geophysical*
801 *Union*, **77(46) Supplement**, F428, Abstract OS41B-10.
- 802
- 803 **North Greenland Ice Core Project Members.** 2004. High-resolution record of Northern
804 Hemisphere climate extending into the last interglacial period. *Nature*, **431**, 147-151.
- 805
- 806 **O'Cofaigh, C.**, J. Taylor, J.A. Dowdeswell, and C.J. Pudsey, 2003: Palaeo-ice streams,
807 trough mouth fans and high-latitude continental slope sedimentation. *Boreas*, **32**, 37-
808 55.
- 809
- 810 **Oerlemans, J.**, 1994: Quantifying global warming from the retreat of glaciers. *Science*,
811 **264**, 243–245.
- 812
- 813 **Oerlemans, J.**, 2001: *Glaciers and Climatic Change*. A.A. Balkema Publishers, Lisse,
814 148 pp.
- 815
- 816 **Otto-Bliesner, B.L.**, J.T. Overpeck, S.J. Marshall, and G. Miller, 2006: Simulating
817 Arctic climate warmth and icefield retreat in the Last Interglaciation. *Science*, **311**,
818 1751-1753.
- 819
- 820 **Overpeck, J.T.**, B.L. Otto-Bliesner, G.H. Miller, D.R. Muhs, R.B. Alley, and J.T. Kiehl,
821 2006: Paleoclimatic evidence for future ice-sheet instability and rapid sea-level rise,
822 *Science*, **311**, 1747-1750.
- 823

- 824 **Parizek**, B.R. and R.B. Alley, 2004: Implications of increased Greenland surface melt
825 under global-warming scenarios: ice-sheet simulations. *Quaternary Science Reviews*,
826 **23**, 1013-1027.
- 827
- 828 **Parnell**, J., S. Bowden, C. Taylor, and J.T. Andrews, 2007: Biomarker determination as a
829 provenance tool for detrital carbonate events (Heinrich events?)—Fingerprinting
830 Quaternary glacial sources in Baffin Bay. *Earth and Planetary Science Letters*, **257**,
831 71-82.
- 832
- 833 **Paterson**, W.S.B., 1994: *The Physics of Glaciers*. Pergamon, Oxford, 3rd ed. 480 pp.
- 834
- 835 **Payne**, A.J., A. Vieli, A.P. Shepherd, D.J. Wingham, and E. Rignot, 2004: Recent
836 dramatic thinning of largest West Antarctic ice stream triggered by oceans.
837 *Geophysical Research Letters*, **31**, L23401. doi: 10.1029/2004GL021284.
- 838
- 839 **Peltier**, W.R., 2004: Global glacial isostasy and the surface of the ice-age Earth—The
840 ICE-5G (VM2) Model and GRACE. *Annual Review of Earth and Planetary Sciences*,
841 **32**, 111-149. (doi:10.1146/annurev.earth.32.082503.144359)
- 842
- 843 **Peltier**, W.R. and R.G. Fairbanks, 2006: Global glacial ice volume and Last Glacial
844 Maximum duration from an extended Barbados sea level record. *Quaternary Science*
845 *Reviews*, **25**, 3322-3337.
- 846
- 847 **Petrenko**, V.V., Severinghaus, J.P., Brook, E.J., Reeh, N., Schaefer, H., 2006: Gas
848 records from the West Greenland ice margin covering the Last Glacial Termination: a
849 horizontal ice core. *Quaternary Science Reviews*, **25**, 865-875.
- 850
- 851 **Plag**, H.-P. and H.-U. Juttner, 2001: Inversion of global tide gauge data for present-day
852 ice load changes. In: *Proceedings of the International Symposium on Environmental*
853 *Research in the Arctic and Fifth Ny-Alesund Science Seminar* [Yamanouchi, T.
854 (ed.)]. *Memoirs of the National Institute of Polar Research (Japan)*, **54**, 301-317.

855

856 **Poore, R.Z.** and H.J. Dowsett, 2001: Pleistocene reduction of polar ice caps—Evidence
857 from Cariaco Basin marine sediments. *Geology*, **29**, 1-74.

858

859 **Raynaud, D.,** J. Chappellaz, C. Ritz, and P. Martinerie, 1997: Air content along the
860 Greenland Ice Core Project core—A record of surface climatic parameters and
861 elevation in central Greenland. *Journal of Geophysical Research*, **102(C12)**, 26,607-
862 26,613.

863

864 **Reeh, N.,** 1984: Reconstruction of the glacial ice covers of Greenland and the Canadian
865 Arctic islands by 3-dimensional, perfectly plastic ice-sheet modeling. *Annals of*
866 *Glaciology*, **5**, 115-121.

867

868 **Reeh, N.,** 1985: Greenland Ice-Sheet Mass Balance and Sea-Level change. In: *Glaciers,*
869 *Ice Sheets, and Sea Level—Effect of a CO₂ induced climatic change.* National
870 Academy Press, Washington D.C., pp. 155-171.

871

872 **Reeh, N.,** 2004: Holocene climate and fjord glaciations in Northeast Greenland—
873 Implications for IRD deposition in the North Atlantic. *Sedimentary Geology*, **165**,
874 333-342.

875

876 **Reeh, N.,** C. Mayer, H. Miller, H.H. Thomsen, and A. Weidick, 1999: Present and past
877 climate control on fjord glaciations in Greenland—Implications for IRD-deposition in
878 the sea. *Geophysical Research Letters*, **26**, 1039-1042.

879

880 **Ridley, J.K.,** P. Huybrechts, J.M. Gregory, and J.A. Lowe, 2005: Elimination of the
881 Greenland Ice Sheet in a high CO₂ climate. *Journal of Climate*, **18**, 3409-3427.

882

883 **Rignot, E.** and P. Kanagaratnam, 2006: changes in the velocity structure of the
884 Greenland Ice Sheet. *Science*, **311**, 986-990.

885

- 886 **Rohling**, E.J., M. Fenton, F.J. Jorissen, P. Bertrand, G. Ganssen, and J.P. Caulet. 1998.
887 Magnitudes of sea-level lowstands of the past 500,000 years. *Nature*, **394**, 162-165.
888
- 889 **Schofield**, J.E., K.J. Edwards, and J.A. McMullen, 2007: Modern pollen-vegetation
890 relationships in subarctic southern Greenland and the interpretation of fossil pollen
891 data from the Norse landnam. *Journal of Biogeography*, **34**, 473-488.
892
- 893 **Severinghaus**, J.P., T. Sowers, E.J. Brook, R.B. Alley, and M.L. Bender, 1998: Timing
894 of abrupt climate change at the end of the Younger Dryas interval from thermally
895 fractionated gases in polar ice. *Nature*, **391**, 141-146.
896
- 897 **Shackleton**, N.J., J. Backman, H. Zimmerman, D.V. Kent, M.A. Hall, D.G. Roberts, D.
898 Schnitker, J.G. Baldauf, A. Desprairies, R. Homrighausen, P. Huddlestun, J.B. Keene,
899 A.J. Kaltenback, K.A.O. Krumsiek, A.C. Morton, J.W. Murray, and J.
900 Westbergsmith, 1984: Oxygen isotope calibration of the onset of ice-rafting and
901 history of glaciation in the North-Atlantic region. *Nature*, **307**, 620-623.
902
- 903 **Sluijs**, A., S. Schouten, M. Pagani, M. Woltering, H. Brinkhuis, J.S.S. Damste, G.R.
904 Dickens, M. Huber, G.J. Reichert, R. Stein, J. Matthiessen, L.J. Lourens, N.
905 Pedentchouk, J. Backman and K. Moran, 2006: Subtropical arctic ocean temperatures
906 during the Palaeocene/Eocene thermal maximum. *Nature*, **441**, 610-613.
907
- 908 **Smith**, J.M.B. and T.P. Bayliss-Smith, 1998: Kelp-plucking—Coastal erosion facilitated
909 by bull-kelp *Durvillaea antarctica* at subantarctic Macquarie Island. *Antarctic*
910 *Science*, **10**, 431-438.
911
- 912 **Souchez**, R., A. Bouzette, H.B. Clausen, S.J. Johnsen, and J. Jouzel, 1998: A stacked
913 mixing sequence at the base of the Dye 3 core, Greenland. *Geophysical Research*
914 *Letters*, **25**, 1943-1946.
915

- 916 **Sowers, T., M. Bender, D. Raynaud, and Y.S. Korotkevich, 1992:** Delta-N-15 of N₂ in
917 air trapped in polar ice—A tracer of gas-transport in the firn and a possible constraint
918 on ice age/gas age-differences. *Journal of Geophysical Research*, **97(D14)**, 15,683-
919 15,697.
- 920
- 921 **Sparrenbom, C.J., O. Bennike, S. Bjorck, and K. Lambeck, 2006a:** Holocene relative
922 sea-level changes in the Qaqortoq area, southern Greenland. *Boreas*, **35**, 171-187.
- 923
- 924 **Sparrenbom, C.J., O. Bennike, S. Bjorck, and K. Lambeck, 2006b:** Relative sea-level
925 changes since 15 000 cal. yr BP in the Nanortalik area, southern Greenland. *Journal*
926 *of Quaternary Science*, **21**, 29-48.
- 927
- 928 **Spencer, M.K., R.B. Alley, and J.J. Fitzpatrick, 2006:** Developing a bubble number-
929 density paleoclimatic indicator for glacier ice. *Journal of Glaciology*, **52(178)**, 358-
930 364.
- 931
- 932 **St. John, K.E. and Krissek, L.A., 2002:** The late Miocene to Pleistocene ice-rafting
933 history of southeast Greenland. *Boreas*, **31**, 28-35.
- 934
- 935 **St. John, K., 2008:** Cenozoic ice-rafting history of the central Arctic Ocean—
936 Terrigenous sands on the Lomonosov Ridge. *Paleoceanography*, **23**, PA1S05.
937 doi:10.1029/2007PA001483.
- 938
- 939 **Stein, A.B., 1996:** Seismic stratigraphy and seafloor morphology of the Kangerlugssuaq
940 region, East Greenland—Evidence for glaciations to the Continental shelf break
941 during the late Weischelian and earlier. MSc thesis, University of Colorado, Boulder,
942 293 pp.
- 943
- 944 **Stein, R., Nam, S.-I., Grobe, H., and Hubberten, H., 1996:** Late Quaternary glacial
945 history and short-term ice-rafted debris fluctuations along the East Greenland
946 continental margin. In: *Late Quaternary Paleooceanography of North Atlantic*

- 947 *Margins* [Andrews, J.T., W.A. Austen, H. Bergsetn, and A.E. Jennings (eds.)].
948 Geological Society, London, pp. 135-151.
949
- 950 **Stirling**, C.H., T.M. Esat, M.T. McCulloch, and K. Lambeck, 1995: High-precision U-
951 series dating of corals from Western Australia and implications for the timing and
952 duration of the last interglacial. *Earth and Planetary Science Letters*, **135**, 115-130.
953
- 954 **Stirling**, C.H., T.M. Esat, K. Lambeck, and M.T. McCulloch, 1998: Timing and duration
955 of the last interglacial—Evidence for a restricted interval of widespread coral reef
956 growth. *Earth and Planetary Science Letters*, **160**, 745-762.
957
- 958 **Stirling**, C.H. T.M., Esat, K. Lambeck, M.T. McCulloch, S.G. Blake, D.-C. Lee, and
959 A.N. Halliday, 2001: Orbital forcing of the marine isotope stage 9 interglacial:
960 *Science*, **291**, 290-293.
961
- 962 **Stocker**, T.F. and S.J. Johnsen, 2003: A minimum thermodynamic model for the bipolar
963 seesaw. *Paleoceanography*, **18**, Art. No. 1087.
964
- 965 **Stoner**, J.S., J.E.T. Channell, and C. Hillaire-Marcel, 1995: Magnetic properties of deep-
966 sea sediments off southwest Greenland—Evidence for major differences between the
967 last two deglaciations. *Geology*, **23**: 241-244.
968
- 969 **Stuiver**, M., T.F. Braziunas, P.M. Grootes, and G.A. Zielinski, 1997: Is there evidence
970 for solar forcing of climate in the GISP2 oxygen isotope record? *Quaternary*
971 *Research*, **48**, 259-266.
972
- 973 **Stuiver**, M., P.J. Reimer, E. Bard, J.W. Beck, K.A. Hughen, B. Kromer, F.G.
974 McCormack, J. van der Plicht, and M. Spurk, 1998: INTCAL98 Radiocarbon age
975 calibration 24,000-0 cal BP. *Radiocarbon*, **40**, 1041-1083.
976

- 977 **Sugden, D.** and B. John, 1976: *Glaciers and Landscape*. Arnold, London, and Halsted,
978 New York, 376 pp.
979
- 980 **Suwa, M., J.C. von Fischer, M.L. Bender, A. Landais, and E.J. Brook,** 2006: Chronology
981 reconstruction for the disturbed bottom section of the GISP2 and the GRIP ice
982 cores— Implications for Termination II in Greenland. *Journal of Geophysical*
983 *Research*, **111(D2)**, Art. No. D02101.
984
- 985 **Syvitski, J.P.M., J.T. Andrews, and J.A. Dowdeswell,** 1996: Sediment deposition in an
986 iceberg-dominated glacial marine environment, East Greenland—Basin fill
987 implications. *Global and Planetary Change*, **12**, 251-270.
988
- 989 **Syvitski, J.P.M., A. Stein, J.T. Andrews, and J.D. Milliman,** 2001: Icebergs and seafloor
990 of the East Greenland (Kangerlussuaq) continental margin. *Arctic, Antarctic and*
991 *Alpine Research*, **33**, 52-61.
992
- 993 **Tang, C.C.L., C.K. Ross, and T. Yao,** 2004: The circulation, water masses and sea-ice of
994 Baffin Bay. *Progress in Oceanography*, **63**, 183-228.
995
- 996 **Tarasov, L. and W. Richard Peltier,** 2002: Greenland glacial history and local
997 geodynamic consequences. *Geophysical Journal International*, **150(1)**, 198-229.
998 doi:10.1046/j.1365-246X.2002.01702.x
999
- 1000 **Tarasov, L. and W.R. Peltier,** 2003: Greenland glacial history, borehole constraints, and
1001 Eemian extent. *Journal of Geophysical Research*, **108(B3)**, Art. No. 2143.
1002
- 1003 **Thiede, J., A. Winkler, T. Wolf-Welling, O. Eldholm, A.M. Myhre, K.H. Baumann, R.**
1004 **Henrick, and R. Stein,** 1998: Late Cenozoic history of the Polar North Atlantic—
1005 Results from ocean drilling. *Quaternary Science Reviews*, **17**, 185-208.
1006

- 1007 **Thomas, R.H.** and PARCA Investigators, 2001: Program for Arctic Regional Climate
1008 Assessment (PARCA) —Goals, key findings, and future directions. *Journal of*
1009 *Geophysical Research*, **106(D24)**, 33,691-33705.
1010
- 1011 **Thomas, R.,** W. Abdalati, E. Frederick, W. Krabill, S. Manizade, and K. Steffen, 2003:
1012 Investigation of surface melting and dynamic thinning on Jakobshavn Isbrae,
1013 Greenland. *Journal of Glaciology*, **49**, 231-239.
1014
- 1015 **Thomas, R.,** E. Frederick, W. Krabill, S. Manizade, and C. Martin, 2006: Progressive
1016 increase in ice loss from Greenland. *Geophysical Research Letters*, **33**, L10503,
1017 doi:10.1029/2006GL026075.
1018
- 1019 **Thompson, W.G.** and S.L. Goldstein, 2005: Open-system coral ages reveal persistent
1020 suborbital sea-level cycles. *Science*, **308**, 401-404.
1021
- 1022 **Toniazzo, T.,** J.M. Gregory, and P. Huybrechts, 2004: Climatic impact of a Greenland
1023 deglaciation and its possible irreversibility. *Journal of Climate*, **17**, 21-33.
1024
- 1025 **van der Plicht, J.,** B. Van Geel, S.J.P. Bohncke, J.A.A. Bos, M. Blaauw, A.O.M.
1026 Speranza, R. Muscheler, and S. Bjorck, 2004: The Preboreal climate reversal and a
1027 subsequent solar-forced climate shift. *Journal of Quaternary Science*, **19**, 263-269.
1028
- 1029 **van der Veen, C.J.,**1999: *Fundamentals of Glacier Dynamics*. Balkema, Rotterdam. 462
1030 pp.
1031
- 1032 **van Kreveld, S.,** M. Sarthein, H. Erlenkeuser, P. Grootes, S. Jung, M.J. Nadeau, U.
1033 Pflaumann, and A. Voelker, 2000: Potential links between surging ice sheets,
1034 circulation changes, and the Dansgaard-Oeschger cycles in the Irminger Sea, 60-18
1035 ka. *Paleoceanography*, **15**, 425-442.
1036

- 1037 **Velicogna, I.** and J. Wahr, 2006: Acceleration of Greenland ice mass loss in spring 2004.
1038 *Nature*, **443**, 329-331.
- 1039
- 1040 **Vorren, T.O.** and J.S. Laberg, 1997: Trough mouth fans—Palaeoclimate and ice-sheet
1041 monitors. *Quaternary Science Reviews*, **16**, 865-886.
- 1042
- 1043 **Weidick, A.** 1993: Neoglacial change of ice cover and the related response of the Earth's
1044 crust in West Greenland. *Grøn. Geol. Unders. Rapp.* **159**, 121–126.
- 1045 **Weidick, A.**, 1996: Neoglacial changes of ice cover and sea level in Greenland—A
1046 classical enigma. In: *The Paleo-Eskimo Cultures of Greenland* [Gronnow, B. and J.
1047 Pind (eds.)]. Danish Polar Center, Copenhagen, pp. 257-270.
- 1048
- 1049 **Weidick, A.**, H. Oerter, N. Reeh, H.H. Thomsen, and L. Thorning, 1990: The recession
1050 of the Inland Ice margin during the Holocene Climatic Optimum in the Jakobshavn-
1051 Isfjord area of west Greenland. *Global and Planetary Change*, **82**, 389-399.
- 1052
- 1053 **Weidick, A.**, M. Kelly, and O. Bennike, 2004: Later Quaternary development of the
1054 southern sector of the Greenland Ice Sheet, with particular reference to the Qassimiut
1055 lobe. *Boreas*, **33**, 284-299.
- 1056
- 1057 **Whillans, I.M.**, 1976: Radio-echo layers and recent stability of West Antarctic ice sheet.
1058 *Nature*, **264**, 152-155.
- 1059
- 1060 **Wilken, M.** and J. Mienert, 2006: Submarine glacial debris flows, deep-sea channels
1061 and past ice-stream behaviour of the East Greenland continental margin. *Quaternary*
1062 *Science Reviews*, **25**, 784-810.
- 1063
- 1064 **Willerslev, E.**, E. Cappellini, W. Boomsma, R. Nielsen, M.B. Hebsgaard, T.B. Brand, M.
1065 Hofreiter, M. Bunce, H.N. Poinar, D. Dahl-Jensen, S. Johnsen, J.P. Steffensen, O.
1066 Bennike, J.L. Schwenninger, R. Nathan, S. Armitage, C.J. de Hoog, V. Alfimov, M.
1067 Christi, J. Beer, R. Muscheler, J. Barker, M. Sharkp, K.E.H. Penkman, J. Haile, P.

1068 Taberlet, M.T.P. Bilbert, A. Casoli, E. Campani, and M.J. Collins, 2007: Ancient
1069 biomolecules from deep ice cores reveal a forested Southern Greenland. *Science*, **317**,
1070 111-114.

1071

1072 **Zielinski**, G.A., P.A. Mayewski, L.D. Meeker, S. Whitlow, M.S. Twickler, M. Morrison,
1073 D.A. Meese, A.J. Gow, and R.B. Alley, 1994: Record of volcanism since 7000 B.C.
1074 from the GISP2 Greenland ice core and implications for the volcano-climate system.
1075 *Science*, **264**, 948-950.

1076

1077 **Zwally**, H.J., W. Abdalati, T. Herring, K. Larson, J. Saba, and K. Steffen, 2002: Surface
1078 melt-induced acceleration of Greenland ice-sheet flow. *Science*, **297**, 218-222.